CHEMICAL REVIEWS

REVIEW

pubs.acs.org/CR

Atmospheric Chemistry of Iodine

Alfonso Saiz-Lopez,[*,†] John M. C. Plane,[*,‡] Alex R. Baker,[§] Lucy J. Carpenter,[∥] Roland von Glasow,[§] Juan C. Gómez Martín,[†] Gordon McFiggans,[⊥] and Russell W. Saunders[‡]

[†]Laboratory for Atmospheric and Climate Science (CIAC), CSIC, Toledo, Spain

[‡]School of Chemistry, University of Leeds, Leeds, LS2 9JT, United Kingdom

[§]School of Environmental Sciences, University of East Anglia, Norwich NR4 7TJ, United Kingdom

[∥]Department of Chemistry, University of York, Heslington, York YO10 5DD, United Kingdom

[⊥]School of Earth, Atmospheric & Environmental Sciences, University of Manchester, Manchester, M13 9PL, United Kingdom

CONTENTS

1. INTRODUCTION

The atmospheric chemistry of iodine is important in diverse ways. First, it provides the route for iodine, which is an essential dietary element for mammals, to be transported from its oceanic source to the continents.[1] Second, iodine chemistry influences the oxidizing capacity of the atmosphere, i.e., the capacity of the atmosphere to oxidize and ultimately remove the large variety of organic and inorganic species which are emitted into it from both natural and anthropogenic sources. This occurs through the catalytic destruction of ozone[2−6] and changes to the important radical

Received: January 19, 2011
Published: October 27, 2011

dx.doi.org/10.1021/cr200029u | *Chem. Rev.* 2012, 112, 1773–1804

Table 1. Summary of Atmospheric Measurements of IO, OIO, I_2, and I (maximum mixing ratio) in a Variety Geographical Locations

		mixing ratio/pptv		
species	location	max	LOD[k]	ref
IO	Antarctica	~10		Frieß et al.[109 I]
		20 ± 1	0.5	Saiz-Lopez et al.[126]
		~12		Saiz-Lopez et al.[33]
		~10		Schönhardt et al.[34 j]
	Arctic	0.8 ± 0.2[a]	0.3	Wittrock et al.[139 I]
		3.4 ± 1.2	1.3	Mahajan et al.[132]
		0.4 ± 0.1	0.2	Oetjen[120 I]
	North Sea (Germany)	2.0 ± 0.7	0.28	Peters et al.[106]
		1.4 ± 0.3	0.14	Oetjen[120 I]
	Mace Head (Ireland)	6.6 ± 0.5	0.9	Alicke et al.[26]
		3.0 ± 0.3	0.2	Allan et al.[27]
		7.0 ± 0.5	0.5	Saiz-Lopez and Plane[18]
		29 ± 9	14[b]	Seitz et al.[104]
		30 ± 1	1.4[c]	Commane et al.[114 h]
	Brittany (France)	7.7 ± 0.5	0.23	Peters et al.[106]
		10.1 ± 0.7	0.5	Mahajan et al.[105]
		54 ± 18	12[d]	Wada et al.[28 h]
		30 ± 7	1.1[e]	Furneaux et al.[115 h]
	Gulf of Maine (USA)	4.0 ± 0.5		Stutz et al.[107]
	Cape Grim (Australia)	2.2 ± 0.3	0.2	Allan et al.[27]
	Heraklion (Greece)	<1.9	0.8	Oetjen[120 I]
	Dead Sea Valley (Israel)	10 ± 1	3	Zingler and Platt[98]
	Tenerife (Spain)	4.0 ± 0.3	0.2	Allan et al.[27]
		0.4 ± 0.2	0.2	Puentedura et al.[125f I]
	Cape Verde Islands	3.1 ± 0.4	0.4	Read et al.[35]
	Maldive Islands	2.8 ± 0.7	0.9	Oetjen[120 I]
	Alcântara (Brazil)	0.8 ± 0.3	0.3	Butz et al.[108]
OIO	Mace Head (Ireland)	3.0 ± 0.4	0.5	Saiz-Lopez and Plane[18]
		9.2 ± 1.3	3.2	Peters et al.[106]
		13 ± 4	4	Bitter et al.[112 h]
	Britanny (France)	8.7 ± 2.3	3	Mahajan et al.[105]
	Gulf of Maine (USA)	27 ± 7[g]		Stutz et al.[107]
	Cape Grim (Australia)	3.0 ± 0.4	0.5	Allan et al.[110]
I_2	Mace Head (Ireland)	93 ± 5	3	Saiz-Lopez and Plane[18]
		61 ± 12	10	Peters et al.[106]
		94 ± 20	20	Bitter et al.[112 h]
	Mweenish Bay (Ireland)	115		Saiz-Lopez et al.[113 h]
		≤302 ± 4	0.2	Huang et al.[116 h]
	Brittany (France)	52 ± 4	5	Mahajan et al.[105]
		50 ± 10	10	Leight et al.[90 h]
	Ría de Arousa (Spain)	300 ± 100	30	Mahajan et al.[111 h]
	California (USA)	4.0 ± 0.6	0.1	Finley and Saltzman[32 h]
I	Mace Head (Ireland)	22 ± 5	2.5	Bale et al.[30 h]
	Ría de Arousa (Spain)	10 ± 5	2	Mahajan et al.[105 h]

[a] Claimed stratospheric IO, in contrast ot other studies.[108,135−137] [b] LP-DOAS 1 km path. [c] A 60 s integration time. Up to 50 ± 9 ppt where observed at 1 s integration. [d] A 30 s integration time. [e] A 10 s integration time. [f] In the free troposphere. [g] Daytime OIO, in contrast to other studies (see table). [h] In-situ measurements. [I] Max-DOAS or Zenith Sky Measurements. [j] Satellite Measurements, No symbol: LP-DOAS. [k] LOD = limit of detection.

species (particularly hydroxyl (OH)) which control the oxidizing chemistry.[2,7,8]

Third, considerable attention has been paid in the past few years to the role of iodine oxides in formation of ultrafine aerosol particles (operationally defined as having a diameter of 3−10 nm). The process of iodine oxide particle (IOP) production is thought to involve the recombination reactions of IO and OIO radicals to form higher oxides which then condense spontaneously to form particles.[9−12] Bursts of IOPs have been observed in certain marine environments. These particles could provide condensation nuclei for other condensable vapors and grow to the point of becoming cloud condensation nuclei (CCN), which would impact the radiative balance of the atmosphere and hence on climate.[9−11,13−22] Fourth, it has been proposed that iodine in the polar atmosphere may enhance depletion of gaseous elemental mercury (Hg^0) by oxidation to reactive gaseous mercuric (Hg^{II}) compounds.[23,24] The oxidized mercury then deposits in the snowpack, part of it may be reduced in the snowpack and released back to the atmosphere, but the remainder runs off in meltwater and can eventually enter the food chain.[25]

During the past decade, the reactive iodine species atomic iodine(I), molecular iodine (I_2), iodine monoxide (IO), and iodine dioxide (OIO) have all been detected in the atmosphere for the first time (Table 1), in locations ranging from Antarctica to the equatorial marine boundary layer (MBL), using the techniques of differential optical absorption spectroscopy (DOAS),[18,26,27] cavity ring-down spectroscopy (CRDS),[28] laser-induced fluorescence (LIF),[29] resonance fluorescence (RF),[30,31] inductively coupled plasma mass spectrometry (ICP-MS),[19] and atmospheric pressure chemical ionization with tandem mass spectrometry (APCI/MS/MS).[32] Measurements of IO have very recently been extended to satellite-based spectroscopy.[33,34] This confirmation of an active widespread atmospheric chemistry of iodine has led to an explosion of interest. Recently, open ocean measurements have revealed significant levels of IO, indicating its possible global importance in the remote ocean environment.[35]

The atmospheric measurements have been complemented by significant developments in laboratory and quantum theory studies of the reaction kinetics, photochemistry, and heterogeneous chemistry of iodine species. In the past 5 years there has been very active research on IO, OIO, $IONO_2$, and the higher iodine oxides (I_2O_x, $x = 2−5$)[36−41]

The last dedicated review on atmospheric iodine[42] focused on the sources and role of organic iodine in the midlatitude MBL. However, even knowledge of the sources of atmospheric iodine has changed dramatically since then. For instance, it has now been shown that probably the major source in the midlatitude coastal MBL is macroalgae which emit mainly I_2 when exposed at low tide.[18] In addition, the recent (and unexpected) discovery of large and geographically widespread IO levels around coastal Antarctica has indicated that there is a substantial source of iodine generated photochemically in snow and sea ice.[33,34] von Glasow and Crutzen included several of these aspects in their updated review on tropospheric halogen chemistry,[43,44] but many exciting discoveries have since been made. Figure 1 summarizes our current understanding and uncertainties of the main gas- and condensed-phase iodine photochemistry processes.

This review comprises the most recent advances in our understanding of the sources of iodine (i.e., biological, gas- and aqueous-phase chemical mechanisms), describes the results of field observations (i.e., ground, balloon, and satellite based), discusses the progress made in laboratory studies of elementary processes and nanoparticle formation as well as numerical modeling of reactive iodine chemistry and particle formation, and

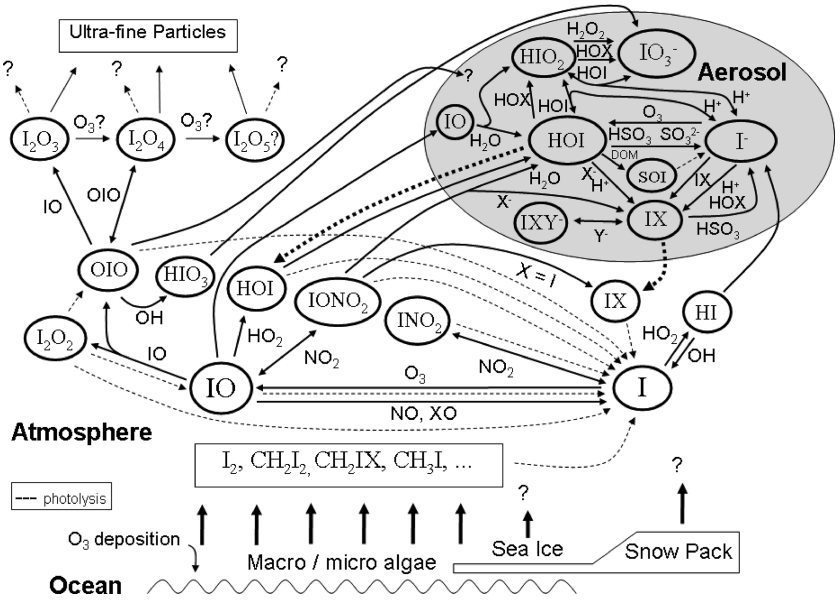

Figure 1. Simplified schematic of atmospheric iodine photochemistry, based upon current knowledge of gas- and condensed-phase processes. Dashed lines represent photolysis, whereas dotted lines illustrate phase equilibration from aerosols. X and Y are halogen atoms, DOM is dissolved organic matter, and SOI is soluble organic iodine.

summarizes our current knowledge of the atmospheric impact of iodine (i.e., ozone depletion, HO_x and NO_x chemistry, Hg oxidation, and new particle formation).

2. SOURCES OF IODINE TO THE ATMOSPHERE

The oceans provide the main source of iodine to the atmosphere through volatilization of iodine carriers including monohalogenated organic compounds such as methyl iodide (CH_3I), ethyl iodide (C_2H_5I), and propyl iodide (1- and 2-C_3H_7I), more reactive polyhalogenated compounds such as chloroiodomethane (CH_2ICl), bromoiodomethane (CH_2IBr), and diiodomethane (CH_2I_2), and I_2. These compounds photodissociate rapidly in the atmosphere to generate iodine atoms, e.g.

$$CH_2I_2 + h\nu \rightarrow \rightarrow CH_2 + 2I \quad (1)$$

$$CH_2IBr + h\nu \rightarrow \rightarrow CH_2 + I + Br \quad (2)$$

$$I_2 + h\nu \rightarrow 2I \quad (3)$$

There have been a number of reviews of organoiodine compounds over the past decade, focusing primarily on CH_3I.[42,45−47] However, even since these relatively recent reviews, key new data have considerably improved knowledge of most of the iodine source gases. A larger database of CH_3I data is now available,[48−50] which has increased previous estimates of the CH_3I global emission rate[48] while consolidating previous suggestions of a largely photochemical source in surface waters.[51,52] Important progress has also been made in understanding the contributions of more reactive iodine source gases. While the WMO 2002 ozone assessment,[46] which used available coastal data and some macroalgal incubation studies, suggested that polyhalogenated iodine compounds (e.g., CH_2ICl, CH_2IBr, CH_2I_2) released from macroalgae make only a very small contribution to the global iodine budget,[53] more recent data suggest that CH_2ICl and CH_2I_2 play a significant role, perhaps contributing as much iodine to the MBL as CH_3I.[47,49,54] In the open ocean, microalgae[55] are a known source of polyhalogenated iodine compounds. New laboratory data has suggested additional abiotic production routes for these compounds in the surface ocean[56−58] and elucidated photochemical removal pathways in seawater.[59,60] Further, there is now incontrovertible evidence for the major contribution of I_2 to iodine in the coastal MBL[18,19,22,61] and indications of a production mechanism via kelp.[62,63] However, there is still insufficient information regarding potential open ocean sources of I_2 to assess its global contribution.

2.1. Atmospheric Mixing Ratios, Seasonality, and Trends in Distributions

Atmospheric mixing ratios of the organoiodines generally decrease in the order $CH_3I > C_2H_5I \approx C_3H_7I > CH_2ICl > CH_2I_2 > CH_2IBr$ (see Table 2), and coastal mixing ratios[50,64] are generally higher than those over the open ocean due to the influence of macroalgae.[65] Two recent comprehensive field studies of CH_3I[48,50] over the Pacific and Atlantic observed generally increasing concentrations from high to low latitudes (although slightly suppressed near the equator). This increase in CH_3I with sea surface temperature (SST) is in accord with earlier studies.[66,67] CH_3I also shows a clear seasonality in midlatitudes with higher concentrations during summer.[50,67−70] These trends broadly reflect the 3D coupled ocean−atmosphere model simulations of Bell et al.,[45] where marine production of CH_3I was parametrized as a scaled product of the solar radiation flux and dissolved organic carbon (DOC) to represent surface photochemical emission.[51,52] The simulated subtropical maxima in CH_3I were a function of high ocean losses in the tropics due to the temperature-dependent reaction with Cl^- (the dominant marine loss process for CH_3I), subtropical maxima in [DOC], and high solar radiation at midlatitudes in summer.

A recent study in the shelf region of the English Channel[68] shows that seawater C_2H_5I, CH_2ICl, CH_2I_2 and CH_2IBr exhibit similar though less pronounced trends in seasonality to CH_3I,

dx.doi.org/10.1021/cr200029u |Chem. Rev. 2012, 112, 1773–1804

Table 2. Atmospheric Mixing Ratios of Organoiodines in the MBL[a]

species	region	mixing ratio/pptv mean	mixing ratio/pptv range	ref
CH_3I	**coastal**			
	Spitzbergen, Norway	1.04	<0.004−2.12	Schall and Heumann[292]
	Mace Head, Ireland (spring)	0.43	0.12−1.47	Carpenter et al.[78]
	Mace Head, Ireland (summer)	3.4	1.9−8.7	Bassford et al.[293]
	Mace Head, Ireland (summer)	3.78	1.3−12.0	Carpenter et al.[80]
	Cape Grim, Australia	2.6	1.0−7.3	Carpenter et al.[80]
	Cape Grim, Australia	1.2		Krummel et al.[294]
	Cape Grim, Australia	0.53	0.14−0.9	Yokouchi et al.[50]
	Okinawa, Japan	1.2	0.5−2.0	Li et al.[295]
	Pacific and Atlantic Coast	0.8	0.4−1.6 [b]	Butler et al.[48]
	Appledore Island, United States	1.39	1.3−1.5	Sive et al.[70]
	NW Pacific Islands [d]	0.86	0.1−4.5	Yokouchi et al.[50]
	San Cristobal Island, Ecuador	1.13	0.53−2.55	Yokouchi et al.[50]
	Antarctic Peninsular	2.4	0.6−7.9	Reifenhäuser and Heuman[296]
	mean	*1.6*	*0.7−4.5* [c]	
	median	*1.2*		
	open ocean			
	Western Pacific	1.07	0.6−1.8	Atlas et al.[297]
	Western Pacific	0.6	0.12−1.15	Blake et al.[66]
	Western Pacific	1.2	0.5−1.9	Yokouchi et al.[298]
	Asian Seas	0.63	0.24−2.0	Yokouchi et al.[298]
	Western Pacific	0.7	0.6−0.8	Li et al.[299]
	Pacific	0.7	0.4−1.6	Butler et al.[48]
	Western Pacific [e]	0.7	0.25−1.7	Yokouchi et al.[50]
	Northern Pacific [f]	0.68	0.19−2.09	Yokouchi et al.[50]
	Atlantic	0.8	0.4−1.2	Butler et al.[48]
	Eastern Atlantic	1.63	0.4−2.24	Chuck et al.[49]
	mean	*0.87*	*0.37−1.58* [c]	
	median	*0.70*		
C_2H_5I	**coastal**			
	Mace Head, Ireland (spring)	0.06	<0.02−0.21	Carpenter et al.[78]
	Mace Head, Ireland (summer)	0.16	<0.02−0.50	Carpenter et al.[80]
	Great Bay, NH, United States	0.07	0.02−0.12	Zhou et al.[300]
	Roscoff, France	0.46	0.21−0.8	Jones et al[64]
	open ocean			
	Asian Seas	0.09	<0.03−0.31	Yokouchi et al.[298]
1-C_3H_7I	**coastal**			
	Spitzbergen, Norway	0.20	<0.02−0.28	Schall and Heumann[292]
	Roscoff, France	0.18	0.08−0.36	Jones et al[64]
2-C_3H_7I	**coastal**			
	Spitzbergen, Norway	2.00	<0.02−5.98	Schall and Heumann[292]
	Roscoff, France	0.47	0.29−0.74	Jones et al[64]
CH_2ICl	**coastal**			
	Mace Head, Ireland (spring)	0.11	<0.02−0.21	Carpenter et al.[78]
	Mace Head, Ireland (summer)	0.16	<0.02−0.50	Carpenter et al.[80]
	Spitzbergen, Norway	0.07	<0.004−0.18	Schall and Heumann[292]
	Norfolk, United Kingdom		0.1−0.5	Baker et al.[101]
	Cape Grim, Australia	0.04	<0.02−0.39	Carpenter et al.[80]
	Appledore Island, United States	0.15	0.01−1.6	Varner et al.[301]

dx.doi.org/10.1021/cr200029u |*Chem. Rev.* 2012, 112, 1773–1804

Table 2. Continued

species	region	mixing ratio/pptv mean	mixing ratio/pptv range	ref
	Thompson Farm, NH, United States	0.68	0.03−3.4	Varner et al.[301]
	Christmas Island, Kiribati	0.10	0.03−0.24	Varner et al.[301]
	Oahu, HI, United States	0.04	0.01−0.07	Varner et al.[301]
	Roscoff, France	0.10	0.03−0.17	Jones et al.[64]
	Outer Hebrides, United Kingdom, kelp beds	1.42	0.94−2.61	Jones et al.[54]
	mean	*0.28*	*0.1−0.9* [c]	
	median	*0.11*		
	open ocean			
	Western Pacific	0	NA	Yokouchi et al.[298]
	Atlantic and Southern Oceans	0.32	0.18−0.71	Chuck et al.[49]
	NE Atlantic (55−60°N), shelf	0.23	<0.08−0.88	Jones et al.[54]
	NE Atlantic (26−36°N)	0.04	<0.1−0.07	Jones et al.[54]
	NE Atlantic (15−25°N)	<0.08	<0.01−0.03	Jones et al.[54]
	mean	*0.12*	*0−0.4* [c]	
	median	*0.04*		
CH_2IBr	**coastal**			
	Mace Head, Ireland (spring)	0.08	0.02−0.32	Carpenter et al.[78]
	Mace Head, Ireland (summer)	0.06	<0.02−0.30	Carpenter et al.[80]
	Roscoff, France	0.06	0.01−0.13	Jones et al.[64]
	Outer Hebrides, United Kingdom, kelp beds	<0.05	NA	Jones et al.[54]
	open ocean			
	Northern Atlantic (15−60°N)	<0.01	0	Jones et al.[54]
CH_2I_2	**coastal**			
	Mace Head, Ireland (spring)	0.05	<0.02−0.36	Carpenter et al.[78]
	Mace Head, Ireland (summer)	0.10	<0.02−0.46	Carpenter et al.[80]
	Spitzbergen, Norway	0.46	<0.08−1.02	Schall and Heumann[292]
	Roscoff, France	0.03	0.01−0.07	Jones et al.[64]
	Outer Hebrides, United Kingdom, kelp beds	0.10	0.02−0.18	Jones et al.[54]
	mean	*0.15*	*0.012−0.42* [c]	
	median	*0.10*		
	open ocean			
	Northern Atlantic (15−60°N)	0.01	<0.01−0.02	Jones et al.[54]

[a] Mean and median values given where ≥5 locations/studies. [b] On the basis of 90% confidence limits. [c] Mean values of minima and maxima. [d] Mean value of data from Cape Ochiishi (43.2°N), Tsukuba (36.0°N), Happo Ridge (36.7°N), and Hateruma Island (24.1°N). [e] Mean of 2 latitudinal bands. [f] Mean of 6 latitudinal bands.

with maxima in the summer months. In contrast, observations by Klick[71] near to seaweed beds on the west coast of Sweden showed distinct spring and autumn peaks in CH_2ICl and CH_2I_2. Generally, atmospheric concentrations of the dihalomethanes are lower or undetectable over open ocean waters compared to coastal/shelf regions (Table 2), making sea−air flux calculations in these regions quite uncertain.

2.2. Emission Rates and Mechanisms

There have been several estimates of CH_3I emissions and attempts to categorize its sources (see Table 3). The top-down estimate of annual ocean emissions by Bell et al.[45] is 191 Gg (I) year^{-1}, falling within an earlier estimate of 114−320 Gg (I) year^{-1}.[72] However, field data from Butler et al.[48] covering seven cruises across the Atlantic, Pacific, and Southern Oceans suggest a total oceanic source more than a factor of 2 higher at ∼550 Gg (I) year^{-1}. Terrestrial sources including rice paddies, wetlands, biomass burning, and terrestrial biomes are suggested to contribute a further 80−110 Gg (I) year^{-1}.[45,70] As discussed earlier, numerous studies point to photochemical production in the surface ocean as the dominant source of CH_3I. An additional dust-stimulated abiotic emission of methyl iodide from the ocean or from marine aerosol was suggested by Williams et al.[73] In contrast, Smythe-Wright et al.[74] attributed extremely high CH_3I seawater and air levels of up to 45 pmol L^{-1} and 100 pptv (parts per trillion in volume, equivalent to pmol mol^{-1}), respectively, in and over low-latitude waters of the Atlantic and Indian Oceans to biological production by the picoplantkon *Prochlorococcus marinus*, suggesting this source alone could contribute 530 Gg (I) year^{-1} as CH_3I, since *Prochlorococcus* are

dx.doi.org/10.1021/cr200029u |*Chem. Rev.* 2012, 112, 1773–1804

Table 3. Estimated Local Lifetimes in the Sunlit MBL and Global Emission Rates for Organoiodine Compounds

species	lifetime	emission rate/Gg (I) year^{-1}	ref
CH_3I	5 days[46]	114−320 total ocean	Moore and Groszko[72]
	6 days[45]	191 total ocean	Bell et al.[45]
		546 total ocean	Butler et al.[48]
		80−110 terrestrial	Bell et al.,[45] Sive et al.[70]
C_2H_5I	4 days[46]	30 total ocean	Jones et al.[54]
CH_2ClI	0.1 days[302]	95 open ocean	Law and Sturges[47] based on data from Chuck et al.[49]
		93 open ocean	Jones et al.[54]
		203 total ocean	Jones et al.[54]
CH_2BrI	~1 h[303]	80 total ocean	Jones et al.[54]
CH_2I_2	2−10 min[303]	223 total ocean	Jones et al.[54]

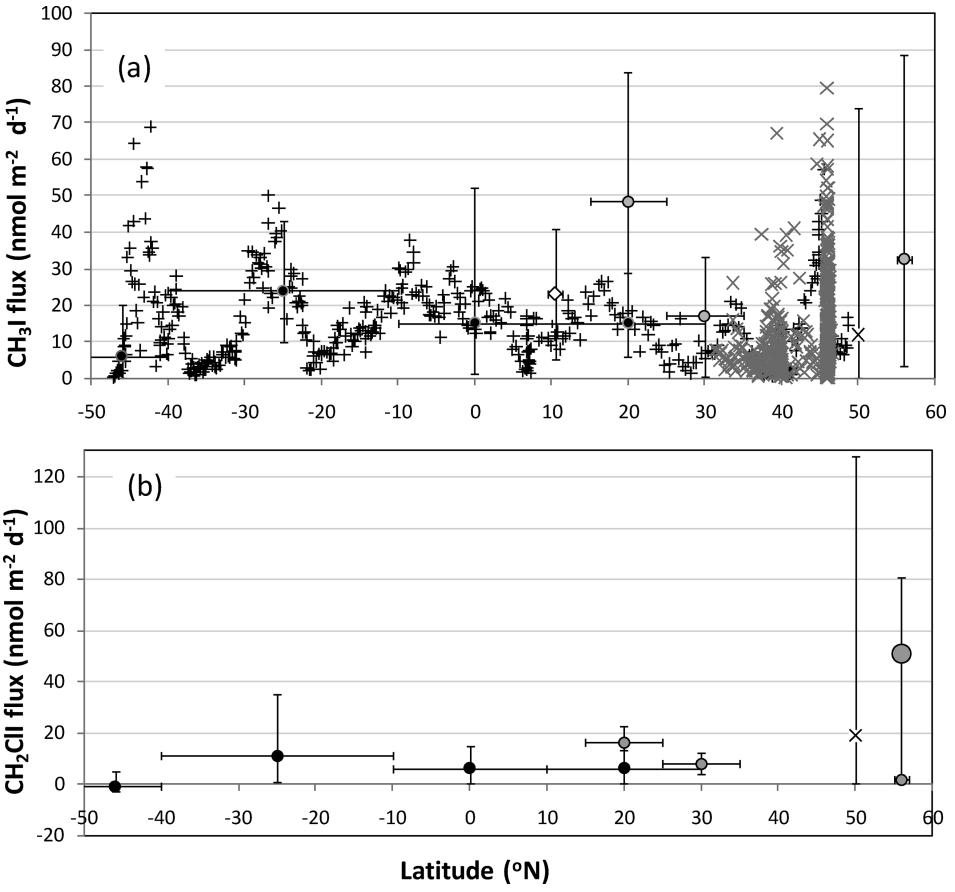

Figure 2. Fluxes of organoiodine compounds from the open Atlantic Ocean. (a) CH_3I: black plus (+), Butler et al.,[48] BLASTII data Oct−Nov 1994 NE and SW Atlantic; gray cross (×), Butler et al.,[48] GASEX98 data May−Jul 1998 E−W transect across N Atlantic; black circles with error bars, mean and range of Chuck et al.,[49] NE and SE Atlantic Sept−Oct 2000; diamond with error bars, mean and range of Richter and Wallace,[327] tropical E Atlantic Oct−Nov 2002; black cross (×) with error bars, annual mean and range of Archer et al.,[68] English Channel; gray circles, mean and range of Jones et al.,[54] − NE (Jun 2006) and tropical E (Jun 2007) Atlantic, excluding coastal data. (b) CH_2ClI: black circles with error bars, mean and range of Chuck et al.,[49] NE and SE Atlantic Sept−Oct 2000; black cross (×) with error bars, annual mean and range of Archer et al.,[68] English Channel; gray circles, mean and range of Jones et al.[54] − NE (Jun 2006) and tropical E (Jun 2007) Atlantic, excluding coastal data. The large gray circle represents the shelf fluxes measured by Jones et al.[54].

abundant in open ocean oligotrophic waters at <40° latitude. These results have been recently contradicted by Brownell et al.,[75] who found that production of CH_3I by *P. marinus* can account for only a small fraction of the estimated global oceanic production. The CH_3I concentrations reported by Smythe-Wright et al.[74] lie above the normal range of other observations in and over open ocean waters[48,49,76] (see Table 2), although similarly high (30−50 pmol L^{-1}) seawater concentrations of CH_3I have been observed in the productive upwelling waters of the eastern Pacific[77] and eastern Atlantic.[54]

While a number of studies[71,78] have identified a range of iodocarbons in coastal regions arising from seaweed emission,[65,79]

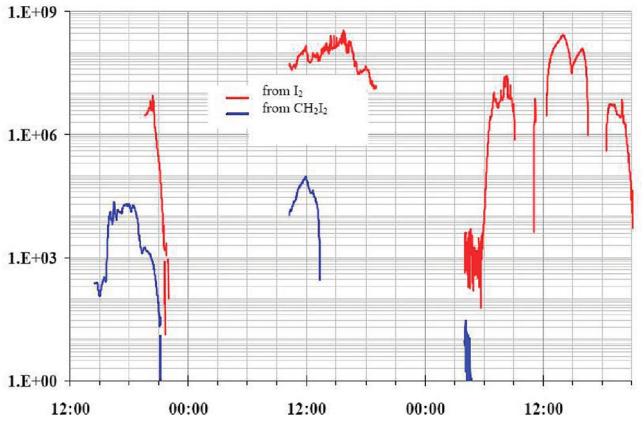

Figure 3. Iodine atom flux from the photolysis of I_2 and CH_2I_2 at Mace Head. Note that there was at least 3 orders of magnitude greater atomic iodine flux from the photolysis of the available I_2 than from the photolysis of CH_2I_2. Reprinted with permission from ref 13. Copyright 2004 European Geosciences Union.

macroalgae produce only ~10 Gg (I) $year^{-1}$ of dihalomethanes (CH_2ICl, CH_2IBr, and CH_2I_2) based on production from midlatitude species[80] and only ~0.5 Gg (I) $year^{-1}$ of CH_3I.[81] These values may be an underestimate if tropical seaweeds are more efficient producers of iodocarbons than midlatitude specimens, as they appear to be for bromoform.[82] However, it is likely that macroalgae represent a minor (0.05−5%) global source of iodocarbons.

An emerging picture is that CH_2ICl and CH_2I_2 are supersaturated in open ocean and shelf surface waters and make an important contribution to the global iodine budget.[49,68] Measurements in the shelf region of the English Channel[68] found that the contribution to the total organoiodine sea-to-air flux from CH_3I, C_2H_5I, CH_2ICl, CH_2I_2, and CH_2IBr (total annual average of 15.5 μmol (I) m^{-2} $year^{-1}$, with summertime fluxes approximately twice this amount) was dominated by CH_2ICl (44%) with CH_3I and CH_2I_2 accounting for 28% and 17%, respectively. These data are very similar to recent results from the subtropical and North Atlantic,[54] where average shelf (off Ireland) total organoiodine fluxes (after accounting for surface photolysis, see discussion below) were 38 μmol (I) m^{-2} $year^{-1}$ in summer, dominated by CH_2ICl (48%) with CH_3I and CH_2I_2 accounting for 26% and 19%, respectively. In the latter study, open ocean total organic iodine fluxes were approximately one-half of the shelf values north of 25°N (mean of 14.5 μmol (I) m^{-2} $year^{-1}$) but similar (mean of 39 μmol (I) m^{-2} $year^{-1}$) in subtropical waters (15−25°N). The contribution of CH_3I was highest in open ocean waters (45−65%), with CH_2ICl accounting for 3−26% and CH_2I_2 9−24% of the total organic iodine sea−air flux. Earlier measurements in the Northwest Atlantic[83] found an average molar concentration ratio and therefore approximate flux ratio of CH_2ICl/CH_3I in surface pelagic waters of 1.06. Extrapolating from coastal, shelf, and open ocean summer data, Jones et al.[54] estimated a total global iodine flux of 1078 Gg (I) $year^{-1}$, of which 531 Gg (I) $year^{-1}$ (49%) is from CH_3I (in good agreement with Butler et al.[48]). The remaining flux is dominated by CH_2ICl (19%) and CH_2I_2 (21%).[71,78]

Correlations between CH_2I_2 and/or CH_2ICl and chlorophyll *a* in the upper water column have been reported from tropical oligotrophic waters in the Bay of Bengal (CH_2I_2 vs Chl-*a*, depth profiles, $R^2 = 0.6$; CH_2ICl vs Chl-*a*, depth profiles, $R^2 = 0.5$[84]), from the Northwest Atlantic (CH_2ICl vs Chl-*a*, depth profiles, $R^2 = 0.9$[83]), and in Atlantic waters (CH_2I_2, surface waters only, $R^2 = 0.4$[54]) suggesting an influence from microalgal sources, and indeed laboratory culture studies of temperate and polar microalgae have identified that they produce a range of organoiodines.[55,85] Other biological mechanisms include methylation of iodine by microalgae[86] and bacteria.[87] Correlation studies between CH_3I and Chl-*a* in the South Atlantic have shown that while in-situ Chl-*a* measurements may not correlate well with CH_3I, the correlation improves significantly if averaged satellite Chl-*a* concentrations along calculated back-trajectories are considered, accounting for spatial and temporal exposure of air masses to biologically active ocean regions upwind of the observation location.[88]

CH_2ICl is also produced photochemically from CH_2I_2 in surface seawater with a molar yield of 0.25−0.35,[59,60] but field data suggest that photoproduction from CH_2I_2 does not fully account for observed surface CH_2ICl concentrations.[54,68] Laboratory determination of the photolysis rates in CH_2I_2 and CH_2ICl in seawater indicate aqueous lifetimes at midday in midlatitudes of 9−12 min for CH_2I_2 and 9−13 h for CH_2ICl.[59,60] Due to rapid photolysis of CH_2I_2 it has been suggested that it is likely to be lost in seawater before transport to the surface.[59,84] However, high-resolution 1-D water column model simulations with photolysis schemes for CH_2I_2 and CH_2ICl suggest that the net sea−air flux of CH_2ICl is essentially unaffected by photolysis, while CH_2I_2 surface concentrations (and therefore approximately fluxes) in the subtropics are reduced compared to concentrations at 6 m by ~30% on average (range 5−90%), with wind speed (which affects mixing within the ocean mixed layer) being the most significant controlling factor.[54]

Recent studies have proposed additional chemical/photochemical mechanisms for the supply of reactive halogens from the ocean surface to the lower atmosphere, which potentially means that subsurface measurements of such species would underestimate their sea−air flux. Martino et al.[57] showed that direct oxidation of I^- in the sea surface microlayer by atmospheric O_3 results in potentially significant production of reactive organoiodine compounds including CH_2I_2, $CHICl_2$, and CH_3I and possibly I_2. These reactions occur in the dark when seawater is exposed to O_3, but so far it is not known whether they are enhanced by solar irradiance due to the complicating factor that polyhalogenated organoiodine compounds are extremely photolabile. Another potential route to direct ocean surface production of small halogen molecules is via oxidation of halogen anions to their radical forms by photosensitizers such as chlorophyll or aromatic ketones, a known component of marine DOC, which in turn will lead to formation of organic halogens in the presence of organic compounds in the sea surface microlayer.[56,58] Oxidation is enhanced in the presence of atmospheric O_3, which acts as an electron acceptor, thus promoting the cationic form of the photosensitizer. The quantity of both molecular and organic halogen emissions from the open ocean via this route remains an open question, although laboratory data suggest this should be elevated in areas of enhanced DOC.

Figure 2 shows current estimates of CH_3I and CH_2ICl fluxes from the open Atlantic Ocean, calculated from the measured partial pressure difference of the gas across the sea surface ($\Delta C = C_{water} - C_{air}/H$, where H is the Henry's Law coefficient) and a wind-dependent gas transfer velocity.[89] For both gases, fluxes tend to be higher over biologically active regions, as demonstrated by the English Channel shelf measurements of Archer[68] and the Irish continental shelf and Mauritanian upwelling measurements of Jones et al.[54] Fluxes of CH_2ICl are generally

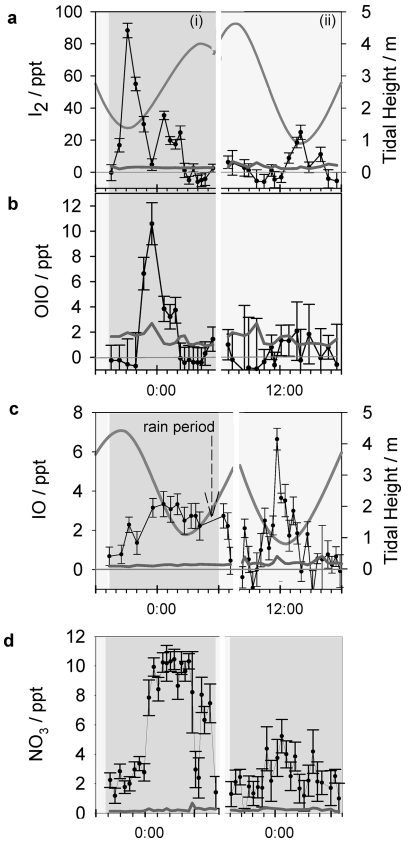

Figure 4. Daytime mixing ratio profiles of I_2, OIO, IO, and NO_3 observed at Mace Head, Ireland, during August 2002. Instrumental detection limit and tidal height are represented by thin black and thin broken lines, respectively. Diurnal and nocturnal measurements periods are plotted as white and gray backgrounds, respectively. Reprinted with permission from ref 18. Copyright 2004 American Geophysical Union.

lower than those of CH_3I over the open ocean but are similar or higher than CH_3I over biologically active regions.

2.3. Molecular Iodine

It was recently discovered that the dominant precursor of reactive iodine in coastal regions is not organic iodine as previously suggested[78] but I_2 emitted by intertidal kelp (see Figure 3).[13,18,19,63,90] Küpper et al.[62] have shown that when kelp are subjected to oxidative stress (e.g., by exposure to high irradiance, desiccation, and atmospheric O_3), high levels of iodide (I^-) are effluxed to the thallus surface and detoxify both aqueous oxidants and ozone, the latter resulting in significant release of I_2 at low tide, as also demonstrated by Ball et al.[91] However, a recent study shows that remarkable amounts of I_2 are released by *Laminaria digitata* even under presumed low-stress conditions.[92] Iodocarbons are also emitted at increased rates after an oxidative burst but at rates amounting to <0.1% of the inorganic iodide efflux.[62]

The findings of high I_2 in coastal regions have led to a resurgence of interest in the historical idea that the open ocean is also a source of I_2.[93−95] Early experiments using UV lamps implied that I_2 could be formed photochemically in the surface ocean via the reaction

$$4I^- + O_2 + 2H_2O + h\nu \rightarrow 2I_2 + 2OH^- \quad (4)$$

Miyake and Tsunogai[94] proposed that this reaction represents a significant source of iodine from the ocean surface to the atmosphere with a rate of 400 Gg (I) year^{-1}. However, Truesdale[96] found that reaction 4 was too slow in sunlight to contribute significant concentrations of I_2 in the oceans with a half-life of 29 months for I^- and suggested that the earlier results[94] were unrepresentative because of the use of UV lamps. Alternatively, Garland et al.[93] and Garland and Curtis[97] proposed that atmospheric O_3 deposited at the sea surface reacts with seawater iodide to evolve I_2 and that this mechanism (reactions 5 and 6) makes an appreciable contribution to the atmospheric iodine budget of 60−120 Gg (I) year^{-1}

$$H^+ + I^- + O_3 \rightarrow HOI + O_2 \quad (5)$$

$$H^+ + HOI + I^- \rightarrow I_2 + H_2O \quad (6)$$

From voltammetry measurements, Möller et al.[95] found the presence of ~10^{-9} mol dm^{-3} I_2 in some samples of surface coastal seawater, but as yet there are insufficient measurements of I_2 in seawater or in open ocean marine air to confirm whether proposed mechanisms for I_2 production operate efficiently in the marine environment. Rapid reactions of O_3 in the interfacial layer are likely to play a role in determining the fraction of iodine which escapes to the atmosphere. There is a suggestion however that such chemistry occurs on the surface of salt lakes, over which high levels (up to 10 pptv) of IO have been observed.[98] The uniquely high halide levels in this environment are conducive to heterogeneous inorganic (IX where X = I, Br, Cl) iodine release induced by liquid-phase ozone reactions or catalytic HOX interactions.[98]

Finally, HOI and I_2 (and HOBr and Br_2), which are in equilibrium in seawater at pH 8 ($HOI + I^- \rightarrow I_2 + OH^-$) with an HOI:$I_2$ ratio of ~500−5000, are a direct product of haloperoxidase activity in micro- and macroalgae. Hill and Manley[99] recently determined very high production rates of HOI and HOBr from polar marine diatoms (abundant under sea−ice), much greater than the previously measured organic halogen rates of release. In the marine environment, it is not yet clear how much, if any, of the reactive iodine species I_2 and/or HOI escape directly from the ocean surface to the atmosphere, but it has been proposed that they may find their way from the underside of sea−ice to the polar MBL via brine channels in the ice.[99,100]

2.4. Summary

It has now been shown that I_2 is the dominant source of reactive iodine in coastal regions,[18] although open ocean I_2 emission remains an open question. Globally, there are without doubt still large uncertainties regarding the total annual iodine input to the atmosphere and its constituent parts. However, recent field data suggests that earlier estimates of oceanic iodocarbon release (114−320 Gg (I) year^{-1} as CH_3I)[45,72] are an underestimate, and the contribution of reactive iodocarbons (particularly CH_2ICl and CH_2I_2) along with higher estimates of CH_3I release imply that the total oceanic input may be ~1 Tg (I) year^{-1} (equating to an average sea−air flux of 22 μmol (I) m^{-2} year^{-1} from organoiodine). This figure is rather higher than the depositional flux of I^- and IO_3^- in rainwater and marine aerosol into the Southern North Sea of 6.3−9.2 μmol (I) m^{-2} year^{-1},[101] although the latter figure does not include soluble organically bound iodine, which can make a significant or even major contribution to precipitation and marine aerosol iodine (see section 6.2).[102,103] If the suggested new chemical[57] and photochemical[56,58] mechanisms for production of reactive iodine from the ocean surface are confirmed to operate efficiently, the global sea−air flux estimate of iodine will become even larger.

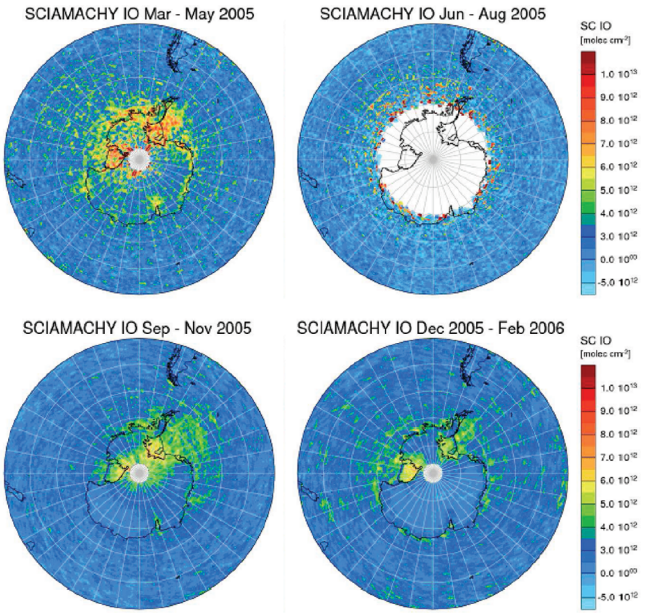

Figure 5. Seasonally averaged slant column densities of IO above Antarctica, explicitly for the periods of March−May, June−August, September−November 2005, and December 2005−February 2006. Maxima in IO columns occur over the Weddell Sea and the Ross Sea and along the coast especially in spring and in autumn. Reprinted with permission from ref 34. Copyright 2008 European Geosciences Union.

The contribution of different chemical and biological sources to gaseous iodine in the marine atmosphere is currently highly uncertain and requires further attention.

3. MEASUREMENTS OF GAS-PHASE REACTIVE IODINE SPECIES

3.1. Coastal Marine Boundary Layer

Measurements of reactive iodine species in the atmosphere have only been made during the past decade. IO was first detected at the coastal site of Mace Head (Ireland) by Alicke et al.[26] using the DOAS technique, and since then further observations reporting IO at levels of a few pptv in the lower troposphere at a variety of coastal locations have revealed the geographical spread of the radical.[18,27,35,104−109] In-situ techniques have also reported IO mixing ratios up to 54 pptv in coastal atmospheres[28,29] (see discussion below comparing in-situ vs integrated long-path measurements).

Observations of other reactive iodine compounds such as OIO, I_2, and I are not as common as for IO. For instance, OIO was first detected at Cape Grim (Tasmania) by Allan et al.;[110] since then observations of this radical have been reported in other coastal locations.[105−107] The first measurement of I_2 was made by Saiz-Lopez and Plane[18] at Mace Head (Figure 4) with mixing ratios up to 93 pptv. Subsequent studies also reported high I_2 levels at the same location.[106,112,19,116] Positive detection of I_2 has also been made at three other sites: Malibu (California),[32] Roscoff (France),[105] and very recently at Galicia (Spain).[111] Atmospheric atomic iodine detection was pioneered by Bale et al.[30] at Mace Head using the resonance fluorescence technique. Those workers reported ambient I atom levels up to 22 pptv during the day. More recently, concurrent observations of I and I_2 via resonance and off-resonance fluorescence have been reported by Mahajan et al.[111] at a coastal site in Galicia. Table 1 summarizes published measurements of IO, OIO, I_2, and I made around the world.

An example of observations of I_2, IO, and OIO at Mace Head is illustrated in Figure 4. I_2 mixing ratios peak at low tide with higher levels observed at night due to the rapid photolysis of the molecule during the day. The nighttime mixing ratios of OIO peaked at 10 pptv, whereas during the day OIO was not observed above the detection limit of the instrument, ~ 2 pptv, consistent with rapid photolysis of the molecule.[37] Note however that one study by Stutz et al.[107] has reported high daytime OIO levels (>20 pptv) in the Gulf of Maine. There have not yet been other reports of measurements of significant OIO concentrations during daytime. Figure 4 also shows nighttime IO mixing ratios up to 3 pptv alongside nitrate radical (NO_3) observations; see section 7.1.3 for the proposed mechanism for the nocturnal formation of IO.

Most of the atmospheric measurements of reactive iodine species in the MBL have been made using the technique of long-path DOAS,[18,26,27,35,98,104−107] which utilizes optical absorption path lengths of several kilometers over coastal locations. This technique is insensitive to inhomogeneities in the spatial distribution of iodine species over the integrated path length, which can be a problem given the localized nature of the biological coastal emissions of iodine precursors and their short atmospheric lifetimes. In fact, point measurements of I_2 by broadband CRDS,[64,112] ICP-MS,[113] and molecular fluorescence,[31] and CRDS and LIF observations of IO[28,29,114] have shown mixing ratios of both molecules that are typically an order of magnitude larger than those reported by the long-path DOAS indicating localized iodine production and chemical processing. For the Mace Head and Roscoff environments, modeling of intertidal I_2 emissions showed that the iodine species (I_2, IO, and OIO) observed by DOAS were concentrated over the intertidal region (typically representing a small portion of the light path) which agreed with in-situ measurements and therefore supported the so-called 'hot spot' hypothesis for iodine emissions in coastal locations.[9,21,90,113,115,116] A combination of long-path DOAS and in-situ techniques is necessary to understand the spatial heterogeneity in the distribution and chemical processing of iodine species in these coastal sites.

3.2. Remote, Open Ocean, and Tropical Marine Boundary Layer

Most MBL field observations of reactive iodine species have been performed in midlatitude coastal locations rich in macroalgae. Hence, a major question remains: how important is iodine chemistry in the open ocean MBL? Evidence comes from studies made off the north coast of Tenerife (Canary Islands),[27] and the Cape Verde Islands,[35,117] which are volcanic peaks with little surrounding coastal shelf, the Atlantic Ocean,[118,119] the Maldive Islands,[120] the Eastern Pacific upwelling region,[121] and the Western Pacific.[122,123] In Tenerife, substantial IO levels up to 3 pptv were observed and the radical concentration exhibited a simple diurnal solar dependence with no tidal correlation. Read et al.[35] reported mixing ratios ranging between 1 and 3 pptv at Cape Verde and indicated that the observed ozone depletion during the same campaign could not be explained in the absence of reactive iodine and bromine compounds. This study constitutes the first measurement of IO in the midocean MBL at a site where local biological sources (such as macroalgae exposed at low tide) were unimportant. Both studies indicate that there may indeed be reactive iodine activity over much of the open ocean.

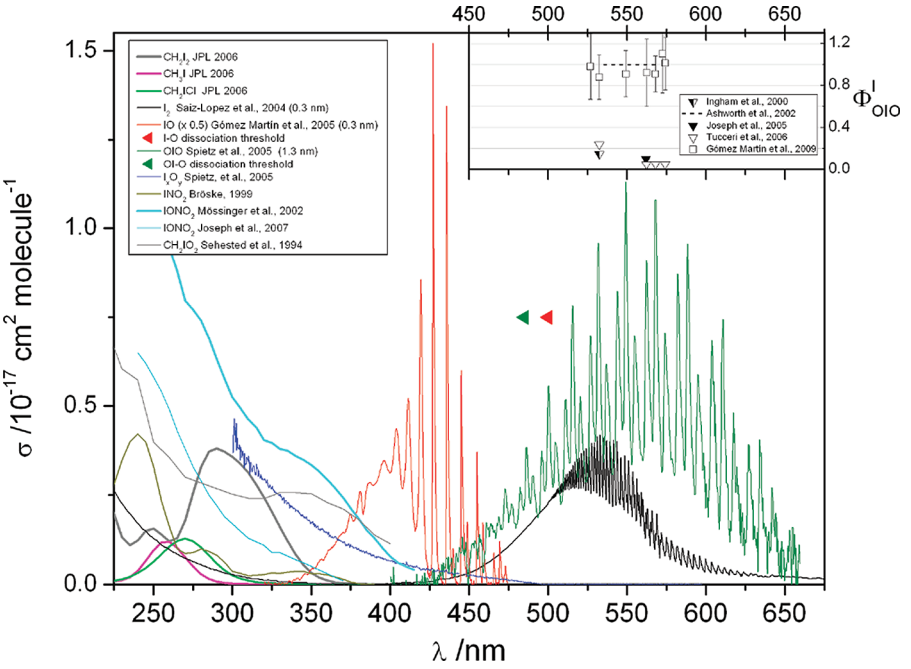

Figure 6. Absorption cross sections of major atmospheric precursors of active iodine (CH_2I_2, CH_3I, CH_2ICl, and I_2) and iodine oxides (IO, OIO, I_xO_y). For clarity, the IO cross sections have been divided by 2. The wavelength thresholds for breaking the I−O and OI−O bonds of IO and OIO, respectively, are shown as triangles of the same color of the corresponding spectra. The two available cross sections of $IONO_2$ (section 4.1.4) and the only available spectra of IONO[328] and CH_2IO_2 (section 4.2.1.1.3) are also shown. The panel on the upper right corner shows the values of the I atom quantum yield from OIO photolysis reported in the literature (section 4.1.2).

This hypothesis has gained momentum after the publication of satellite slant column measurements corresponding to the 2005−2009 period showing detectable levels of IO in the upwelling region of the southeastern Pacific, along the South American coast and around the Galapagos Archipelago.[34,124] More recent multiaxis DOAS (Max-DOAS) measurements from a ship-based campaign in 2008 also report the presence of IO in the Eastern Pacific, although suggesting lower levels than those detectable from satellite-borne instruments.[121] The influence of the El Niño/La Niña-Southern Oscillation (ENSO) on the biological activity in surface water may be an explanation for such variability, although quantitative IO measurements from satellite platforms over the ocean must still be treated with caution. This is because the ocean surface is a relatively poor reflector of sunlight, so that satellite observations over the ocean have to work with comparatively low signal to noise.[124]

Very recently, there has been some evidence that IO may also be present in the free troposphere at concentrations detectable by Max-DOAS instruments.[121,125]

3.3. Polar Boundary Layer

Frieß et al.[109] measured IO differential slant columns densities of up to 10^{14} molecules/cm^2 above coastal Antarctica (Neumayer station) and concluded from the diurnal variation that most IO would be located in the boundary layer with mixing ratios up to 10 pptv. They also observed a seasonal cycle with higher IO columns in summer. Strikingly, IO mixing ratios over 20 pptv have been observed in the coastal Antarctic boundary layer during springtime,[126] and satellite measurements[33,34] have now shown that IO can be detected over large areas in and around the continent (see Figure 5). Measurement of IO from space has been a major development in recent years, demonstrating that the radical is more widespread over the Antarctic coast and continent than previously realized. In this environment, IO exhibits similar seasonal cycles to those of bromine oxide (BrO) with a distinct maximum in spring followed by a decrease during summer and then a secondary maximum during autumn.[34,126] Recent MAX-DOAS measurements and snow pit sample analyses at the Antarctic Neumayer Station suggest extremely large mixing ratios of IO of up to 50 ppbv (parts per billion in volume, equivalent to nmol mol^{-1}) within the snowpack.[127] Such high IO mixing ratios are difficult to reconcile with the current understanding of the iodine chemistry, and they remain to be confirmed. In any case, the reported high levels of IO and the widespread spatial distribution unexpectedly makes Antarctica the most iodine active environment in the world. Yet, the sources of such a large iodine burden in the Antarctic atmosphere remain in debate.[100,128]

In the Arctic, by contrast, although filterable iodine has been measured on aerosols,[129] active gas-phase iodine chemistry seemingly occurs only on a very localized scale. Martinez et al.[130] used long-path DOAS and neutron activation to measure IO and total gaseous iodine at Ny-Ålesund, Spitzbergen, with IO detection limits of 2−4 pptv. Total gaseous iodine was typically 1−2 pptv, but a maximum of 8 pptv was measured during an event of high bromine loadings. IO was never measured above the detection limit, not even in the case with 8 pptv of total gaseous iodine. Hönninger[131] could detect IO only in one instance above the detection limit in Alert in spring 2000. The column density of about 2×10^{13} molecules cm^{-2} would correspond to a mixing ratio of about 0.7 pptv if IO were homogeneously distributed in a 1 km layer. However, Mahajan et al.[132] reported detection of up to 3.4 pptv of IO at Hudson Bay in the Canadian Arctic. The IO was very sporadic and appeared to coincide with emission of iodocarbons from open water 'polynyas' formed in the sea ice. This striking asymmetry in iodine activity between the Arctic and

Table 4. Updated Enthalpies of formation at 298 K of Selected Iodine-Containing Species

species	$\Delta_f H^\circ_{298}$ /kJ mol^{-1}	ref	source of data
IO	$122.3^{+0.8}_{-1.7}$	Dooley et al.[226]	velocity map imaging
OIO	118.5 ± 2.0	Gómez Martín and Plane[160]	photofragment excitation spectroscopy
IOIO	141.3 ± 9	Kaltsoyannis and Plane[39]	quantum chemistry calculations
	152.4 ± 4	Grant et al.[227]	
IOOI	179.9 ± 9	Kaltsoyannis and Plane[39]	quantum chemistry calculations
	177.9 ± 4	Grant et al.[227]	
OI(I)O	157.9 ± 9	Kaltsoyannis and Plane[39]	quantum chemistry calculations
	138.6 ± 4	Grant et al.[227]	
I_2O_3	64.0 ± 9	Kaltsoyannis and Plane[39]	quantum chemistry calculations
I_2O_4	111.3 ± 9	Kaltsoyannis and Plane[39]	quantum chemistry calculations
I_2O_5	33.0 ± 9	Kaltsoyannis and Plane[39]	quantum chemistry calculations
$IONO_2$	33.1 ± 9	Kaltsoyannis and Plane[39]	quantum chemistry calculations

the Antarctic remains an area of ongoing research. It should also be noted that the sporadic, localized appearance of IO in the Arctic is in stark contrast to the observations of regional scale 'clouds' of BrO triggered by the bromine explosion.[25]

3.4. Salt Lakes and Volcanoes

In summer 2001, Zingler and Platt[98] identified IO in addition to BrO in the Dead Sea basin. The IO mixing ratios were in the 0.5−6 pptv range with maxima of more than 10 pptv. They suggested that microbiological processes were not involved in formation of organic iodine compounds at this location. Instead, they proposed inorganic reaction cycles similar to those for bromine in polar regions, which released iodine from salt deposits. However, a study by Amachi et al.[87] identified iodide-oxidizing bacteria in natural gas brines and seawater that produce I_2, CH_2I_2, and CH_2ClI. This shows that, in principle, extremophile bacteria could also be involved in mechanisms of iodine release in the Dead Sea and other salt deposits. Smoydzin[133] attempted to reproduce the IO measurements with a one-dimensional model and concluded that the most likely source of iodine would be the surface water of the Dead Sea.

Aiuppa et al.[134] measured emissions of bromine and iodine from Mt. Etna passively with base-treated filters that capture only acidic species. They extrapolated their measurements, utilizing halide:SO_2 ratios, and estimated mean global source strengths of 13 (range 3−40) Gg (Br) year^{-1} and 0.11 (range 0.04−6.6) Gg (I) year^{-1}.

3.5. Stratospheric IO

A modeling study by Solomon et al.[5] showed that even relatively small amounts of iodine (compared with bromine and chlorine), which reached the stratosphere through deep convective cloud pumping in the tropics of species such as CH_3I, could contribute significantly to the O_3 depletions reported in the tropical lower stratosphere. However, only upper limits of 0.2 ppt for IO in the upper troposphere and stratosphere have been reported from ground-based measurements in Arizona (United States)[135] and balloon-borne instruments launched at mid- and high-latitude European locations[136−138] and in a low-latitude location in Brasil.[108] Measurements from balloon-borne UV−vis spectrometers are performed by solar occultation. These observations suggest that iodine plays a minor role in ozone loss in the upper troposphere and lower stratosphere. In contrast, one study[139] has reported mixing ratios up to 0.8 pptv of IO in the high-latitude winter stratosphere using the ground-based zenith-sky spectroscopy technique. To date, in-situ measurements of active iodine in the upper troposphere and lower strastosphere have not been reported.

4. LABORATORY AND THEORETICAL STUDIES OF ATMOSPHERIC IODINE CHEMISTRY

The 2003 special issue of *Chemical Reviews* discussed a substantial body of experimental data for gas-phase reactions of I and IO.[140] Heterogeneous processes involving iodine-containing species[141] as well as aqueous-phase and interfacial iodine chemistry[142] were also reviewed. More recent laboratory studies have focused on chemical sources of IO_x (= I + IO), reactions affecting the IO_x partitioning, the photochemistry of OIO and $IONO_2$, and heterogeneous mechanisms. New experimental and theoretical work on the thermochemistry of iodine species is also available. Current data evaluations include work on iodine chemistry up to 2005.[143,144] This section therefore focuses on results published since 2005 as well as on several controversial issues and remaining uncertainties. Note that following this criterium some relevant processes are not discussed in this review. Laboratory studies on IOP formation and growth are described in section 5.2.

4.1. Spectroscopy and Photochemical Reactions

4.1.1. Iodine Monoxide. New studies of the absolute absorption cross section of IO at 427.2 nm[145,146] have confirmed the determination by Harwood et al.[147] Some effort has been directed to understanding the IO spectrum and the observed underlying continuum,[148,149] and wavelength-dependent absorption cross sections have been measured at appropriate resolution for atmospheric spectroscopy and for computing photodissociation rate coefficients (see Figure 6).[146] Harwood et al. reported a temperature-independent cross section for the IO($A^2\Pi_{3/2}$ − $X^2\Pi_{3/2}$, 4−0) band, while Bloss et al.[150] observed a significant negative temperature dependence. Laboratory data and spectral simulations show that the IO ro-vibrational bands are higher and narrower at low temperatures (253 K) due to depopulation of high rotational levels.[151]

The photodissociation coefficients (J) reported by Bloss et al.[150] and Gómez Martín et al.[146] are in excellent agreement (J = 0.14 s^{-1} for midday during summer solstice at 40°N). Laszlo et al.[152] and Harwood et al.[147] estimated higher J values, most likely because the broad underlying absorptions of other species were not subtracted from their measured IO spectra.

dx.doi.org/10.1021/cr200029u |*Chem. Rev.* 2012, 112, 1773–1804

4.1.2. Iodine Dioxide. The absolute absorption cross sections of OIO in its visible band system (480−630 nm) are now well established.[146,149,150,153,154] The photolysis pathways of OIO

$$OIO + h\nu \rightarrow I(2P_J) + O_2 \quad (7a)$$

$$\rightarrow O(^3P) + IO \quad (7b)$$

have been a matter of debate since the late 1990s[155] due to (a) the potentially important impact on the O_3-depleting potential of iodine, (b) rapid photolysis being an explanation for the low levels of OIO observed during daytime,[113,156] and (c) the potential role of OIO in new particle formation (see section 5). The I-atom quantum yield from channel 7a ($\phi(I)$) has been controversial for many years (see inset in Figure 6). The first study by Ingham et al.[157] concluded that OIO is probably stable with respect to photolysis in the 480−660 nm band as their results suggested that the I atom would only be formed in a sequential two-photon process. However, high-resolution spectroscopy of OIO revealed the absence of rotational structure which, combined with the absence of fluorescence, provided evidence for a very short-lived excited state (~200 fs) and indicated photolysis of OIO via eq 7a.[158] However, subsequent studies reported upper limits of $\phi(I) < 0.1$ at 567.9 nm and $\phi(I) < 0.05$ at 560−580 nm.[153,154] However, very recently, Gómez Martín et al.[37] determined that $\phi(I) = 1.07 \pm 0.15$ between 500 and 650 nm, in an experiment which utilized simultaneous measurements of OIO by CRDS and atomic I by RF. A new theoretical study employing multireference configuration interaction calculations supports this observation.[159] An OIO photolysis quantum yield of unity results in an atmospheric photolysis rate of $J(OIO) = 0.4\ s^{-1}$ at noon during summer solstice at 40° N.

This result is also in accord with the observation that the yield of atomic O from channel 7b is negligible when OIO is photolyzed at 532 nm.[157] Recently, a threshold for the appearance of IO from photolysis of OIO at ~480 nm has been reported,[160] in agreement with new quantum calculations of the O−IO bond energy.[39,159] Although production of IO via channel 7b is not atmospherically relevant, this observation allowed the first experimental determination of $\Delta H_f(OIO)$ (Table 4).[160]

4.1.3. Higher Iodine Oxides. The higher oxides I_2O_x ($x = 2$, 3, or 4) should form from recombination of IO with itself ($x = 2$), IO and OIO ($x = 3$), or OIO with itself ($x = 4$); all these reactions are exothermic, and I_2O_3 should be particularly stable at typical MBL temperatures.[39] Bloss et al.[150] and Gómez Martín et al.[146] reported a featureless absorption, increasing monotonically from 460 nm to shorter wavelengths (Figure 6), in flash photolysis experiments where IO and OIO were also observed. The growth kinetics were found to be roughly consistent with a product of the IO self-reaction (I_2O_2, identified as the asymmetric dimer IOIO by Gómez Martín et al.[146]) or a superposition of I_2O_2 and I_2O_3. The I_2O_2 absorption cross section was estimated to be $\sim 2 \times 10^{-18}$ cm^2 molecule^{-1} at 340 nm. The estimated photolysis rate at noon during summer solstice at 40°N is $J(I_2O_2) \approx 0.03\ s^{-1}$.[146] Further information on the higher iodine oxides in the gas phase, beyond qualitative observations,[147,161−163] is not available (the bulk properties of iodine oxides are discussed in section 5.2.1). New studies aimed at clarifying the photochemistry of I_xO_y must address the problem of the unambiguous assignment of the different species.

4.1.4. Photolysis of $IONO_2$. Iodine nitrate ($IONO_2$) forms from recombination of IO and NO_2 (reaction 8) and is likely to be the major gas-phase iodine species in semipolluted atmospheres, i.e., $NO_2 > 1$ ppbv.[105] Photolysis of $IONO_2$ then becomes important as a route for recycling this reservoir species to IO_x

$$IO + NO_2(+M) \rightarrow IONO_2 \quad (8)$$

$$IONO_2 + h\nu \rightarrow IO + NO_2 \quad (9a)$$

$$\rightarrow I + NO_3 \quad (9b)$$

$$\rightarrow I + NO_3 \quad (9c)$$

$$I + O_3 \rightarrow IO + O_2 \quad (10)$$

O_3 depletion will only be significant if channel 9b is significant. However, the NO_3 fragment formed will photolyze to $NO_2 + O$ with a branching ratio of 0.9.[164] The resulting atomic oxygen will recombine with O_2 to form O_3, which thus reduces the overall O_3-depleting efficiency of channel 9b.

Two recent high-level quantum chemistry calculations have reported new heats of formation for $IONO_2$ which are in good agreement: $\Delta H_f^{298K} = 32.5$[39] and 36.5 kJ mol^{-1}.[165] Adopting the first of these values, the threshold for channel 9a is then 118 kJ mol^{-1} and that for channel 9b is 131 kJ mol^{-1}, so both channels could potentially be open to photolysis throughout the visible region of the spectrum. Although channel 9c is in principle accessible (threshold = 167 kJ mol^{-1}), this channel involves significant internal rearrangement and should have a large barrier.[40] A recent experimental study of $IONO_2$ photochemistry,[41] where the photolysis quantum yields for IO and NO_3 production at 248 nm were measured using LIF of IO at 445 nm and CRDS of NO_3 at 662 nm, showed that the yields were $\phi(IO) \leq 0.02$ and $\phi(NO_3) = 0.21 \pm 0.09$. However, quantum chemistry calculations[41] show that photolysis to $I + NO_3$ is likely to be the only significant channel, and the low $\phi(NO_3)$ is explained by production of 'hot' NO_3, most of which dissociates to $NO_2 + O$.

There have been two fairly recent measurements of the absolute absorption cross section of $IONO_2$ (Figure 6).[41,166] Because $IONO_2$ is rather unstable and cannot be stored and purified (cf. $ClONO_2$), the molecule was made in both studies by laser flash photolysis of N_2O at 193 nm, followed by reaction of the resulting O atoms with CF_3I to make IO, which then recombined in an excess of NO_2 (reaction 8). Time-resolved UV−vis spectroscopy was used to measure the absorption spectrum from 240 to 370 nm[41] or 245 to 415 nm.[166] In both studies, the $IONO_2$ spectrum was determined by fitting and subtracting reference spectra for CF_3I and NO_2 in these wavelength ranges. Unfortunately, there is poor agreement: the absorption cross sections from the earlier study by Mössinger et al.[166] are significantly larger than those of Joseph et al.[41] by a factor of 1.7 at 245 nm increasing to 6.9 at 350 nm. The reasons for this disagreement are unclear. One point in favor of the Joseph et al. absorption cross section is that it is red shifted by ~1.2 eV from the spectrum of $BrONO_2$,[167] which is close to the prediction from quantum chemistry calculations,[41] compared with a red shift of ~2.1 eV required to overlap with the spectrum of Mössinger et al.[166] It is important that this issue is resolved because the two cross sections yield photolysis frequencies which differ by more than an order magnitude from $J(IONO_2) = (3.0 \pm 2.1) \times 10^{-3}\ s^{-1}$[41] to $4.0 \times 10^{-2}\ s^{-1}$.[166]

4.2. Kinetics and Chemical Mechanisms

4.2.1. Gas-Phase Reactions. *4.2.1.1. IO_x Sources.* The main fate of I_2 and small iodoalkanes during daytime is photodissociation.

dx.doi.org/10.1021/cr200029u |*Chem. Rev.* 2012, 112, 1773–1804

In the particular case of di-iodomethane (CH_2I_2), rapid release of the second I atom depends on the products of the reaction $CH_2I + O_2$.[36] I atoms react with O_3 to produce IO. A steady state between I and IO is reached rapidly as a result of the photolysis of IO (see section 4.1.1), and therefore, they can be collectively termed *active iodine* (IO_x). Additional chemical paths to IO_x are the reactions of iodoalkanes with Cl[168−170] and OH.[170,171] Reaction of I_2 with NO_3[162] has been invoked as a nighttime source of IO_x, which could explain the observation of high mixing ratios of IO and OIO in the nighttime coastal MBL.[18] Potential paths to IO_x from reactions of CH_3I and CH_2I_2 with NO_3 have been suggested as well.[172,173]

4.2.1.1.1. Iodoalkanes + Cl. The importance of chemical removal of iodoalkanes increases with increasing chain length.[168] The RCH_2I + Cl reactions are known to involve a complex mechanism.[174] A number of recent studies have reported the spectroscopic detection and analysis of some of these RCH_2I−Cl adducts (R = H, CH_3, Cl, Br, I) using CRDS,[175−177] LIF,[178] and UV−vis absorption spectroscopy.[179] According to these studies, adduct formation tends to dominate for the short chain iodoalkanes and is usually reversible under atmospheric conditions. In addition, these adducts do not undergo significant reaction with O_2, with upper limits of 2.5×10^{-17} cm^3 molecule^{-1} s^{-1} for R = H, CH_3 at 250 K and 1×10^{-16} cm^3 molecule^{-1} s^{-1} for R = H, I at 296 K.[179] Therefore, RCH_2I−Cl adducts are unlikely to play any atmospheric role.

Loss of the iodopropanes by reaction with OH may be as important as by photolysis,[170,171,180] but their reactions with atomic Cl only start to be significant for [Cl] ≥ 10^5 atoms cm^{-3}.[180] Ultimately, degradation of iodoalkanes by chemical pathways in the presence of O_2 leads to release of IO_x.[169,180,181]

4.2.1.1.2. I_2 and Iodoalkanes + NO_3. There is only one channel accessible for reaction 11 at room temperature, yielding atomic I and $IONO_2$. According to the recently published enthalpy of formation of $IONO_2$ (see section 4.1.4),[39] reaction 11 is essentially thermoneutral

$$I_2 + NO_3 \rightarrow I + IONO_2 \quad (11)$$

There is a single determination of the rate coefficient for reaction 11 by Chambers et al.,[162] who obtained $k_{11} = (1.5 \pm 0.5) \times 10^{-12}$ cm^3 molecule^{-1} s^{-1}, independent of temperature between 292 and 423 K. Kaltsoyannis and Plane[39] estimated a rate coefficient for the reverse reaction, $k_{-11} \approx (5.5-9.4) \times 10^{-11}$ cm^3 molecule^{-1} s^{-1}, using quantum chemistry calculations on $IONO_2$ to estimate the equilibrium constant and applying detailed balance. Chambers et al. also reported a determination of the rate coefficient for I + NO_3, which was 4 times larger than the most recent determination by Dillon et al.[36] (see section 4.2.1.2.3). Measurement of k_{11} presented fewer complications than measurement of k(I + NO_3). Nevertheless, in view of this disagreement and considering the key role played by reaction 11 in nighttime iodine chemistry and the potential importance of the reverse reaction in semipolluted environments,[105] new experimental studies on these reactions would be very desirable.

It has been proposed that the reaction between CH_3I and NO_3 could occur via the bimolecular channel

$$CH_3I + NO_3 \rightarrow CH_2I + HNO_3 \quad (12)$$

and $k_{12} \approx 1 \times 10^{-17}$ cm^3 molecule^{-1} s^{-1} was measured initially.[182] More recently, Nakano et al.[183] reported a rate coefficient for this close to the thermoneutral reaction of $k_{12} = (4.1 \pm 0.2) \times 10^{-13}$ cm^3 molecule^{-1} s^{-1}, based on analysis of the decays of NO_3 measured by CRDS in the presence of excess CH_3I. However, Dillon et al.[36] suggested that, in view of the large rate coefficient for the I + NO_3 reaction,[36,162] reaction with I atoms generated from photolysis of the precursor could account for most of the observed NO_3 loss.

Nakano el al.[173] also studied the reaction

$$CH_2I_2 + NO_3 \rightarrow \text{products} \quad (13)$$

by analyzing the NO_3 decays measured by CRDS in the presence of excess CH_2I_2. They obtained a rate coefficient very close to the value of k_{12} reported by the same group. The same criticism for the previous reaction can be invoked here.[36]

4.2.1.1.3. Reaction of CH_2I Radical with O_2. The mechanism, rate coefficient, and product branching ratios of this reaction have been the subject of intensive research in the past few years.[36,148,177,184−187] Data published recently suggested that it could have bimolecular channels producing both I and IO[184−186] alongside an association channel

$$CH_2I + O_2 \rightarrow HCHOO + I \quad (14a)$$

$$\rightarrow HCHO + IO \quad (14b)$$

$$(+M) \rightarrow CH_2IO_2 \quad (14c)$$

Masaki et al.[188] and Eskola et al.[185] found that reactions 14a−14c are pressure independent up to ∼50 Torr at room temperature, indicating that only the bimolecular channels 14a and 14b are active. The rate coefficients at 298 K reported in these two studies, obtained from the observed decay of CH_2I, are in good agreement: $k_{14} = (1.6 \pm 0.2) \times 10^{-12}$ cm^3 molecule^{-1} s^{-1}[1188] and $k_{14} = (1.37 \pm 0.32) \times 10^{-12}$ cm^3 molecule^{-1} s^{-1}.[185] According to Eskola et al., the rate coefficient shows a negative temperature dependence in the 220−450 K range. Enami et al. performed two studies of this reaction by monitoring the growth of IO by time-resolved CRDS. In the first study,[184] CH_2I was generated from photolysis of CH_2I_2, and $k_{14} = (4.0 \pm 0.4) \times 10^{-12}$ cm^3 molecule^{-1} s^{-1} was determined. In the second study,[177] CH_2I was generated from H-atom abstraction by Cl, and $k_{14} = (1.28 \pm 0.22) \times 10^{-12}$ cm^3 molecule^{-1} s^{-1} was found. The authors attributed the higher value of their first study to the large amount of I atoms generated from the 266 nm photolysis of CH_2I_2, which would subsequently react with CH_2IO_2 to form IO.

Sehested et al.[187] found that the adduct CH_2IO_2 would be the major product under atmospheric conditions, based on the observation of a nascent broadband absorption (see Figure 6). Enami et al.[184] claimed an IO yield of unity from this reaction, while Eskola et al.[185] observed an I-atom yield that was close to unity, with a minor channel generating IO. In the latter work, formation of I and IO were observed on the same time scale as the loss of CH_2I. Stefanopoulos et al.[186] observed HCHO and HCOOH at P < 3 mTorr (∼0.4 Pa) using two independent detection techniques, suggesting production of both I and IO. However, there is only tentative evidence that these species are the *final* products of the CH_2I oxidation by O_2. Dillon et al.[36] and Gravestock[148] found, using photolysis of CH_2I_2 in the presence of O_2, that IO is most likely not a direct product of reactions 14a−14c but originates from secondary chemistry. Dillon et al.[36] determined an upper limit of 0.1 for the yield of IO based on a cross calibration of the IO LIF signal with the IO yield from the O + CH_2I_2 reaction. Gravestock[148] presented evidence for a

close to unity yield of the association channel, but the absence of both HCOOH and CH_2IO_2 signals in their mass spectra precluded a quantitative statement. Finally, the new study by Enami et al.[177] reports pressure- and temperature-dependent yields of IO, possibly reflecting formation of CH_2IO_2, with a value of 0.17 ± 0.12 at 298 K and 760 Torr. In summary, there seems to be some convergence that the IO yield from reactions 14a−14c is small.

4.2.1.2. IO_x and OIO Sinks. 4.2.1.2.1. Formation of Iodine Oxides. The highly exothermic reaction between IO and O_3 has been discounted as an efficient atmospheric source of OIO: Dillon et al.[189] confirmed a low upper limit for this rate coefficient ($<5 \times 10^{-16}$ cm^3 molecule^{-1} s^{-1}), consistent with the one previously reported.[190] The major atmospheric sources of OIO are the reaction IO + BrO and the IO self-reaction

$$\mathrm{IO} + \mathrm{IO} \rightarrow \mathrm{I} + \mathrm{OIO} \quad (15a)$$

$$\rightarrow \mathrm{IOIO} \quad (15b)$$

$$\rightarrow \text{other products} \quad (15c)$$

The recommended value at 298 K of $k_{15} = 9.9 \times 10^{-11}$ cm^3 molecule^{-1} s^{-1} [143] is based on the good agreement of several studies.[147,150,152,157] Gómez Martín et al.[191] pointed out that the IO + OIO recombination reaction could be effectively included in a second-order decay analysis of IO, causing a ∼20% overestimation. The branching of the IO self-reaction as a function of pressure in the range 10−400 Torr has been reported.[191] Extrapolation to atmospheric conditions agrees well with a previous determination by Bloss et al.[150] and with the pressure dependence of the channel-specific rate coefficient in the presence of O_3.[147,192] The dominant channels at atmospheric pressure are the channel forming the IO dimer (∼50%) and the OIO forming channel (∼40%). Theoretical calculations and experimental data indicate that the lifetime of IOIO against dissociation to I + OIO should be only around 1 s under atmospheric conditions at 290 K.[39,160]

Regarding the fate of OIO (other than photolysis, see section 4.1.2), Gómez Martín et al.[191] proposed the reactions

$$\mathrm{IO} + \mathrm{OIO} + \mathrm{M} \rightarrow \mathrm{I_2O_3} + \mathrm{M} \quad (16)$$

$$\mathrm{OIO} + \mathrm{OIO} + \mathrm{M} \rightarrow \mathrm{I_2O_4} + \mathrm{M} \quad (17)$$

to explain rapid removal of OIO in the presence of excess O_3. Recent theoretical work on I_2O_3[39] has shown that this molecule is extremely stable ($\Delta H(16) = -166$ kJ mol^{-1} at 0 K). New laboratory work is needed in order to unambiguously establish the OIO loss mechanism by observing the higher iodine oxides evolving from the gas phase and contributing to nucleation of IOPs (see section 5).

4.2.1.2.2. HO_x Reactions. The reaction between OIO and OH could have several channels

$$\mathrm{OIO} + \mathrm{OH}(+\mathrm{M}) \rightarrow \mathrm{HOIO_2} \quad \Delta H_0 = -204 \text{ kJmol}^{-1} \quad (18a)$$

$$\rightarrow \mathrm{IO} + \mathrm{HO_2} \quad \Delta H_0 = -25 \text{ kJmol}^{-1} \quad (18b)$$

$$\rightarrow \mathrm{HOI} + \mathrm{O_2} \quad \Delta H_0 = -222 \text{ kJmol}^{-1} \quad (18c)$$

where the reaction enthalpy changes are derived from quantum chemistry calculations.[40] The recombination pathway (eq 18a) involves simple attachment of the oxygen atom of OH to the iodine atom of OIO to yield the most stable isomer of $HOIO_2$, whereas theoretical studies of the IO + HO_2 and HOI + O_2 potential surfaces show that these contain significant energy barriers.[40,193] Application of Rice−Ramsperger−Kassel−Marcus (RRKM) theory shows that recombination should proceed at the high-pressure limit at atmospheric pressure, governed by the dipole−dipole capture rate between OIO and OH.[40] Reaction 18a is particularly interesting because the iodine atom is oxidized to the +5 oxidation state, so that uptake of gas-phase $HOIO_2$ on sea−salt aerosol should provide a route to the iodate ion, which is often the major form of iodine in marine aerosols (see section 6).[101] However, the recent experimental demonstration[37] that OIO photolyses to I + O_2 with $J \approx 0.4$ s^{-1} means that reaction with OH would be uncompetitive.

4.2.1.2.3. NO_x Reactions. NO Reactions. The reaction between OIO and NO could proceed via four channels

$$\mathrm{OIO} + \mathrm{NO} \rightarrow \mathrm{IO} + \mathrm{NO_2} \quad \Delta H_0 = -70 \text{ kJmol}^{-1} \quad (19a)$$

$$(+\mathrm{M}) \rightarrow \mathrm{IONO_2} \quad \Delta H_0 = -166 \text{ kJmol}^{-1} \quad (19b)$$

$$\rightarrow \mathrm{I} + \mathrm{NO_3} \quad \Delta H_0 = -50 \text{ kJmol}^{-1} \quad (19c)$$

$$\rightarrow \mathrm{INO} + \mathrm{O_2} \quad \Delta H_0 = -104 \text{ kJmol}^{-1} \quad (19d)$$

where the reaction enthalpy changes are determined from quantum calculations.[40] Calculations of the potential energy surface show that although recombination to produce $IONO_2$ is the most exothermic channel, this pathway 19b involves significant rearrangement. In fact, reactions 19a−19d are only likely to proceed via channel 19a. The rate coefficient has been measured by time-resolved CRDS of OIO[40,194] and found to have a small negative temperature dependence and be significantly faster than the analogous reactions of OClO and OBrO. No pressure dependence between 10 and 100 Torr has been observed. Reaction 19a leads to a null O_3-depleting cycle when the OIO has come from the IO self-reaction (reaction 15a) because the NO_2 produced will photolyze to generate O and hence O_3, thereby canceling out the O_3 removed by the I atom produced in reaction 15a. However, the rate coefficient $k_{19}(300\text{ K}) = (6.0 \pm 1.1) \times 10^{-12}$ cm^3 molecule^{-1} s^{-1} implies that during daytime the reaction will only compete with photolysis of OIO (which is O_3 depleting; see above) if NO > 2 ppbv, i.e., in a semipolluted environment.

NO_2 Reactions. In polluted environments, the second most important loss of iodine atoms after reaction 10 is[195]

$$\mathrm{I} + \mathrm{NO_2} + \mathrm{M} \rightarrow \mathrm{INO_2} + \mathrm{M} \quad \Delta H_0 = -59.5 \text{ kJmol}^{-1} \quad (20a)$$

$$\rightarrow \mathrm{IONO} + \mathrm{M} \quad \Delta H_0 = -44.8 \text{ kJmol}^{-1} \quad (20b)$$

Tucceri et al.[196] measured pressure dependence rate coefficients for reaction 20a in He and N_2 bath gases, which were then combined with previous data sets[197−199] to derive new falloff expressions. The prevailing association channel is expected to depend strongly on the external conditions.[195]

dx.doi.org/10.1021/cr200029u |*Chem. Rev.* 2012, 112, 1773–1804

The most recent study[200] of the recombination reaction between IO and NO_2 reports measurements of k_8(IO + NO_2 + M) over a wide range of temperatures (223−294 K) and pressures (18−760 Torr). The results are in good agreement with previous determinations by Allan and Plane[201] and Daykin and Wine[202] using N_2 as the bath gas but 25% larger than that determination by Hölscher and Zellner[203] with air as a third body. In fact, Dillon et al. found that there were no significant differences in the rate coefficient in air, O_2, or N_2. The RRKM fit over a large range of temperature (216−474 K) and pressure (20−760 Torr) reported by Allan and Plane[201] fits well the low-pressure data reported by Maguin et al.[204] However, Golden[205] pointed out that the Lennard−Jones parameters describing the collision frequency between the third body (N_2) and the energized IO−NO_2 complex in the RRKM fit were too large. This problem has now been resolved[39] with the new IO−NO_2 bond energy, D_0 = 118 kJ mol^{-1}, which is 22 kJ mol^{-1} larger than the earlier theoretical estimate of 95 ± 10 kJ mol^{-1} used by Allan and Plane[201] and in reasonably good agreement with D_0 = 114 ± 3 kJ mol^{-1} calculated by Marshall.[165]

The revised RRKM fit can now be used to obtain a revised expression for the thermal dissociation of $IONO_2$ in 760 Torr N_2: $k_{-8}(240-300\ K) = 2.1 \times 10^{15} \exp(-13\,670/T)\ s^{-1}$. The lifetime of $IONO_2$ against thermal dissociation is then 39 h at 290 K (a typical temperature of the midlatitude MBL). Marshall's own RRKM calculations yield a faster decomposition rate which converts to a lifetime of 6 h, although the quoted uncertainty is a factor of 3.5, reflecting a high sensitivity to the D_0 value.[165] According to Kaltsoyannis and Plane,[39] even with the theoretical lower limit of D_0(IO−NO_2) ≥ 110 kJ mol^{-1}, then the lower limit to the lifetime of 2.2 h is significantly longer than the photolysis lifetime at midday of ∼300 s (see section 4.1.4). However, Marshall's results seem to suggest that thermal decomposition could compete with aerosol uptake during nighttime.[39]

NO_3 Reactions. Reaction between I and NO_3 may compete with O_3 removal of I atoms in polluted or semipolluted environments during nighttime. Dillon et al.[36] studied reactions of I and IO with NO_3 using a pulsed laser photolysis-LIF technique where IO radicals produced from these reactions were monitored in situ. They found the rate coefficient of the reaction I + NO_3 to be $k_{21} = (1.0 \pm 0.3) \times 10^{-10}$ cm^3 $molecule^{-1}$ s^{-1}, i.e., smaller by a factor of ∼4 than the only previous determination[162] but still close to the gas kinetic collision rate at all pressures (25−90 Torr), indicating the dominant bimolecular reaction

$$I + NO_3 \rightarrow IO + NO_2 \quad (21)$$

Chambers et al.[162] used a discharge−flow technique and monitored decay of I atoms. Curvature of the bimolecular plot was observed and attributed to wall losses related to formation of iodine oxides. In contrast, reasonably linear bimolecular plots were observed by Dillon et al.[36] Cross-calibration experiments using O + CF_3I as a source of IO allowed Dillon et al. to determine the IO yield of reaction 21, which was found to be close to unity.

Reaction between IO and NO_3 has been invoked to explain the anomalous [IO]/[OIO] nighttime ratios observed recently in a semipolluted environment.[105] It has three exothermic bimolecular channels and a possible association channel

$$IO + NO_3 \rightarrow OIO + NO_2 \quad (22a)$$

$$\rightarrow IOO + NO_2 \rightarrow I + O_2 + NO_2 \quad (22b)$$

$$\rightarrow INO_2 + O_2 \quad (22c)$$

$$(+M) \rightarrow IOONO_2 \quad (22d)$$

A rate coefficient for the non-I-atom-forming channels has been measured by Dillon et al.,[36] who followed the IO decay in the presence of excess NO_3 (any I atoms formed via this reaction would be converted immediately to IO by reaction with excess NO_3, see above). The channel-specific rate coefficient was found to be pressure independent between 25 and 70 Torr N_2, having a value of $k_{22a} = (9 \pm 4) \times 10^{-12}$ cm^3 $molecule^{-1}$ s^{-1}. If, by analogy with IO + NO_2, the association channel is assumed to be close to its low-pressure limit, the lack of pressure dependence may indicate that this channel is not significant. Formation of INO_2 seems to be mechanistically unlikely. Thus, Dillon et al. proposed that the OIO-forming channel 22a is responsible for removal of IO observed.

4.2.1.2.4. Reactions of IO_x with Organics. Nakano et al.[183] reported a rate coefficient for reaction of IO and dimethyl sulfide (DMS)

$$IO + DMS \rightarrow I + DMSO \quad (23a)$$

$$(+M) \rightarrow IO{-}DMS \rightarrow I + DMSO \quad (23b)$$

of $k_{23} = (2.5 \pm 0.2) \times 10^{-13}$ cm^3 $molecule^{-1}$ s^{-1} at 298 K and 100 Torr, which was an order of magnitude larger than the previously recommended value.[206−208] This motivated two subsequent studies by Gravestock et al.[38] and Dillon et al.,[209] which confirmed the earlier much lower rate coefficient. There is now sufficient evidence that this reaction is characterized by a pressure-independent rate coefficient of $k_{23} < 3 \times 10^{-14}$ cm^3 $molecule^{-1}$ s^{-1} at 298 K. The I-atom yield from this reaction has been found to be close to 1 by Dillon et al.

Reactions 24a−24c could potentially contribute to O_3 loss or provide an additional source of OIO[210]

$$IO + CH_3O_2 \rightarrow I + O_2 + CH_3O \quad (24a)$$

$$\rightarrow OIO + CH_3O \quad (24b)$$

$$\rightarrow \text{products} \quad (24c)$$

Dillon et al.[189] reported k_{24}(30−318 Torr) = (2 ± 1) × 10^{-12} cm^3 $molecule^{-1}$ s^{-1}, 30 times smaller than Bale et al.[211] and Enami et al.[212] However, determinations of $k(CF_3O_2 + IO)$ reported in these three papers are in good agreement, suggesting that the disagreement about k_{24} lies in chemical interference from CH_3O or HO_2, which could remove IO efficiently.[189] Bale et al. observed a high yield of I atoms (k_{24a}/k_{24} = 0.4−1.0), and Enami et al. determined an upper limit of <0.1 for the yield of OIO (eq 24b), while the observed temperature dependence was invoked to discount a major CH_3IO producing channel, thus suggesting that channel 24a is dominant. In that case, it could have some impact on O_3 depletion if the reported higher values of k_{24}[211,212] are correct. A new experimental study using an independent technique would be valuable to clarify this.

dx.doi.org/10.1021/cr200029u |*Chem. Rev.* 2012, 112, 1773–1804

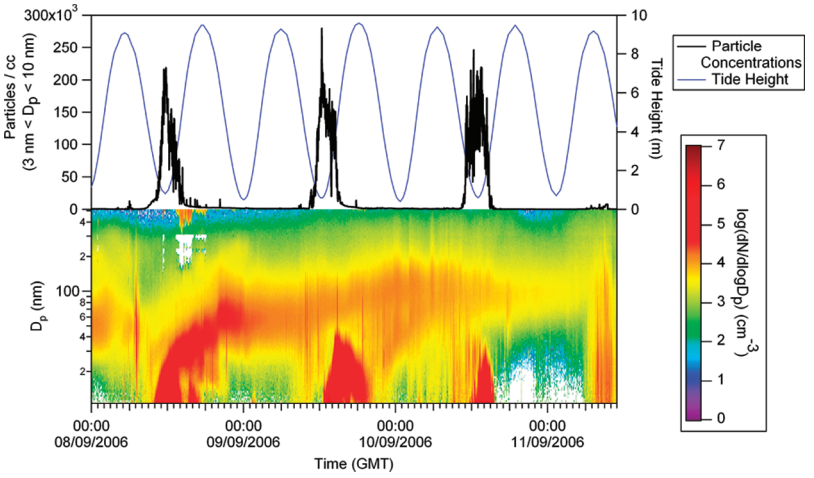

Figure 7. Particle number concentrations and size distribution evolution during the RHaMBLe Roscoff field project.

4.2.2. Heterogeneous Reactions. Rossi's 2003 review[141] on atmospherically relevant heterogeneous chemistry discussed a comparatively small body of laboratory work on the uptake of HOI and ICl on solid (dry or frozen) halide surfaces. Since then, Braban et al.[213] extended the study of HOI, ICl, and IBr uptake on aqueous salt surfaces. They have shown that uptake of HOI on aqueous halide salt films at 274 K leads to activation of bromine and chlorine by release of IBr and ICl into the gas phase. This work confirmed previous studies[214,215] showing that the presence of bromine in the sea−salt substrate switches chlorine activation into bromine activation, rendering HOI-driven chlorine activation from sea−salt aerosol much less important. Uptake of ICl and HOI on bromine-containing substrates gave the same IBr yield. ICl was used as a proxy for HOI in uptake experiments on NaBr aerosols, where a large yield of IBr per ICl molecule taken up was observed.

Iodine-mediated chlorine and bromine activation mechanisms have also recently been studied by Enami et al.,[216] who found that I^- catalyzes oxidation of Br^- and Cl^- in aqueous nanodroplets exposed to ozone (essentially as a result of formation of HOI). An analogous mechanism has been proposed for iodine self-activation: Sakamoto et al.[217] reported production of gas-phase I_2 from the heterogeneous reaction of O_3 on the surface of iodide-containing solutions, which confirms previous work.[97] In addition, Sakamoto et al. reported for the first time direct formation of gaseous IO from the heterogeneous reaction of I^- and O_3. It has also been shown very recently[218] that this heterogeneous reaction is hindered in the presence of typical phenols with $pK_a \approx 10$ due to the fast reaction of phenolates with O_3.

Martino et al.[57] have shown that the interaction of dissolved iodide, dissolved organic matter, and ozone can lead to the sea−surface production of CH_2I_2, $CHClI_2$, and CHI_3; this is a significant finding since it provides a ubiquitous source of iodine to the marine atmosphere (see section 2.2). Recently, Wren et al.[219] have shown that halide ions that have been excluded to the ice surface of frozen salt solutions react heterogeneously with ozone to produce molecular halogens, suggesting that a surface reaction between gas-phase ozone and frozen iodide could be responsible for the presence of IO in the polar boundary layer.

4.2.3. Aqueous and Interface Phase Reactions and Photochemistry. Recently, a series of studies on the speciation of iodine in rain, snow, and aerosol have been published that challenge the role of iodine in aerosol formation and its processing in the aqueous phase[102,103,220] (see also section 6.2). It was found that soluble organically bound iodine is the dominant fraction, with smaller amounts of iodide and iodate. Baker[102] suggested that this organically bound iodine forms by aqueous-phase chemistry in the aerosol. Very little is known about such chemistry, and further research in this area is required. In principle, the main consequence of this soluble organically bound iodine is an increase of the residence time of iodine within the particles. Interestingly, recent laboratory results show that *n*-butanol and malonic acid, which are ubiquitously found in atmospheric aerosols, are inert toward HOI and other intermediate species as $IOOO^-$. Similarly, no evidence was found for formation of anionic organoiodine products from ozonolysis of I^- + phenol mixtures.[218]

During the past few years some work has been conducted on the role of halogen activation of the iodide contained in aqueous solutions, both as a result of heterogeneous processes (see above) and aqueous-phase reactions. O'Driscoll et al.[221,222] have shown that a nitrite/iodide solution (two known sea−salt aerosol components) does not have to be strongly acidified to cause release of I_2 and NO, *if* such a mixed solution undergoes a freeze−thaw process. Acceleration of the NO_2^-/I_2^- reaction observed by these authors was attributed to the freeze−concentration effect, according to which H^+ ions rejected from a growing ice phase become concentrated in liquid "micropockets" within the ice, following the phase diagram of the solution. It is proposed that protonation of HONO generates the nitroacidium ion (H_2ONO^+), which then reacts with iodide to yield INO, and subsequently I_2 and NO are formed via two parallel paths. It was also observed that the amount of dissolved oxygen has a large effect on the yield of I_3^- (used as a proxy of I_2). This was rationalized in terms of a chain reaction mechanism involving oxidation of NO to NO_2 by O_2 and subsequent regeneration of H_2ONO^+.

Martino et al.[59,223] and Jones and Carpenter[60] have shown that CH_2I_2 is very photolabile in the near UV (300−350 nm) in seawater, leading to more photochemically stable products such as CH_2ICl which are then emitted to the atmosphere. Jones and Carpenter[224] also studied the degradation of a series of iodocarbons by hydrolysis and chlorination reactions, which can be rapid enough to limit the flux of these species to the atmosphere.

Overall there are still important gaps in our understanding of the aqueous-phase chemistry of iodine (see Figure 1 and discussion in Pechtl et al.[225]) that are also apparent in the shortcomings of model predictions of the iodine speciation in hydrometeors (see section 6.2).

4.3. Thermochemistry

The only experimental thermochemical data on the iodine oxides are recent spectroscopic determinations of the heats of formation ($\Delta_f H°_{298}$) of IO[226] and OIO.[160] The heats of formation of the higher oxides and $IONO_2$ have recently been reported using quantum theory at the coupled cluster level, including spin−orbit coupling of iodine.[39,227] All these results are listed in Table 4.

5. IODINE-MEDIATED ULTRAFINE PARTICLES IN THE ATMOSPHERE

5.1. Field Observations

5.1.1. Historical Context. The presence of fine particles in the coastal atmosphere has been long established, from the earliest observations in Scotland[228] and France[229] to Australia[230] and more recently Antarctica.[231,232] Initially it was postulated that their secondary production (i.e., growth through condensation of vapor rather than primary emission into the atmosphere) implicated sulfuric acid, likely derived from oxidation of DMS.[233] This hypothesis prevailed through to the late 1990s, being invoked to account for coastal atmospheric particle formation in Antartica[231] and investigated in great detail in particle bursts observed in Ireland.[234] However, identification of the daytime tidal cycles in iodocarbons,[78] IO,[26,27] and ultrafine particle bursts[16,234] provided the first evidence for a role for iodine compounds. On this basis it was suggested that halocarbons might play a role in particle formation. Such a relationship alone does not exclude participation of H_2SO_4 in either nucleation or condensational growth, but simulations using classical binary (H_2SO_4/H_2O) or ternary ($H_2SO_4/NH_3/H_2O$) nucleation and growth by first-order phase transition from gas to particles clearly showed that an additional component was required to explain new particle formation at Mace Head.[234]

5.1.2. Recent Field Investigations. In the past decade a number of comprehensive field investigations have been carried out to resolve aspects of iodine-mediated particle formation. The most comprehensive characterization of ultrafine particle properties and behavior was carried out within the Particle Formation in the Coastal Environment (PARFORCE) project[235] between September 1998 and June 1999. This project employed both long-term and intensive measurements at Mace Head. A marked and abrupt increase in the number concentration of particles between 3 and 10 nm diameter was consistently observed with a daytime low tidal signature, when particles formed on 90% of the days. Within PARFORCE, a wide range of analytical techniques was employed to categorize and interpret the aerosol measurements. The estimated range of the new particle growth rate, estimated 1 nm cluster concentration and condensable vapor source rate were derived from the combination of measurement and model application.[236] Direct micrometeorological flux determinations[237] determined particle number fluxes during bursts of 10^9-10^{10} m^{-2} s^{-1} and noted a close correlation between the concentration and the net positive flux of ultrafine aerosol particles during single-source events at Mace Head. This implies that the particle flux can be estimated from the measured particle concentration under similar conditions.

There is an indication from the contemporaneous reduction in measured gaseous H_2SO_4 concentration, increase in nucleation mode surface area, and increase in nucleation mode hygroscopicity that condensation of H_2SO_4 plays a role in the growth of particles, once formed. This has since been confirmed by a laboratory study (section 5.2.3).[12] Furthermore, the only analysis of particle composition from the field identified the presence of both iodine and sulfur in the majority of particles collected at Mace Head during episodes of elevated new particle production.[238]

More recently, the combination of inorganic and organic gaseous iodine and other trace gas speciation with aerosol measurements allowed the North Atlantic Marine Boundary Layer Experiment (NAMBLEX) project[239] (also carried out at Mace Head) to address many of the outstanding linkages between iodine and particle formation. All previous experiments had employed long-path DOAS instruments to detect reactive halogen species IO or OIO. Modeling studies incorporating a relatively explicit clustering of iodine oxides, tuned to reproduce laboratory experiments,[9] indicated that the ambient atmospheric levels of IO and OIO were 1−2 orders of magnitude too low to explain the observed particle distributions. The NAMBLEX project employed long-path DOAS to measure I_2, and it was demonstrated[18] that I_2, rather than organic iodine-containing compounds, was the source of gaseous reactive iodine. Furthermore, Saiz-Lopez et al.[19] proposed that most of the I_2 would be located in a very narrow strip (where macroalgae were exposed at low tide) comprising only 8% of the 4.2 km DOAS light path, where new particles were being formed from highly concentrated, localized pockets of iodine oxides. Indeed, Pechtl et al.[21] used a laboratory-derived parametrization for new particle formation and found that bursts of particles can only be explained from "hot spots". Subsequent in-situ measurements of I_2 and IO in Mace Head and Roscoff confirmed the "hot spot" theory.[19,114,115,240] Another modeling study[19] driven by I_2 emissions and sequential condensation of higher iodine oxides was able to reproduce the observed particle bursts and suggested that they could contribute to the regional ambient CCN burden, hence affecting radiative forcing as previously postulated.[241]

5.1.3. Further Afield. It has been important to establish whether iodine-mediated particles are formed at sites other than Mace Head. During the Reactive Halogens in the Marine Boundary Layer (RHaMBLe) coastal experiment,[242] direct micrometeorological measurements of particle emission and corresponding ozone depositional fluxes were made in Roscoff (Brittany) on the northwest coast of France.[243] Particle formation showed the same daytime low-tidal signature that was observed at Mace Head, as did path-integrated IO measured by long-path DOAS[105] and the even higher in-situ IO concentrations measured by CRDS[28] and LIF[29]). The concentration of particles with diameters between 3 and 10 nm was measured to be up to 3×10^5 cm^{-3}, at an apparent emission flux rate of up to 2×10^9 m^{-2} s^{-1}, consuming ozone such that it manifested a deposition velocity of up to 3 mm s^{-1} at the deepest low tides. Under appropriate conditions, the inferred growth of particles to sizes at which they were CCN active was observed (see Figure 7). The air was continuously semipolluted (NO_2 at ppbv levels) during the RHaMBLe coastal project, demonstrating that (i) the most likely I_xO_y formation channel was not quenched by reactions with NO, (ii) formation of $IONO_2$ via reaction 8 does not prevent particle

dx.doi.org/10.1021/cr200029u |Chem. Rev. 2012, 112, 1773–1804

formation, most likely because $IONO_2$ is recycled to IO via an autocatalytic reaction with atomic I (reaction $^{-11}$, see section 4.2.1.1.2),[39,105] and (ii) the significant condensational sink to pre-existing pollutant aerosol is unable to prevent formation. These observations are consistent with the "hot spot" formation of particles at extremely high iodine concentrations close to their source, where the ratio of NO_x to IO_x is too low to prevent their formation. Additional supporting evidence for the hot spot iodine-mediated formation of particles in Roscoff and Mace Head has been recently published.[104,115,116]

5.2. Laboratory Studies of Particle Formation and Growth

5.2.1. Laboratory Evidence for Particle Formation from Iodine Oxides. Direct formation of iodine oxide particles (IOPs) has been observed in numerous laboratory studies of iodine photochemistry.[9−12,14,15,155,161] Mass spectrometric analysis of the IOPs produced by photo-oxidation experiments of elevated (ppbv) concentrations of CH_2I_2 in the presence of O_3 revealed IO^-, IO_2^-, and IO_3^- fragments, which were postulated to be evidence for polymers produced from sequential addition of OIO to initial I_2O_4 dimers. This would be consistent with the reported low HTDMA-derived hygroscopicity of freshly formed particles probed at Mace Head[244] (though it must be noted that such measurements conflate compositional and morphological dependence). This mechanism was further employed (and extended) in a comprehensive investigation of CH_2I_2 photo-oxidation in a coupled chamber and modeling study[15] that revealed an aerosol mass spectrometer (AMS) fingerprint of the particles consistent with iodine oxides and oxy acids and a particle structure consistent with fractal agglomerates that collapsed under increased humidity. Particle formation was found not to occur if any one of CH_2I_2, O_3, or UV radiation were absent. To produce sufficient particle mass, the modeling in this study indicated that mass transfer between the gas and particles required accommodation coefficients of near unity for the postulated condensing components and that an additional iodine source was required to explain atmospheric observations. Extending this analysis to investigate formation and growth of aerosol from iodocarbon emissions in the remote marine atmosphere, O'Dowd et al.[17] postulated that the enhancement of marine particle number might be sufficient to impact on global radiative forcing.

The most probable solid particle compositions resulting from direct oxidation of reactive gas-phase iodine are I_2O_4 and I_2O_5,[10,12] whose crystal structures have been documented.[245,246] While laboratory studies of particle formation from photolysis of CH_2I_2 have indirectly inferred the tetraoxide form,[15] transmission electron microscope analysis of particles generated photochemically from molecular I_2 and O_3 in dry conditions (<2% relative humidity) showed that the IOPs were essentially I_2O_5.[10] These two solid iodine oxides have markedly different bulk hygroscopic properties, with the pentaoxide (the anhydride of iodic acid, HIO_3) being very hygroscopic and having a high solubility in water (molality of ∼7.6 mol per kg or 71.7 wt % for a saturated solution at room temperature), while I_2O_4 has a low hygroscopicity but is known to decompose to I_2 and HIO_3 on prolonged exposure to water.[247] The role of relative humidity (RH) levels in excess of 80% (i.e., typical of the MBL) has recently been examined in a study which explored the deliquescence behavior of the solid oxides and the water activities of aqueous solutions of iodine oxides.[248]

Saunders and Plane[10] speculated that I_2O_5 might form in the gas phase through oxidation of I_2O_4 by O_3 and that this very

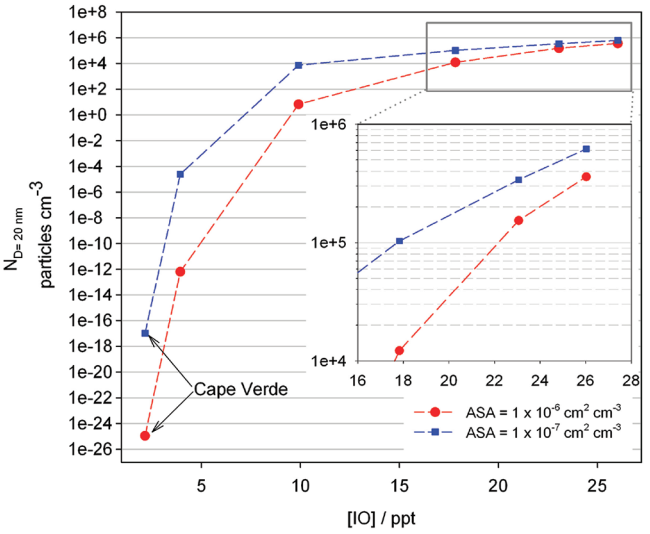

Figure 8. Number of potential CCN predicted to form in the remote MBL after 24 h as a function of the mean daytime IO concentration at 10 m. [IO] is changed by altering the sea-to-air flux of I_2. Two cases are illustrated in the figure to show the sensitivity to the background aerosol surface area, which is set to a typical remote MBL value of 1×10^{-6} cm^2 cm^{-3} (red) or an ultraclean value of 1×10^{-7} cm^2 cm^{-3} (blue). Reprinted with permission from ref 117. Copyright 2010 European Geosciences Union.

stable iodine oxide then polymerized to produce IOPs (thus explaining observation that dry IOPs consist of I_2O_5). However, a recent study[12] has shown that IOPs can form *without* O_3 being present. In this study, N_2O was photolyzed using a 193 nm excimer laser to produce O atoms, which then reacted with I_2 to make IO. IOP formation is thus almost certainly initiated by polymerization of I_2O_3 and I_2O_4, which are formed in reactions 16 and 17. The bond energies between these higher iodine oxides ($\Delta H_0(I_2O_3 + I_2O_4 \rightarrow I_4O_7) = -171$ kJ mol^{-1}; $\Delta H_0(I_2O_4 + I_2O_4 \rightarrow I_4O_8) = -208$ kJ mol^{-1}) are large enough to make the polymerization spontaneous.[12] The particles must then restructure in the solid phase to I_2O_5 and I_2. Under dry conditions, a kinetic study of IOP formation showed that the particles form fractal-like, aggregate structures,[11] which were observed to collapse when humidifed.[12] It therefore seems probable that IOPs which form in humid marine environments are either aqueous droplets of HIO_3 composition (or possibly the anhydro form, $I_2O_5 \cdot HIO_3$[249]) or I_2O_4 particles which undergo (at least partial) hydrolysis to HIO_3 and I_2. I_2 can then either recycle into the gas phase or exist with I^- in the aqueous phase $I_2 + I^- \leftrightarrow I_3^-$ equilibrium.[250]

5.2.2. Particle Formation in Macroalgal Incubation Experiments. There have been a number of macroalgal incubation studies to resolve aspects of iodine-mediated particle formation. The first of these,[22] which tested the exposure of single macroalgal fronds to ambient levels of light and O_3, demonstrated formation of particles from *Laminaria digitata* samples. Such particles were identical to those formed in the photo-oxidation of I_2 or CH_2I_2 insofar as their composition measured by an AMS and their physical properties were concerned. This study[22] therefore linked the macroalgal exposure at low tide to molecular I_2 emission and IOP formation. Subsequent chamber incubations of mixed macroalgae under near-ambient conditions[20] attempted to relate quantitatively the particle growth rates to macroalgal

Table 5. Summary of Total Aerosol Iodine Concentrations Reported for Open Ocean, Island, Coastal, and Continental Locations

location	iodine concentration/ng m^{-3}	ref
open ocean sites		
Equatorial Atlantic	2−24	Rancher and Kritz[304]
Eastern Tropical North Atlantic	4.6−13	Gilfedder et al.[273]
Western Pacific	1.3−5.1	Gilfedder et al.[273]
island sites		
Hawaii	1.3−25	Duce et al.[305]
Hawaii	0.8−4	Duce et al.[262]
Hawaii	1.4−5.2	Moyers and Duce[306]
Enewetak Atoll, tropical Pacific	0.67−7.9	Duce et al.[307]
Canadian Arctic	<0.1−4	Sturges and Barrie[308]
Alert, Canadian Arctic	0.05−1.4	Barrie and Barrie[309]
Alert, Canadian Arctic	0.2−1.9	Barrie et al.[310]
Alert, Canadian Arctic	0.03−2	Sirois and Barrie[129]
Barbados	0.35−19	Arimoto et al.[311]
Tenerife	0.25−15	Arimoto et al.[311]
Moana Loa Observatory, Hawaii	1.8 ± 1.2	Zieman et al.[312]
Uto, Finland	0.90 mean	Jalkanen and Manninen[313]
Hong Kong	0.3−11.6	Cheng et al.[314]
coastal sites		
Barrow, Alaska	0.3−10	Duce et al.[315]
Cambridge, Massachusetts	2−10	Lininger et al.[316]
McMurdo, Antarctica	0.93 ± 0.39	Duce et al.[317]
Tokyo, Japan	1.7−12.7	Tsukada et al.[271]
Mace Head, Ireland	0.4−21	Arimoto et al.,[311]
Ibaraki, Japan	0.3−3.4	Yoshida and Muramatsu[318]
Virolahti, Finland	0.75 mean	Jalkanen and Manninen[313]
Weybourne, United Kingdom	0.68−6.4	Baker et al.[220]
Mace Head, Ireland	1.7−5.7	Gilfedder et al.[273]
continental sites		
South Pole	0.49 ± 0.12	Duce et al.[317]
South Pole	0.07−0.09	Maenhaut et al.[319]
South Pole	0.18 ± 0.04 winter 0.08 ± 0.04 summer	Cunningham et al.[320]
South Pole	0.13 ± 0.04 winter 0.26 ± 0.06 summer	Tuncel et al.[321]
Eastern Transvaal	2.7−3.3 (medians)	Maenhaut et al.[322]

emissions of I_2 produced per unit mass of algae. A model using the emitted I_2 as the primary condensable material source and including clustering of OIO and I_2O_3 as the initial nucleating mechanism was able to reproduce characteristics of the observed particle formation.[251] Further chamber experiments[61,63] have demonstrated the large biological (and temporal) variability in the emission of gaseous precursors and subsequent formation of particles as well as quantifying the O_3 consumption rate during *Laminaria* incubations.

5.2.3. Iodine Oxide Particle Growth to Potential Cloud Condensation Nuclei. One important question concerns the growth of IOPs in the presence of condensable vapors, such as water, ammonia, and both mineral and organic acids, in the marine atmosphere. This is because the supply of iodine oxides is limited, so that once IOPs form they will only grow by condensation of these other vapor species to sizes where the particles have a significant impact on climate either directly (scattering and absorption of solar radiation) or indirectly (enhancement of CCN).[252] Although it has long been known that particle size is a more dominant factor in CCN activity than chemical composition, the latter is most likely to control the rate of growth from freshly nucleated particles to potentially active sizes (>50 nm diameter).

A recent laboratory study[12] has shown that the initial rate of formation and growth of IOPs in humid conditions is actually slower than in very dry conditions, because H_2O forms relatively stable complexes with I_2O_3 and I_2O_4, inhibiting their polymerization. This study also showed that the accommodation of H_2SO_4 vapor on IOPs is very efficient, particularly at high relative humidities: the accommodation coefficient is around 0.75 at RH = 90%. Growth of IOPs in the remote MBL to sizes at which their role as CCN may become important is therefore likely to be governed by the uptake of H_2SO_4, accompanied by H_2O and NH_3 to maintain the pH close to neutral.[253−255]

Regarding the uptake of possible organic species, the most likely candidates are the short chain dicarboxylic acids ($HOOC-(CH_2)_n-COOH$; $n \geq 0$), which have a variety of biogenic and anthropogenic sources[256] and have been identified as the major contributors to the water-soluble organic carbon fraction of atmospheric aerosols in a variety of locations.[257] Reaction of aqueous solutions of these organic acids in the presence of concentrated HIO_3 solution and subsequent formation of I_2 in both aqueous and solid phases has been observed in the case of oxalic ($n = 0$) and malonic ($n = 1$) acids (the species found to be most abundant in atmospheric aerosols in marine environments).[258−260] Therefore, these acids could potentially provide a route for the recycling of I_2 from aerosols. However, a recent study[12] has shown that the accommodation coefficient of oxalic acid on hydrated IOPs was less than 10^{-3}, so the uptake of organic acids is probably less important than H_2SO_4.

5.3. Unresolved Aspects of Iodine-Mediated Particle formation

There are several outstanding areas of interest relating to IOP formation. The first concerns the mechanism for forming the initial iodine oxide polymers. Although progress has been made in this area (section 5.2.1), direct observation of I_2O_x species in the laboratory and measurement of the rates of polymerization of these species remain an experimental challenge. Apart from a single study,[238] there is no compositional information for particles below about 100 nm diameter (many hours to days of growth after nucleation) with which to evaluate any hypothesized formation and growth mechanisms. There is also little information regarding the relative roles of iodine oxides and other condensing vapors in the nucleation and growth stages. Given the very rapid formation rates of I_xO_y it might appear obvious that the higher iodine oxides are more important close to the iodine sources (where nucleation occurs) compared to their decreased

dx.doi.org/10.1021/cr200029u |*Chem. Rev.* 2012, 112, 1773–1804

Table 6. Summary of Iodine Speciation Determinations in Samples of Rain, Snow, and Aerosol from Various Locations[a]

location	sample type	sample numbers	species measured	species calculated	iodide	iodate	SOI	insoluble iodine	combinations	ref
				open ocean sites						
Weddell Sea	aerosol	1	TII, A	B	23					Gäbler and Heumann[323]
Tropical South Atlantic	aerosol	1	A, B		17	83				Wimschneider and Heumann[324]
Southern North Sea	rain	14	TII, A	B	21−99					Campos et al.[276]
Tropical North Atlantic	aerosol	28	TSI, A, B	C	5−26	8−72	16−79			Baker,[102,325]
North and South Atlantic	aerosol	22	TSI, A, B	C	15−66	8−79	2−65			Baker[102]
North and South Pacific	aerosol	57	TSI, A, B, C^{+}	C	<1−74	<1−46	7.5−100			Lai et al.[267]
Tropical North Atlantic	aerosol	14	TSI, A, B	C	11−39	24−69	14−50			Allan et al.[326]
Northwest Pacific and Arctic	aerosol	28	TI, TSI, A, B	C, D		8−82	0−35	4−42		Xu et al.[272]
Eastern Tropical North Atlantic	aerosol	3	TI, TSI	D				20−25		Gilfedder et al.[273]
North and South Pacific	aerosol	5	TI, TSI	D				27−48		Gilfedder et al.[273]
				coastal sites						
German North Sea coast	submicrometer aerosol	1	A, B			<10				Gäbler and Heumann[323]
SE England	rain	26	TII, A	B	9−100					Campos et al.[276]
SE England	aerosol	16	TI, TSI, TII	C, D			0−93	4−50	3−74 (A+B)	Baker et al.[220]
SE England	aerosol	30	TSI, B	A+C		<1−93				Baker et al.[101]
SE England	rain	58	TII, A	B	3−96					Baker et al.[101]
Mace Head, Ireland	aerosol	18	TSI, A, B, C^{+}	C		<1−6	83−97			Gilfedder et al.[103]
Mace Head, Ireland	PM 2.5 aerosol	9 (morning)	TSI, A, B, C^{+}	C	4.5−21	0.2−7.2	78−95			Gilfedder et al.[103]
Mace Head, Ireland	PM 2.5 aerosol	9 (afternoon)	TSI, A, B, C^{+}	C	5.4−30	0.1−7.2	69−94			Gilfedder et al.[103]
Mace Head, Ireland	PM 2.5 aerosol	9 (night)	TSI, A, B, C^{+}	C	3.7−20	0.15−2.7	78−96			Gilfedder et al.,[103]
Mace Head, Ireland	rain	8	TSI, A, B, C^{+}	C	11−31	3.3−18	51−84			Gilfedder et al.,[103]
Roskilde, Denmark	rain and snow	94 (^{127}I)	TSI, B, C^{+}			43−97			7−57 (A + C)	Hou et al.[274]
Roskilde, Denmark	rain and snow	94 (^{129}I)	TSI, A, B	C	20−100	1−50	0−77			Hou et al.,[274]
Mace Head, Ireland	aerosol	3	TI, TSI	D				17−53		Gilfedder et al.[273]
				terrestrial sites						
Tokyo, Japan	aerosol	3	TSI, B, D			3−11		36−57	44−61 (A+B+C)	Tsukada et al.[271]
Regensburg, Germany	aerosol	4	A, B		12−31	69−88				Wimschneider and Heumann[324]
Mainland United Kingdom (4 sites)	rain	215	TII, B	A		50 (average)				Truesdale and Jones[275]
Germany	snow		TSI, A, B, C^{+}	C	24−64	<1−16	21−76			Gilfedder et al.[265]
Lake Constance, Germany	rain	21	TSI, A, B, C^{+}	C	11−61	2−48	13−82			Gilfedder et al[266]
Lake Constance, Germany	snow	15	TSI, A, B, C^{+}	C	32−66	<1−6	33−67			Gilfedder et al.[266]
Swiss Alps	rain	1	TSI, A, B, C^{+}	C	41	2	57			Gilfedder et al.[266]
Mummelsee, Germany	rain	1	TSI, A, B, C^{+}	C	24	14	62			Gilfedder et al.[266]
Mummelsee, Germany	snow	4	TSI, A, B, C^{+}	C	41	<1	59			Gilfedder et al.[266]
Patagonia, Chile	rain	3	TSI, A, B, C^{+}	C	67	<1	33			Gilfedder et al.[266]
Australia, New Zealand,	rain	3	TSI, A, B, C^{+}	C	19−35	9−13	58−63			Gilfedder et al.[103]
Greenland	snow	6	TSI, A, B, C^{+}	C	10	∼2	88			Gilfedder et al.[103]

[a] For each study the species determined are given using the following codes: iodide (A), iodate (B), soluble organic iodine (C), anionic soluble organic iodine (C^{+}), nonionic soluble (organic) iodine (C‡), insoluble iodine (D), or combinations of those codes where the analytical techniques used gave determinations of more than one species. The proportions of the species determined are given expressed as a percentage of the total measured iodine concentration: TI, total iodine; TSI, total soluble iodine; TII, total inorganic iodine. The speciation is shown in percentages.

dx.doi.org/10.1021/cr200029u |Chem. Rev. 2012, 112, 1773–1804

role on dilution away from the seaweed beds, when the role of other condensing vapors becomes more important.

A firm mechanistic understanding of particle formation is therefore still some way off. Care must be taken when using parametrizations[21,22,261] that have been developed relating particle formation to the I_xO_y concentration or production rate, prior to such an understanding. Any mechanism must be able to reproduce both laboratory and field observations before its predictions can be trusted to extrapolate beyond the scope of existing field observations. Nevertheless, these models can be used for helpful sensitivity studies and to direct future studies especially as the details of the nucleation process are not resolved yet.

A further uncertainty surrounds the wider significance of coastal particle formation. While coastal new particle formation has been routinely observed at a number of locations, it is far from clear that coastal sources impact on radiation through the ability of particles to act as CCN at a regional, let alone global, scale. First, it is necessary to establish unambiguously whether, once particles that have been formed from macroalgal exposure at low tide have grown to "CCN-active sizes", they act efficiently as CCN at realistic marine supersaturations. Second, it is not clear that the areas where significant numbers of efficient CCN are produced from IOPs are sufficiently large to produce significant radiative impacts.

A final major area of uncertainty surrounds iodine-mediated particle formation in the remote MBL. Extrapolating from coastal measurements, using laboratory-based mechanisms, to global scales is highly uncertain because of the high order of dependence on the concentration of IO. This is illustrated in Figure 8, which shows the number of particles which are predicted in a 1-D modeling study[22] to grow large enough (diameter >20 nm) after 24 h to have a good chance of surviving to become CCN after 24 h as a function of the mean daytime IO concentration. Two cases are illustrated in the figure to show the sensitivity to the background aerosol surface area (*ASA*), which is set to a typical remote MBL value of 1×10^{-6} cm^2 cm^{-3} or an ultraclean value of 1×10^{-7} cm^2 cm^{-3}. The figure shows that the predicted number of particles is highly sensitive to (i) the background *ASA*, because the loss to background aerosols through uptake is usually faster than growth by coagulation and condensation (except at high [IO]), and (ii) the IO concentration, because the rates of formation of OIO and I_2O_4 depend nonlinearly on [IO]. The figure demonstrates the extremely small probability of forming potential CCN when [IO] < 5 ppt, which seems to be the case \in the remote MBL.[22,27,35] However, the model results show that for higher [IO], such as observed in midlatitude coastal areas[19,28,29] and Antarctica,[126] IOPs may well produce CCN.

6. ACCUMULATION OF IODINE IN AEROSOL

6.1. Iodine Concentrations in Aerosol

Iodine has been found at the low ng m^{-3} level in atmospheric aerosols from a wide variety of environments. Table 5 lists data from a number of these regions. Although the table contains little data from nonmarine influenced sites, the strong concentration difference apparent between measurements at the South Pole and at other locations is consistent with the dominant source of iodine to the atmosphere being marine. Iodine concentrations in aerosol are considerably enriched over seawater composition, as indicated by I/Cl and I/Na ratios.[220,262] This enrichment may be to some extent a result of emission of iodine-enriched material from the sea surface microlayer during bubble bursting[263] but also reflects the transfer of volatile iodinated gases from the sea surface (see section 2).

6.2. Iodine Speciation

A range of inorganic iodine species are potentially present in aerosol (e.g., I^-, HOI, I_2, ICl, IBr, IO_3^-, see preceding sections), but because HOI is potentially reactive and the IX (X = Cl, Br, I) species are insoluble (and photochemically active), only the ionic species I^- and IO_3^- are expected to accumulate appreciably. Of these, I^- participates in halogen activation reactions to yield IX,[6] and so older model studies concluded on this basis that IO_3^- would be the only stable iodine species in aerosol.[3,6] However, measurements of I^-/IO_3^- speciation in (mostly) marine rainwater and aerosol have shown that the ratio between these two species is highly variable (Table 6) with at present no clear mechanism understood to control this ratio.

Several studies performed a decade ago provided evidence for the existence of an organic fraction of soluble iodine in rainwater[264] and aerosol.[220] Subsequent reports indicate that soluble organic iodine (SOI) is ubiquitous in both.[102,103,265−267] As with inorganic iodine speciation, the proportion of soluble iodine in organic form appears to be highly variable, although SOI is frequently found to constitute the major fraction of soluble iodine (Table 6). Some caution may be necessary when interpreting the SOI data obtained by extracting aerosol samples with the aid of ultrasonication. Baker et al.[220] showed that extended periods of ultrasonication (in their case >5 min) appear to cause conversion of inorganic iodine to SOI. More detailed work by Xu et al.[268] indicates that iodide is the species removed, with losses being greater from cellulose filters than from glass fiber filters; iodate concentrations were unaffected by ultrasonication. Formation of oxidizing species, such as H_2O_2 and superoxide, during acoustic cavitation (see, e.g., ref 269) may be responsible for the disappearance of iodide. It has been shown that ultrasonication of aerated solutions of iodide liberates iodine,[270] and this iodine may then react with organic substrates to produce SOI. Nevertheless, the widespread occurrence of SOI in nonultrasonically treated rainwater and snow[103,264−266] confirms that it is a significant component of atmospheric iodine. Attempts to identify the components of SOI have so far had limited success, with anionic SOI species being reported to comprise 5−20% of total soluble iodine in rain, snow, and aerosol samples[103,265,266] and only one SOI component tentatively identified as iodoacetic acid.[103,265,266]

To date, only Tsukada and co-workers[271] appear to have directly measured the insoluble fraction of aerosol iodine while other workers[220,272,273] have inferred the presence of an insoluble fraction from the difference between total iodine concentrations and soluble iodine concentrations. Those studies suggest that insoluble iodine also appears to account for a significant fraction of total aerosol iodine. There are very few potential candidate species for insoluble inorganic iodine, and Baker et al.[220] suggested on this basis that the insoluble fraction of aerosol iodine was likely to be organic, although Gilfedder et al.[273] noted that iodine adsorbed to mineral or black carbon surfaces may also contribute to the insoluble fraction.

We are still some way from a complete understanding of the presence of and chemical interrelationships between these various inorganic and organic fractions of iodine. Hydration of the higher iodine oxides (I_2O_4, I_2O_5) associated with nucleation of iodine-containing particles (see section 5) can account for the presence of aerosol iodate. Baker et al.[101] reported a lower proportion of soluble aerosol iodine in the iodate form in air masses that had arrived in the southern United Kingdom from Europe than in other air masses that had spent much longer over the ocean before arrival. Since the European air had only been

subject to marine iodine emissions shortly before sample collection, Baker and co-workers suggested that this implied a relatively slow formation rate for aerosol iodate. Recent results on the speciation of stable (^{127}I) and radioiodine (^{129}I) in rainfall in Denmark may support that conclusion. The major source of ^{129}I to the environment in Europe is its release, principally into seawater, from the nuclear reprocessing facilities in Sellafield, U.K., and Le Hague, France. In a 6 year record of monthly rainfall samples, Hou et al.[274] observed the median proportion of soluble ^{127}I in the form of iodate to be 67%, which is consistent with previous reports of inorganic iodine speciation in rain.[101,275,276] The speciation of ^{129}I in the Danish rain was dramatically different, with almost all radioiodine (median 87%) present as iodide.[274] Similarly to the case of European air reported by Baker et al.,[101] the dominant source of ^{129}I in Danish rain is emitted relatively close to the point of collection of the samples, and thus, the time available for iodate formation is relatively short compared to stable iodine emitted from further away.

Aerosol SOI may be introduced by primary emissions of iodinated organic matter from the sea surface during bubble bursting, as suggested for example by Seto and Duce.[263] The sea surface microlayer is enriched in organic matter, and reactions of O_3 and I^- at the sea surface are known to produce iodinated organic matter,[57] so it is reasonable to assume that some of the organic matter ejected to the atmosphere during bubble bursting[277] is iodinated. There is also a potential secondary mechanism for formation of SOI through reaction of aerosol organic matter with HOI.[102] Studies of equivalent reactions in seawater have shown this reaction to be highly pH dependent, with optimum pH values being above 8.[278] This would appear to be at odds with the high abundance of sulfuric acid in submicrometer aerosol, where the majority of SOI has also been observed.[102,103] Results obtained with single-aerosol mass spectrometers provide some useful insights into the mixing states of iodine, sulfate, and organic matter that are not available from the large sample, filtration-based studies discussed above. At Cape Grim (Tasmania), iodine-containing particles were positively correlated with organic-containing particles and negatively correlated with sulfate-containing particles,[279] i.e., iodine was positively correlated with organics in particles that contained little sulfate.[280] A positive correlation between iodine and organics was also observed in particles at altitudes between 5 and 19 km above North America.[281] These results[279,280] indicate that aerosol organics are present in a higher pH environment than would be expected of sulfuric acid aerosol and may therefore exist under conditions conducive to iodination by HOI. Alternatively, this distribution of organics and iodine in low sulfate particles may be a consequence of primary production of iodinated organic aerosol from the sea surface. However SOI is formed, its presence provides a potential source of aerosol iodide through photolysis of C−I bonds. Pechtl et al.[225] proposed a mechanism by which iodate may be reduced in acidic aerosol based on known inorganic chemistry. This mechanism greatly improved their model's ability to reproduce measured I^-/IO_3^- ratios by including (less well known) organic−iodine interactions.

6.3. Key Uncertainties

It would seem that the interactions of iodine and organic matter are the most significant unknowns in aerosol iodine chemistry at present. The results of Pechtl and co-workers[225] suggest that these interactions potentially hold the key to a quantitative understanding of inorganic iodine speciation in aerosol and that they may thus play a significant role in regulating the recycling of halogens to the gas phase. Laboratory studies investigating potential routes for formation and degradation of organoiodine compounds under conditions relevant to aerosols will be necessary in order to improve parametrizations of these interactions in models. The diverse nature of aerosol organic matter will make these experiments challenging. It is to be hoped that further developments in field observations, such as better characterization of the components of aerosol organic iodine and further insight into the mixing state of relevant species (iodine, organics, sulfate, seasalt), will aid this work. Other processes that merit investigation include an assessment of the relative rates of production of aerosol organic iodine via primary and secondary mechanisms, since these mechanisms imply very different impacts on aerosol HOI concentrations, and the effects of organic surface films on aerosol−gas transfer processes for HOI and IX.

7. IMPACTS AND MODELING OF REACTIVE IODINE SPECIES

The potential relevance of iodine to the gas-phase chemistry of the troposphere was realized more than 30 years ago,[2] including its importance for ozone destruction and the potential to lead to significant shifts in the HO_x and NO_x ratios.[2] However, one common conclusion of the early modeling studies on iodine chemistry in the atmosphere[2,5,52,282−284] was that a significant lack of kinetic data and missing information on reactive iodine precursor gas fluxes, especially from the ocean, made solid assessments of the importance of iodine chemistry very difficult. Nevertheless, the large potential of reactive iodine for destruction of O_3 was already indicated in these studies. Davis et al.,[284] for example, estimated that under conditions typical for the tropical marine environment about 6% of total tropospheric column O_3 destruction was due to iodine chemistry and that in regions of high marine biological activity this could as high as 30%.

Since these studies our knowledge of the atmospheric concentrations of short-lived organic and inorganic iodine compounds, their fluxes, their speciation in aerosol particles, rain, and snow, and the pertinent reaction kinetics have greatly improved (sections 2 − 6). In the following few paragraphs we summarize the findings from model studies from the past decade. Even though great progress has been made, several important open questions remain which we will highlight at the end of this section.

7.1. Impacts of Iodine Chemistry

7.1.1. Ozone Depletion. The iodine-catalyzed depletion of O_3 occurs in the lower troposphere via a number of catalytic cycles. IO can deplete O_3 through its self-reaction.

Cycle 1

Cycle 1

$$(\mathrm{I} + \mathrm{O_3} \rightarrow \mathrm{IO} + \mathrm{O_2}) \times 2 \quad (10)$$

$$\mathrm{IO} + \mathrm{IO} \rightarrow \mathrm{I} + \mathrm{OIO} \quad (15a)$$

$$\mathrm{OIO} + h\nu \rightarrow \mathrm{I} + \mathrm{O_2} \quad (7a)$$

net: $2\mathrm{O_3} \rightarrow 3\mathrm{O_2}$

IO can also react with BrO in a cross-reaction that produces OIO and Br (80%) and I + Br (20%).[144] The photodissociation of OIO to I + O_2 with a quantum yield close to 1 increases the overall O_3-depleting efficiency of the IO self-reaction and the IO + BrO cross-reaction.[37] Note that OIO can also react with NO (reaction 19a−19d). Cycle 1 will dominate O_3 destruction

when relatively high mixing ratios of halogen oxides are present (typically, more than 2 pptv of IO and BrO). At lower halogen oxide concentrations, reaction with HO_2 radicals becomes important.

Cycle 2

Cycle 2

$$I + O_3 \rightarrow IO + O_2 \quad (10)$$

$$IO + HO_2 \rightarrow HOI + O_2 \quad (25)$$

$$HOI + h\nu \rightarrow I + OH \quad (26)$$

net: $HO_2 + O_3 \rightarrow OH + 2O_2$

In semipolluted environments, $IONO_2$ formation can also lead to O_3 depletion.

Cycle 3

Cycle 3

$$I + O_3 \rightarrow IO + O_2 \quad (10)$$

$$IO + NO_2 \rightarrow IONO_2 \quad (8)$$

$$IONO_2 + h\nu \rightarrow I + NO_3 \quad (9)$$

$$NO_3 + h\nu \rightarrow NO + O_2 \quad (27)$$

$$NO + O_3 \rightarrow NO_2 + O_2 \quad (28)$$

net: $2O_3 \rightarrow 3O_2$

However, although the quantum yield of reactions 9a−9c is large,[41,164] the major photolysis pathway of NO_3 produces NO_2 + O, leading to no overall O_3 depletion. In addition, the $IONO_2$ formed can also be removed from the gas phase by recycling through sea-salt aerosol, which provides an efficient route for converting NO_x to NO_3^- ions in the aerosol,[105,107] but little is known about the uptake rates or condensed phase chemistry. However, the uptake of HOI and $IONO_2$ enhances release of chlorine and bromine from sea-salt particles into the gas phase, which can then cause further O_3 depletion.[285] Two recent studies have shown high levels of IO and OIO in polluted environments.[105,107] Stutz et al.[107] compared model and field data and proposed that the $IONO_2$ reservoir must be short lived for the model calculations to be consistent with the field data. Subsequent work by Kaltsoyannis and Plane[39] has shown, using quantum chemistry calculations, that $IONO_2$ will rapidly recycle back to I_2 by reaction with I

$$IONO_2 + I \rightarrow I_2 + NO_3 \quad (-11)$$

The resulting I atoms, from I_2 photolysis, will react with $IONO_2$, rather than O_3, if the ratio $[IONO_2]/[O_3]$ is >0.01.[39] This sequence represents an autocatalytic cycle that will limit the build up of $IONO_2$ and suggests that iodine chemistry should still be active even in a relatively high NO_x environment.

7.1.2. Influence on the NO_x and HO_x Balance. The ratio of NO_2 to NO is controlled principally by the reactions

$$NO_2 + h\nu(\lambda < 400\text{nm}) \rightarrow NO + O(^3P) \quad (29)$$

$$NO + O_3 \rightarrow NO_2 + O_2 \quad (28)$$

In the presence of significant halogen concentrations, the balance will be shifted toward NO_2[3,8,242]

$$IO + NO \rightarrow I + NO_2 \quad (30)$$

This reaction therefore plays a similar role to peroxy radicals such as HO_2 and CH_3O_2. Note, however, that reaction 30 would be followed by reaction 10, thereby consuming O_3 and the NO_2 would photolyze to produce an O_3, so the overall effect is a null cycle in terms of O_3 change.

In the remote MBL, the HO_2 radical is formed from OH through the sequence

$$OH + CO \rightarrow H + CO_2(+O_2) \rightarrow HO_2 \quad (31)$$

In the presence of IO, the HO_2/OH ratio will be reduced[2,3,7,8,78,242,282,284]

$$IO + HO_2 \rightarrow HOI + O_2 \quad (25)$$

$$HOI + h\nu \rightarrow OH + I \quad (26)$$

As compared to bromine chemistry, this cycle is particularly important in the case of iodine, because the IO + HO_2 reaction is fast and HOI photolyses more readily than HOBr.[144,164]

7.1.3. Nighttime Iodine Chemistry. Nocturnal IO observations were first reported by Saiz-Lopez and Plane.[18] In the same study the presence of I_2 was suggested to explain the daytime and nighttime measurements of IO through photolysis during the day (reaction 3) and reaction with NO_3 during the night (reaction 11) to give I atoms, followed by reaction with O_3 (reaction 10). Reaction between IO and NO_3 (reactions 22a−22d) then produces OIO, which has also been observed at night.[18,113] Reactions 22a−22d have recently been studied in the laboratory and shown to be relatively fast.[36]

7.1.4. Oxidation of Elemental Mercury. Gaseous elemental mercury (Hg^0) is emitted to the atmosphere from a variety of sources, principally coal combustion. The elemental form has an atmospheric lifetime of about 1 year, except during the polar spring when Hg^0 is converted to reactive gaseous mercury (RGM) on a time scale of only a few hours. As most Hg^I is thermally unstable,[24] the Hg in RGM is in the +2 oxidation state, probably as the mercuric halides ($HgBr_2$/$HgCl_2$) and possibly as mercuric oxide (HgO).[25] The nature of this conversion process is currently an important research area, because the soluble RGM, following methylation, quickly enters the food chain in the Arctic ecosystem. While the mechanism for Hg^0 oxidation is not completely understood, it has been observed that Hg^0 depletion events correlate with polar O_3 depletion events and elevated levels of BrO radicals observed in the springtime polar boundary layer.[25,286] Using reaction rate calculations by Goodsite et al.,[24] recent modeling studies have suggested that iodine in the polar atmosphere enhances depletion of Hg^0 by oxidation to Hg^{II},[23,126] although oxidation is almost certainly initiated by bromine chemistry.[25] In coastal Antarctica, where IO levels up to 20 pptv were reported, theoretical calculations of mercury oxidation by iodine show that iodine could lead to a 40% reduction of the Hg lifetime compared to removal by bromine chemistry acting alone.[126]

7.2. Modeling Iodine Atmospheric Domains

7.2.1. Polar Boundary Layer. Although the presence of IO in polar regions was only confirmed recently,[109,126,132] the presence of organic iodine compounds in the polar regions prompted an earlier modeling study by Sander et al.[287] which investigated the potential impact of iodine on Arctic ozone depletion events. The results of this study suggested a contribution of 20% of iodine chemistry to O_3 destruction if IO was present at 1 pptv as well as a 2−3-fold increase in OH and a related decrease in HO_2 radicals.

Saiz-Lopez et al.[8] used a 1-D model to reproduce their measurements of halogen oxides in coastal Antarctica.[126] They assumed the boundary layer to be well mixed and were able to reproduce the measured IO mixing ratios of up to 20 pptv by using a reactive iodine flux of the order of 10^{10} I atom cm^{-2} s^{-1}. This flux is too high to be provided by photolysis of organic iodine precursors. The source of iodine is most likely from the snowpack through the recycling of previously deposited iodine that originated from the ocean,[219] but direct proof of this is still missing. In order to reproduce satellite observations of atmospheric columns of IO,[33,34] Saiz-Lopez et al.[8] had to assume that higher iodine oxides undergo photolysis in addition to uptake on existing aerosol particles and formation of new particles. The heterogeneous recycling of HOI and $IONO_2$ was also required to reproduce the measurements. The modeled I_2O_x mixing ratios of up to 25 pptv imply that formation of new particles should be possible under these circumstances. Interestingly, the modeled destruction of O_3 (in the presence of BrO) was much greater than observed, indicating either a rather strong downward flux of O_3 from the free troposphere or missing processes in the model. The halogens also cause significant changes to the vertical profiles of OH and HO_2 and the NO_2/NO ratio.

As discussed in section 3.3, reactive inorganic iodine compounds seem to have much higher concentrations in the Antarctic than the Arctic. Possible reasons for this difference between the polar regions may include different sea−ice thicknesses and/or different biological communities, as the iodine precursors could be related to enrichment of iodine from the ocean water by (ice) algae.

7.2.2. Marine Boundary Layer. *7.2.2.1. Gas-Phase Iodine Chemistry.* Model studies have been used to try to reproduce measured concentrations of I, IO, OIO, and I_2 and observed new particle formation as well as shifts in the observed ratios of OH/HO_2 and NO/NO_2 in order to test our current understanding of the iodine chemistry involved. In order to do this a variety of models have been employed, mainly box and 1-D models. In some model studies the concentrations of a number of reactive noniodine species have been constrained to measured values in order to quantify the iodine precursor fluxes needed to reproduce measured iodine concentrations, whereas other studies do not prescribe any concentrations and then test the combination of all included processes and especially of nonlinearities in the chemistry. Some of the models use an explicit description of aqueous-phase (aerosol particles and cloud droplets) processes; others only consider heterogeneous reactions on particles assuming that uptake is the rate-limiting step and an essentially infinite supply of condensed phase reactants.

Vogt et al.[6] developed a combined gas and aerosol box model using CH_2I_2, CH_2ClI, CH_3I, and i-C_3H_7I as precursor gases for iodine. They predicted IO mixing ratios on the order of 1 pptv and found a strong impact of gas-phase iodine chemistry on the O_3 concentration, with destruction rates of up to 1 ppbv d^{-1}, which under their conditions was faster than O_3 destruction by the O_3 + HO_2 reaction. They also demonstrated strong chemical coupling between reactive I, Cl, and Br compounds, with the iodine compounds accelerating release of bromine and chlorine from sea-salt aerosol (section 4.2.2). This model also predicted significant uptake of iodine to particles, consistent with observations of a large enrichment of iodine in aerosol particles. However, almost all particulate iodine was present in the form of IO_3^-, because cycling between other aqueous-phase species is efficient and creates temporary reservoirs only. As discussed in section 6, this is inconsistent with available measurements pointing to some missing understanding in the aqueous-phase chemistry of iodine.

To ameliorate this problem, Baker[102] suggested the reaction of HOI with organic matter in particles to produce I^-. Pechtl et al.[225] modified the inorganic reaction mechanism of Vogt et al.,[6] especially improving the description of the cycling between HOI_{aq}, IO_3^-, and I^- and including reaction of HOI with organic material. They were able to reproduce measured iodine speciation (section 6) when the pseudo-first-order rate constant of this reaction was assumed to be at least 5×10^{-6} s^{-1}. This highlights the importance of further kinetic studies into the aqueous-phase production and cycling of organic iodine compounds.

The study by von Glasow et al.[288] employed the mechanisms of Vogt et al.[6] in a 1-D model. Maxima of ICl and IBr concentrations were calculated to be located below the inversion that caps the cloud-free MBL (pointing to the importance of acid-catalyzed cycling in the sea-salt aerosol), whereas maxima of IO and OIO were predicted to be near the ocean surface (i.e., near the source of the precursors).

Whereas the aforementioned studies aimed mainly at understanding the general cycling and speciation of iodine compounds, the following studies aimed at reproducing specific conditions encountered during field measurements. Stutz et al.[289] used a quasi-steady-state box model, which did not include the aerosol phase, to explain the measurements of iodine oxides at Mace Head. They reproduced the measured IO mixing ratios of around 6 pptv by prescribing the required precursor fluxes and found that for these conditions, cycles involving production of HOI by reaction of IO with HO_2 and subsequent photolysis of HOI would lead to an O_3 destruction rate of about 12.5 ppbv day^{-1}, whereas the IO self-reaction would lead to an O_3 destruction rate of about 3.8 ppbv day^{-1}.

McFiggans et al.[3] used a box model with a chemical scheme based on that of Vogt et al.[6] but without explicit treatment of the aerosol chemistry. The model was constrained with data from measurements and with iodine precursor fluxes to reproduce the measured IO concentration for field campaigns at Mace Head and Tenerife. They showed that under these conditions iodine chemistry was of similar importance to odd-hydrogen chemistry for ozone destruction, that uptake of iodine to aerosol particles could lead to significant enrichment of iodine in particles compared to seawater ratios, and that iodine chemistry would speed up denoxification of the marine boundary layer.

Peters et al.[106] compared field measurements from Brittany with a 1-D model that was initialized with field data. They were able to reproduce the observed mixing ratios of IO with the observed alkyl iodides as the only precursors. Even though I_2 was never measured above the rather high detection limit around 20 pptv, the model showed that the iodine chemistry could also be dominated by very small, and therefore undetectable, I_2 fluxes.

Bloss et al.[7] and Sommariva et al.[290] investigated different aspects of the influence of iodine chemistry on the photochemistry at Mace Head. They found with observationally constrained models that the IO + HO_2 reaction accounted for up to 40% of the HO_2 sink, whereas subsequent photolysis of HOI comprised up to 15% of the daytime OH source.[7] Sommariva et al.[290] confirmed these results and highlighted the relevance of the choice of uptake coefficients for HOI and HO_2 for the impact of iodine on HO_x photochemistry.

Read et al.[35] employed a box model to quantify the impact of measured BrO and IO concentrations on O_3 photochemistry and found that the daytime destruction of O_3 could only be explained by invoking halogen chemistry. If their data are indeed representative of large ocean regions, this would support the suggestions from previous model studies that halogen chemistry needs to be considered on a global scale. In a subsequent study with a 1-D model of the MBL, Mahajan et al.[22] showed that the "top-hat" diurnal profile of IO could not be modeled satisfactorily without invoking a daytime iodine source which peaked around noon. This could be indirect evidence for a photochemical source of I_2 or other photolabile iodine species from the sea surface (section 2.2).

Mahajan et al.[105] used a 1-D model to reproduce I_2 and IO measurements at a semipolluted environment, Roscoff. This study suggested that the $IONO_2$ + I reaction plays an important role in recycling iodine species, concluding that this recycling mechanism was needed to account for the observed levels of I_2 and IO at Roscoff.

The photochemistry of OIO (section 4.1.2) has confused the community for years. Stutz et al.[107] reported daytime measurements of OIO at Appledore Island under high NO_x concentrations, which they showed to be unreconcilable with the knowledge about iodine−NO_x interaction. They reported that there would have to be a fast recycling of $IONO_2$ to avoid it becoming the main iodine reservoir. They suggested the net reaction $IONO_2 + O_3 \rightarrow OIO + NO_2 + O_2$ with which they were able to reproduce the measurements of IO and OIO. More recent quantum dynamical calculations by Kaltsoyannis and Plane[39] suggested that the reaction −11 was more likely to explain the proposed rapid loss of $IONO_2$. The recent study by Gómez Martín et al.[37] showed the efficient photolysis of OIO, highlighting the need for yet another chemical mechanism to explain the daytime observations of OIO by Stutz et al.[107]

7.2.2.2. Iodine Oxide Particle Formation. This topic has been covered in detail in section 5, which describes the results from field campaigns[19,106,242,291] and laboratory experiments.[9−13,15] The box model study of Saiz-Lopez et al.[19] used an explicit nucleation scheme for higher iodine oxides from monomers to polymers and "real" aerosol particles. They showed that the assumption of higher iodine oxide concentrations in hot spots which are still consistent with the long-path DOAS measurements are sufficient to reproduce nucleation events in the model similar to those observed in the field. Pirjola et al.[251] analyzed the chamber data of Sellegri et al.[20] with a sectional model where stable thermodynamic clusters, the precursors for nucleation mode particles, are formed from OIO dimer formation. Coagulation of the particles was calculated taking the fractal particle geometry into account. The modeled results were in good agreement with the chamber studies. On the basis of their chamber results and a seaweed survey around Mace Head, Sellegri et al.[20] constructed an emission inventory and included it into a regional 3-D model. The modeled nucleation mode concentrations were about 5 times smaller than the observed ones, which might be caused by uncertainties in the seaweed distribution and possible chamber-specific effects that are reflected in the derived seaweed-mass−nucleation relationship. The model suggested that the plume of newly formed nucleation mode particles can reach up to 600 m in height 10 km inland of the seaweed areas.

On the basis of the experiments of Burkholder et al.,[9] Pechtl et al.[21] developed a two-step nucleation parametrization to investigate the homogeneous nucleation of OIO under various atmospheric conditions in a 1-D model where a column of air was assumed to be moving over "hot spots" with increased iodine precursor fluxes. For scenarios with clean marine air, OIO was found to contribute both to homogeneous nuclei formation and to growth of pre-existing clusters to detectable particle sizes. In model runs with initially polluted air (continental outflow), OIO concentrations were lower and the homogeneous nucleation could not compete with ternary H_2SO_4−NH_3−H_2O nucleation; however, they pointed out that OIO did contribute substantially to the "apparent" nucleation rate, even though they did not include the recycling of INO_3 in their model runs, which would have led to even higher OIO mixing ratios.[242,243]

7.3. Key Uncertainties

Even though a lot of new information regarding iodine chemistry has become available in the past decade, the main conclusions from the early model studies on iodine chemistry remain valid, i.e., that there is a lack of information in the following areas: the photochemistry of reactive iodine, e.g., gas-phase reactions of IO, OIO, and higher iodine oxides as well as iodine−NO_x interactions; aqueous-phase chemistry, especially to explain the observed particulate iodine speciation; and on the fluxes of alkyl iodides and inorganic iodine (particularly I_2) from the oceans and macroalgae exposed at low tide. Most data comes from the field campaigns at Mace Head and in Brittany; however, results from Appledore Island suggest that there might be some regional differences. This urges us to continue studying these processes at various locations to eventually be able to assess the importance of these processes on a regional and global scale.

Even though a lot of progress has been made, many important questions remain. There are still important gaps in our knowledge of the kinetics of reactions involving the higher iodine oxides, which hinder further progress in modeling, although recent laboratory and theoretical investigations have helped to elucidate the mechanisms. The details of new particle formation from iodine oxides are also not yet resolved. In terms of ozone destruction the relevance of these fairly localized events of very high iodine loadings might be limited, and although there are indications that the fine particles produced in these bursts can grow to CCN sizes, more studies are needed to test on what spatial scale this might be of relevance, especially when viewed in the context of competition with other continental particle sources.

AUTHOR INFORMATION

Corresponding Author

*E-mail: a.saiz-lopez@ciac.jccm-csic.es (A.S.-L); j.m.c.plane@leeds.ac.uk (J.M.C.P.).

BIOGRAPHIES

Alfonso Saiz-Lopez studied Chemistry in Ciudad Real, Spain. In 2005 he received his Ph.D. degree in Atmospheric Physical Chemistry

at the University of East Anglia, focused on absorption spectroscopy for atmospheric measurement and marine boundary layer halogen chemistry. After a brief postdoctoral stay at the University of Leeds, he was a NASA Postdoctoral Scholar at the Jet Propulsion Laboratory and Research Associate at the Harvard-Smithsonian Center for Astrophysics. In 2009 he moved to Toledo, Spain, where he was appointed Senior Research Scientist, and currently heads the Laboratory for Atmospheric and Climate Science at the Spanish Research Council (CSIC). Since 2009 he has been Affiliate Scientist at NCAR. His research group focuses on atmospheric measurement, modeling, and laboratory studies of tropospheric halogens.

John Plane was educated at Cambridge University (1976−1983). He was a Research Fellow at St. John's College, Cambridge, from 1982 to 1985 and then Associate Professor at the Rosenstiel School of Marine and Atmospheric Science, University of Miami. In 1991 he moved to the School of Environmental Sciences, University of East Anglia, becoming Professor of Environmental Science in 1999. He has been Professor of Atmospheric Chemistry in the School of Chemistry at the University of Leeds since 2006.

Alex Baker received his Ph.D. degree in Marine Chemistry from the University of Southampton in 1992 before conducting postdoctoral work at the University of the West Indies, University of Liverpool, and University of East Anglia. He has studied the marine and industrial chemistry of humic material and the biogeochemistry of trace metals in seawater and, since 1997, has worked primarily on aerosol biogeochemistry in the marine boundary layer. He is currently a Reader in Marine and Atmospheric Chemistry at the University of East Anglia.

Lucy Carpenter, born in Salisbury, England, received her B.Sc. (Hons) degree in Chemistry from the University of Bristol in 1991 and, following a gap year, studied for her Ph.D. degree in the subject of peroxy radicals in the lower atmosphere at the University of East Anglia under the supervision of Professor Stuart Penkett (awarded 1996). After postdoctoral research at UEA and the University of Leeds, she moved to the University of York as a Lecturer in 2000 and is currently a Professor in the Department of Chemistry. Her research addresses the atmospheric impacts of marine-derived trace gases, particularly organohalogens. In 2006 she was awarded a Philip Leverhulme prize in Earth Ocean and Atmospheric Sciences.

Roland von Glasow studied atmospheric physics in Mainz, Germany. His Ph.D. thesis, which he worked on at the Max-Planck-Institute for Chemistry in Mainz, Germany, focussed on reactive halogens and sea salt chemistry. After 2 years as a postdoctoral fellow at the Scripps Institution of Oceanography, San Diego, CA, he was awarded an Emmy Noether stipend by the German Deutsche Forschungsgemeinschaft which enabled him to start an independent Junior Research Group at the Institute of Environmental Physics at the University of Heidelberg, Germany. In 2007 he moved to the University of East Anglia, where he is a Reader in Atmospheric Chemistry. The work of his group focusses on tropospheric halogen chemistry (marine boundary layer, polar regions, volcanic plumes, salt lakes, free troposphere), links between halogen and sulfur

chemistry, the background chemistry of the marine boundary layer, and the microphysics of aerosols and clouds in the marine boundary layer.

Juan Carlos Gómez Martin studied Physics in Granada, Spain. He conducted his Ph.D. work on gas-phase halogen atmospheric photochemistry, kinetics, and spectroscopy at the Institute for Environmental Physics and Remote Sensing of the University of Bremen. After a brief postdoctoral study in Bremen, he was appointed as Post Doctoral Research Assistant in the School of Chemistry of the University of Leeds, where he worked for 2.5 years on the photochemistry and gas-to-particle conversion processes of mesospheric and tropospheric interest. In 2009 he moved to Toledo, Spain, where he works currently as Research Associate at the Laboratory for Atmospheric and Climate Science at the Spanish Research Council (CSIC). His research is focused on the design, development, and field deployment of spectroscopy-based instruments for in-situ measurements of halogen precursors, active halogens, and reservoir species.

Gordon McFiggans conducted his Ph.D. studies in Marine Boundary Layer Chemistry at the University of East Anglia, investigating multiphase halogen photochemistry and ultrafine particle formation before taking a Fellowship in the Atmospheric Physics Group in UMIST, modeling tropospheric multicomponent aerosol. He led the Reactive Halogens in the Marine Boundary Layer (RHaMBLe) consortium project and is currently Professor of Atmospheric Multiphase Processes in the Centre for Atmospheric Sciences at the University of Manchester.

Russell Saunders received his M.S. degree in Chemistry from the University of Bath in 2001 and Ph.D. degree for work on inorganic secondary aerosol formation and properties from the University of East Anglia (UEA), Norwich, in 2005. He then moved to the University of Leeds, where he is currently a postdoctoral researcher. His interests combine laboratory and modeling studies of iodine-containing aerosol and also 'meteoric smoke' particles comprised of iron, magnesium, and silicon oxides and metal silicate species.

REFERENCES

(1) Whitehead, D. C. *Environ. Int.* **1984**, *10*, 321.
(2) Chameides, W. L.; Davis, D. *J. Geophys. Res.* **1980**, *85*, 7383.
(3) McFiggans, G.; Plane, J. M. C.; Allan, B. J.; Carpenter, L. J.; Coe, H.; O'Dowd, C. *J. Geophys. Res., [Atmos.]* **2000**, *105*, 14371.
(4) Calvert, J. G.; Lindberg, S. E. *Atmos. Environ.* **2004**, *38*, 5087.
(5) Solomon, S.; García, R. R.; Ravishankara, A. R. *J. Geophys. Res.* **1994**, *99*, 20491.
(6) Vogt, R.; Sander, R.; Glasow, R. V.; Crutzen, P. J. *J. Atmos. Chem.* **1999**, *32*, 375.
(7) Bloss, W. J.; Lee, J. D.; Johnson, G. P.; Sommariva, R.; Heard, D. E.; Saiz-Lopez, A.; Plane, J. M. C.; McFiggans, G.; Coe, H.; Flynn, M.; Williams, P.; Rickard, A. R.; Fleming, Z. L. *Geophys. Res. Lett.* **2005**, *32*, L06814.
(8) Saiz-Lopez, A.; Plane, J. M. C.; Mahajan, A. S.; Anderson, P. S.; Bauguitte, S. J.-B.; Jones, A. E.; Roscoe, H. K.; Salmon, R. A.; Bloss, W. J.; Lee, J. D.; Heard, D. E. *Atmos. Chem. Phys.* **2008**, *8*, 887.
(9) Burkholder, J. B.; Curtius, J.; Ravishankara, A. R.; Lovejoy, E. R. *Atmos. Chem. Phys.* **2004**, *4*, 19.
(10) Saunders, R. W.; Plane, J. M. C. *Environ. Chem.* **2005**, *2*, 299.
(11) Saunders, R. W.; Plane, J. M. C. *J. Aerosol Sci.* **2006**, *37*, 1737.
(12) Saunders, R. W.; Mahajan, A. S.; Gómez Martín, J. C.; Kumar, R.; Plane, J. M. C. *Z. Phys. Chem. (Munich)* **2010**, *224*, 1095.
(13) McFiggans, G.; Coe, H.; Burgess, R.; Allan, J.; Cubison, M.; Alfarra, M. R.; Saunders, R.; Saiz-Lopez, A.; Plane, J. M. C.; Wevill, D. J.; Carpenter, L. J.; Rickard, A. R.; Monks, P. S. *Atmos. Chem. Phys.* **2004**, *4*, 701.
(14) Hoffmann, T.; O'Dowd, C. D.; Seinfeld, J. H. *Geophys. Res. Lett.* **2001**, *28*, 1949.
(15) Jimenez, J. L.; Bahreini, R.; Cocker, D. R., III; Zhuang, H.; Varutbangkul, V.; Flagan, R. C.; Seinfeld, J. H.; O'Dowd, C. D.; Hoffmann, T. *J. Geophys. Res.* **2003**, *108*, 4318.
(16) O'Dowd, C. D.; Geever, M.; Hill, M. K.; Smith, M. H.; Jennings, S. G. *Geophys. Res. Lett.* **1998**, *25*, 1661.
(17) O'Dowd, C. D.; Jimenez, J. L.; Bahreini, R.; Flagan, R. C.; Seinfeld, J. H.; Hameri, K.; Pirjola, L.; Kulmala, M.; Jennings, S. G.; Hoffmann, T. *Nature* **2002**, *417*, 632.
(18) Saiz-Lopez, A.; Plane, J. M. C. *Geophys. Res. Lett.* **2004**, *31*, L04112.

(19) Saiz-Lopez, A.; Plane, J. M. C.; McFiggans, G.; Williams, P. I.; Ball, S. M.; Bitter, M.; Jones, R. L.; Hongwei, C.; Hoffmann, T. *Atmos. Chem. Phys.* **2006**, *6*, 883.
(20) Sellegri, K.; Yoon, Y. J.; Jennings, S. G.; O'Dowd, C. D.; Pirjola, L.; Cautenet, S.; Chen, H.; Hoffmann, T. *Environ. Chem.* **2005**, *2*, 260.
(21) Pechtl, S.; Lovejoy, E. R.; Burkholder, J. B.; von Glasow, R. *Atmos. Chem. Phys.* **2006**, *6*, 505.
(22) Mahajan, A. S.; Plane, J. M. C.; Oetjen, H.; Mendes, L.; Saunders, R. W.; Saiz-Lopez, A.; Jones, C. E.; Carpenter, L. J.; McFiggans, G. B. *Atmos. Chem. Phys.* **2010**, *10*, 4611.
(23) Calvert, J. G.; Lindberg, S. E. *Atmos. Environ.* **2004**, *38*, 5105.
(24) Goodsite, M. E.; Plane, J. M. C.; Skov, H. *Environ. Sci. Technol.* **2004**, *38* (6), 1772.
(25) Simpson, W. R.; von Glasow, R.; Riedel, K.; Anderson, P.; Ariya, P.; Bottenheim, J.; Burrows, J.; Carpenter, L. J.; Frieß, U.; Goodsite, M. E.; Heard, D.; Hutterli, M.; Jacobi, H.-W.; Kaleschke, L.; Neff, B.; Plane, J.; Platt, U.; Richter, A.; Roscoe, H.; Sander, R.; Shepson, P.; Sodeau, J.; Steffen, A.; Wagner, T.; Wolff, E. *Atmos. Chem. Phys.* **2007**, *7*, 4375.
(26) Alicke, B.; Hebestreit, K.; Stutz, J.; Platt, U. *Nature* **1999**, *397*, 572.
(27) Allan, B. J.; McFiggans, G.; Plane, J. M. C.; Coe, H. *J. Geophys. Res., [Atmos.]* **2000**, *105*, 14363.
(28) Wada, R.; Beames, J.; Orr-Ewing, A. *J. Atmos. Chem.* **2007**, *58*, 69.
(29) Whalley, L.; Furneaux, K.; Gravestock, T.; Atkinson, H.; Bale, C.; Ingham, T.; Bloss, W.; Heard, D. *J. Atmos. Chem.* **2007**, *58*, 19.
(30) Bale, C.; Ingham, T.; Commane, R.; Heard, D.; Bloss, W. *J. Atmos. Chem.* **2008**, *60*, 51.
(31) Gómez Martín, J. C.; Blahins, J.; Gross, U.; Ingham, T.; Goddard, A.; Mahajan, A. S.; Ubelis, A.; Saiz-López, A. *Atmos. Meas. Tech.* **2011**, *4*, 29.
(32) Finley, B. D.; Saltzman, E. S. *J. Geophys. Res.* **2008**, *113*, D21301.
(33) Saiz-Lopez, A.; Chance, K.; Liu, X.; Kurosu, T. P.; Sander, S. P. *Geophys. Res. Lett.* **2007**, *34*, L12812.
(34) Schönhardt, A.; Richter, A.; Wittrock, F.; Kirk, H.; Oetjen, H.; Roscoe, H. K.; Burrows, J. P. *Atmos. Chem. Phys.* **2008**, *8*, 637.
(35) Read, K. A.; Mahajan, A. S.; Carpenter, L. J.; Evans, M. J.; Faria, B. V. E.; Heard, D. E.; Hopkins, J. R.; Lee, J. D.; Moller, S. J.; Lewis, A. C.; Mendes, L.; McQuaid, J. B.; Oetjen, H.; Saiz-Lopez, A.; Pilling, M. J.; Plane, J. M. C. *Nature* **2008**, *453*, 1232.
(36) Dillon, T. J.; Tucceri, M. E.; Sander, R.; Crowley, J. N. *Phys. Chem. Chem. Phys.* **2008**, *10*, 1540.
(37) Gómez Martín, J. C.; Ashworth, S. H.; Mahajan, A. S.; Plane, J. M. C. *Geophys. Res. Lett.* **2009**, *36*, L09802.
(38) Gravestock, T.; Blitz, M. A.; Heard, D. E. *Phys. Chem. Chem. Phys.* **2005**, *7*, 2173.
(39) Kaltsoyannis, N.; Plane, J. M. C. *Phys. Chem. Chem. Phys.* **2008**, *10*, 1723.
(40) Plane, J. M. C.; Joseph, D. M.; Allan, B. J.; Ashworth, S. H.; Francisco, J. S. *J. Phys. Chem. A* **2006**, *110*, 93.
(41) Joseph, D. M.; Ashworth, S. H.; Plane, J. M. C. *Phys. Chem. Chem. Phys.* **2007**, *9*, 5599.
(42) Carpenter, L. J. *Chem. Rev.* **2003**, *103* (12), 4953.
(43) von Glasow, R.; Crutzen, P. J. In *Treatise on Geochemistry*; Heinrich, D. H., Karl, K. T., Eds.; Pergamon: Oxford, 2003; Vol. 4.
(44) von Glasow, R.; Crutzen, P. J. In *Treatise on Geochemistry*; Heinrich, D. H., Karl, K. T., Eds.; Pergamon: Oxford, 2007; Vol. 4.02.
(45) Bell, N.; Hsu, L.; Jacob, D. J.; Schultz, M. G.; Blake, D. R.; Butler, J. H.; King, D. B.; Lobert, J. M.; Maier-Reimer, E. *J. Geophys. Res.* **2002**, *107* (D17), 4340.
(46) Ko, M. K. W.; Poulet, G.; Blake, D. R.; Boucher, O.; Burkholder, J. H.; Chin, M.; Cox, R. A.; George, C.; Graf, H.-F.; Holton, J. R.; Jacob, D. J.; Law, K. S.; Lawrence, M. G.; Midgley, P. M.; Seakins, P. W.; Shallcross, D. E.; Strahan, S. E.; Wuebbles, D. J.; Yokouchi, Y.; Blake, N. J.; Butler, J. H.; Douglass, A. R.; Dvortsov, V. L.; Folkins, I.; Haynes, P. H.; Mellouki, A.; Prather, M. J.; Rodríguez, J. M.; Schauffler, S. M.; Shepherd, T. G.; Textor, C.; Timmreck, C.; Weisenstein, D. K. *Very short-lived halogen and sulfur substances, Chapter 2 in Scientific Assessment of Ozone Depletion:* 2006; Global Ozone Research and Monitoring Project; Report no. 50; World Meteorological Organization (WMO): Geneva, 2007; 572 pp.
(47) Law, K. S.; Sturges, W. T.; Blake, D. R.; Blake, N. J.; Burkholder, J. B.; Butler, J. H.; Cox, R. A.; Haynes, P. H.; Ko, M. K. W.; Kreher, K.; Mari, C.; Pfeilsticker, K.; Plane, J. M. C.; Salawitch, R. J.; Schiller, C.; Sinnhuber, B.-M.; Glasow, R. v.; Warwick, N. J.; Wuebbles, D. J.; Yvon-Lewis, S. A.; Butz, A.; Considine, D. B.; Dorf, M.; Froidevaux, L.; Kovalenko, L. J.; Livesey, N. J.; Nassar, R.; Sioris, C. E.; Weisenstein, D. K. *Halogenated very short-lived substances, Chapter 2 in Scientific Assessment of Ozone Depletion:* 2006; Global Ozone Research and Monitoring Project; Report no. 50; World Meteorological Organization (WMO): Geneva, 2007; 572 pp.
(48) Butler, J. H.; King, D. B.; Lobert, J. r. M.; Montzka, S. A.; Yvon-Lewis, S. A.; Hall, B. D.; Warwick, N. J.; Mondeel, D. J.; Aydin, M.; Elkins, J. W. *Global Biogeochem. Cycles* **2007**, *21*, GB1023.
(49) Chuck, A. L.; Turner, S. M.; Liss, P. S. *J. Geophys. Res.* **2005**, *110*, C10022.
(50) Yokouchi, Y.; Osada, K.; Wada, M.; Hasebe, F.; Agama, M.; Murakami, R.; Mukai, H.; Nojiri, Y.; Inuzuka, Y.; Toom-Sauntry, D.; Fraser, P. *J. Geophys. Res.* **2008**, *113*, D18311.
(51) Happell, J. D.; Wallace, D. W. R. *Geophys. Res. Lett.* **1996**, *23*, 2105.
(52) Moore, R. M.; Zafiriou, O. C. *J. Geophys. Res.* **1994**, *99*, 16415.
(53) Giese, B.; Laturnus, F.; Adams, F. C.; Wiencke, C. *Environ. Sci. Technol.* **1999**, *33*, 2432.
(54) Jones, C. E.; Hornsby, K. E.; Sommariva, R.; Dunk, R. M.; von Glasow, R.; McFiggans, G.; Carpenter, L. J. *Geophys. Res. Lett.* **2010**, *37*, L18804.
(55) Moore, R. M.; Webb, M.; Tokarczyk, R.; Wever, R. *J. Geophys. Res.* **1996**, *101*, 20899.
(56) Jammoul, A.; Dumas, S.; D'Anna, B.; George, C. *Atmos. Chem. Phys.* **2009**, *9*, 4229.
(57) Martino, M.; Mills, G. P.; Woeltjen, J.; Liss, P. S. *Geophys. Res. Lett.* **2009**, *36*, L01609.
(58) Reeser, D. I.; Jammoul, A.; Clifford, D.; Brigante, M.; D'Anna, B.; George, C.; Donaldson, D. J. *J. Phys. Chem. C* **2008**, *113*, 2071.
(59) Martino, M.; Liss, P. S.; Plane, J. M. C. *Environ. Sci. Technol.* **2005**, *39*, 7097.
(60) Jones, C. E.; Carpenter, L. J. *Environ. Sci. Technol.* **2005**, *39*, 6130.
(61) Dixneuf, S.; Ruth, A. A.; Vaughan, S.; Varma, R. M.; Orphal, J. *Atmos. Chem. Phys.* **2009**, *9*, 823.
(62) Küpper, F. C.; Carpenter, L. J.; McFiggans, G. B. *Proc. Natl. Acad. Sci. U.S.A.* **2008**, *105* (19), 6954.
(63) Palmer, C. J.; Anders, T. L.; Carpenter, L. J.; Küpper, F. C.; McFiggans, G. B. *Environ. Chem.* **2005**, *2*, 282.
(64) Jones, C. E.; Hornsby, K. E.; Dunk, R. M.; Leigh, R. J.; Carpenter, L. J. *Atmos. Chem. Phys.* **2009**, *9*, 8757.
(65) Carpenter, L. J.; Malin, G.; Liss, P. S.; Kupper, F. C. *Global Biogeochem. Cycles* **2000**, *14*, 1191.
(66) Blake, N. J.; Blake, D. R.; Chen, T.-Y.; J., C., Jr.; Sachse, G.; Anderson, B.; Rowland, F. S. *J. Geophys. Res.* **1997**, *102* (D23), 28315.
(67) Yokouchi, Y.; Nojiri, Y.; Barrie, L. A.; Toom-Sauntry, D.; Fujinuma, Y. *J. Geophys. Res.* **2001**, *106*, 12661.
(68) Archer, S. D.; Goldson, L. E.; Liddicoat, M. I.; Cummings, D. G.; Nightingale, P. D. *J. Geophys. Res.* **2007**, *112*, C08009.
(69) Cohan, D. S.; Sturrock, G. A.; Biazar, A. P.; Fraser, P. J. *J. Atmos. Chem.* **2003**, *44*, 131.
(70) Sive, B. C.; Varner, R. K.; Mao, H.; Blake, D. R.; Wingenter, O. W.; Talbot, R. *Geophys. Res. Lett.* **2007**, *34*, L17808.
(71) Klick, S. *Limnol. Oceanogr.* **1992**, *37*, 1579.
(72) Moore, R. M.; Groszko, W. *J. Geophys. Res.* **1999**, *104*, 11163.
(73) Williams, J.; Gros, V.; Atlas, E.; Maciejczyk, K.; Batsaikhan, A.; Schöler, H. F.; Forster, C.; Quack, B.; Yassaa, N.; Sander, R.; Van Dingenen, R. *J. Geophys. Res.* **2007**, *112*, D07302.
(74) Smythe-Wright, D.; Boswell, S. M.; Breithaupt, P.; Davidson, R. D.; Dimmer, C. H.; Eiras Diaz, L. B. *Global Biogeochem. Cycles* **2006**, *20*, GB3003.

(75) Brownell, D. K.; Moore, R. M.; Cullen, J. J. *Global Biogeochem. Cycles* **2010**, *24*, GB2002.
(76) Butler, J. H.; Bell, T. G.; Hall, B. D.; Quack, B.; Carpenter, L. J.; Williams, J. *Atmos. Chem. Phys.* **2010**, *10*, 327.
(77) Singh, H. B.; Salas, L. J.; Stiles, R. E. *J. Geophys. Res.* **1983**, *88*, 3684.
(78) Carpenter, L. J.; Sturges, W. T.; Penkett, S. A.; Liss, P. S.; Alicke, B.; Hebestreit, K.; Platt, U. *J. Geophys. Res., [Atmos.]* **1999**, *104*, 1679.
(79) Pedersén, M.; Collén, J.; K., A.; Ekdahl, A. *Sci. Mar.* **1996**, *60*, 257.
(80) Carpenter, L. J.; Liss, P. S.; Penkett, S. A. *J. Geophys. Res.* **2003**, *108*, 4256.
(81) Manley, S. L.; Dastoor, M. N. *Limnol. Oceanogr.* **1987**, *32*, 709.
(82) Yokouchi, Y.; Hasebe, F.; Fujiwara, M.; Takashima, H.; Shiotani, M.; Nishi, N.; Kanaya, Y.; Hashimoto, S.; Fraser, P.; Toom-Sauntry, D.; Mukai, H.; Nojiri, Y. *J. Geophys. Res.* **2005**, *110*, D23309.
(83) Moore, R. M.; Tokarczyk, R. *Geophys. Res. Lett.* **1992**, *19*, 1779.
(84) Yamamoto, H.; Yokouchi, Y.; Otsuki, A.; Itoh, H. *Chemosphere* **2001**, *45*, 371.
(85) Hughes, C.; Malin, G.; Nightingale, P. D.; Liss, P. S. *Limnol. Oceanogr.* **2006**, *51*, 2849.
(86) Itoh, N.; Tsujita, M.; Ando, T.; Hisatomi, G.; Higashi, T. *Phytochemistry* **1997**, *45*, 67.
(87) Amachi, S.; Kamagata, Y.; Kanagawa, T.; Muramatsu, Y. *Appl. Environ. Microbiol.* **2001**, *67*, 2718.
(88) Arnold, S. R.; Spracklen, D. V.; Gebhardt, S.; Custer, T.; Williams, J.; Peeken, I.; Alvain, S. *Environ. Chem.* **2010**, *7*, 232.
(89) Nightingale, P. D.; Malin, G.; Law, C. S.; Watson, A. J.; Liss, P. S.; Liddicoat, M. I.; Boutin, J.; Upstill-Goddard, R. C. *Global Biogeochem. Cycles* **2000**, *14* (1), 373.
(90) Leigh, R. J.; Ball, S. M.; Whitehead, J.; Leblanc, C.; Shillings, A. J. L.; Mahajan, A. S.; Oetjen, H.; Dorsey, J. R.; Gallagher, M.; Jones, R. L.; Plane, J. M. C.; Potin, P.; McFiggans, G. *Atmos. Chem. Phys.* **2010**, *10*, 11823.
(91) Ball, S. M.; Hollingsworth, A. M.; Humbles, J.; Leblanc, C.; Potin, P.; McFiggans, G. *Atmos. Chem. Phys.* **2010**, *10*, 6237.
(92) Nitschke, U.; Ruth, A.; Dixneuf, S.; Stengel, D. *Planta* **2010**, *233*, 737.
(93) Garland, J. A.; Elzerman, A. W.; Penkett, S. A. *J. Geophys. Res.* **1980**, *85*, 7488.
(94) Miyake, Y.; Tsunogai, S. *J. Geophys. Res.* **1963**, *68*, 3989.
(95) Möller, A.; Lovric, M.; Scholz, F. *Int. J. Environ. Anal. Chem.* **1996**, *63*, 99.
(96) Truesdale, V. W. *Mar. Chem.* **2007**, *12*, 3.
(97) Garland, J. A.; Curtis, H. *J. Geophys. Res.* **1981**, *86*, 3183.
(98) Zingler, J.; Platt, U. *J. Geophys. Res.* **2005**, *110*, D07307.
(99) Hill, V. L.; Manley, S. L. *Limnol. Oceanogr.* **2009**, *54*, 812.
(100) Saiz-Lopez, A.; Boxe, C. S. *Atmos. Chem. Phys. Disc* **2008**, *8*, 2953.
(101) Baker, A. R.; Tunnicliffe, C.; Jickells, T. D. *J. Geophys. Res., [Atmos.]* **2001**, *106*, 28743.
(102) Baker, A. R. *Environ. Chem.* **2005**, *2*, 295.
(103) Gilfedder, B. S.; Lai, S.; Petri, M.; Biester, H.; Hoffmann, T. *Atmos. Chem. Phys.* **2008**, *8*, 6069.
(104) Seitz, K.; Buxmann, J.; Pöhler, D.; Sommer, T.; Tschritter, J.; O'Dowd, C.; Platt, U. *Atmos. Chem. Phys.* **2010**, *10*, 2117.
(105) Mahajan, A. S.; Oetjen, H.; Saiz-Lopez, A.; Lee, J. D.; McFiggans, G. B.; Plane, J. M. C. *Geophys. Res. Lett.* **2009**, *36*, L16803.
(106) Peters, C.; Pechtl, S.; Stutz, J.; Hebestreit, K.; Hönninger, G.; Heumann, K. G.; Schwarz, A.; Winterlik, J.; Platt, U. *Atmos. Chem. Phys.* **2005**, *5*, 3357.
(107) Stutz, J.; Pikelnaya, O.; Hurlock, S. C.; Trick, S.; Pechtl, S.; von Glasow, R. *Geophys. Res. Lett.* **2007**, *34*, L22816.
(108) Butz, A.; Boesch, H.; Camy-Peyret, C.; Chipperfield, M. P.; Dorf, M.; Kreycy, S.; Kritten, L.; Prados-Roman, C.; Schwaerzle, J.; Pfeilsticker, K. *Atmos. Chem. Phys.* **2009**, *9*, 7229.
(109) Frieß, U.; Wagner, T.; Pundt, I.; Pfeilsticker, K.; Platt, U. *Geophys. Res. Lett.* **2001**, *28*, 1941.
(110) Allan, B. J.; Plane, J. M. C.; McFiggans, G. *Geophys. Res. Lett.* **2001**, *28*, 1945.
(111) Mahajan, A. S.; Sorribas, M.; Gómez Martín, J. C.; MacDonald, S. M.; Gil, M.; Plane, J. M. C.; Saiz-Lopez, A. *Atmos. Chem. Phys.* **2010**, *10*, 27227.
(112) Bitter, M.; Ball, S. M.; Povey, I. M.; Jones, R. L. *Atmos. Chem. Phys.* **2005**, *5*, 2547.
(113) Saiz-Lopez, A.; Shillito, J. A.; Coe, H.; Plane, J. M. C. *Atmos. Chem. Phys.* **2006**, *6*, 1513.
(114) Commane, R.; Seitz, K.; Bale, C. S. E.; Bloss, W. J.; Buxmann, J.; Ingham, T.; Platt, U.; Pöhler, D.; Heard, D. E. *Atmos. Chem. Phys.* **2011**, *11*, 6721.
(115) Furneaux, K. L.; Whalley, L. K.; Heard, D. E.; Atkinson, H. M.; Bloss, W. J.; Flynn, M. J.; Gallagher, M. W.; Ingham, T.; Kramer, L.; Lee, J. D.; Leigh, R.; McFiggans, G. B.; Mahajan, A. S.; Monks, P. S.; Oetjen, H.; Plane, J. M. C.; Whitehead, J. D. *Atmos. Chem. Phys.* **2010**, *10*, 3645.
(116) Huang, R. J.; Seitz, K.; Buxmann, J.; Pöhler, D.; Hornsby, K. E.; Carpenter, L. J.; Platt, U.; Hoffmann, T. *Atmos. Chem. Phys.* **2010**, *10*, 4823.
(117) Mahajan, A. S.; Plane, J. M. C.; Oetjen, H.; Mendes, L.; Saunders, R. W.; Saiz-Lopez, A.; Jones, C. E.; Carpenter, L. J.; McFiggans, G. B. *Atmos. Chem. Phys.* **2010**, *10*, 4611.
(118) Großmann, K.; Tschritter, J.; Holla, R.; Pöhler, D.; Frieß, U.; Platt, U. *Geophys. Res. Abs.* **2011**, *13*, EGU2011–8054−1.
(119) Lampel, J.; Niebling, S.; Tschritter, J.; Frieß, U.; Platt, U. *Geophys. Res. Abs.* **2011**, *13*, EGU2011–11845.
(120) Oetjen, H. Ph.D. Thesis, University of Bremen, Bremen, Germany, 2009.
(121) Volkamer, R.; Coburn, S.; Dix, B.; Lechner, M.; Sinreich, R.; Duhl, T.; Guenther, A. *Geophys. Res. Abs.* **2011**, *13*, EGU2011–13678.
(122) Großmann, K.; Frieß, U.; Tschritter, J.; Peters, E.; Wittrock, F.; Quack, B.; Krüger, K.; von Glasow, R.; Sommariva, R.; Pfeilsticker, K.; Platt, U. *Geophys. Res. Abs.* **2011**, *13*, EGU2011–12176−2.
(123) Peters, E.; Großmann, K.; Frieß, U.; Wittrock, F.; Richte, A.; Burrows, J. P. *Geophys. Res. Abs.* **2011**, *13*, EGU2011–758.
(124) Schönhardt, A. Ph.D. Thesis, University of Bremen, Bremen, Germany, 2009.
(125) Puentedura, O.; Gil, M.; Saiz-Lopez, A.; Hay, T.; Navarro-Comas, M.; Gómez-Pelaez, A.; Cuevas, E.; Iglesias, J. *Atmos. Chem. Phys. Discuss.* **2011**, *11*, 27833.
(126) Saiz-Lopez, A.; Mahajan, A. S.; Salmon, R. A.; Bauguitte, S. J.-B.; Jones, A. E.; Roscoe, H. K.; Plane, J. M. C. *Science* **2007**, *317*, 348.
(127) Frieβ, U.; Deutschmann, T.; Gilfedder, B. S.; Weller, R.; Platt, U. *Atmos. Chem. Phys.* **2010**, *10*, 2439.
(128) Atkinson, H. M.; Roscoe, H. K.; Liss, P.; Hughes, C. In *International Polar Year Oslo Science Conference*; Elsevier: Oslo, Norway, 2010.
(129) Sirois, A.; Barrie, L. A. *J. Geophys. Res.* **1999**, *104*, 11599.
(130) Martinez, M.; Arnold, T.; Perner, D. *Ann. Geophys.* **1999**, *17*, 941.
(131) Hönninger, G. Ph.D. Thesis, University of Heidelberg, Heidelberg, Germany, 2002.
(132) Mahajan, A. S.; Shaw, M.; Oetjen, H.; Hornsby, K. E.; Carpenter, L. J.; Kaleschke, L.; Tian-Kunze, X.; Lee, J. D.; Moller, S. J.; Edwards, P.; Commane, R.; Ingham, T.; Heard, D. E.; Plane, J. M. C. *J. Geophys. Res., [Atmos.]* **2010**, *115*, D20303.
(133) Smoydzin, L. Ph.D. Thesis, University of Heidelberg, Heidelberg, Germany, 2008.
(134) Aiuppa, A.; Federico, C.; Franco, A.; Giudice, G.; Gurrieri, S.; Inguaggiato, S.; Liuzzo, M.; McGonigle, A. J. S.; Valenza, M. *Geochem. Geophys. Geosyst.* **2005**, *6*, Q08008.
(135) Wennberg, P. O.; Brault, J. W.; Hanisco, T. F.; Salawitch, R. J.; Mount, G. H. *J. Geophys. Res.* **1997**, *102*, 8887.
(136) Pundt, I.; Pommereau, J.-P.; Phillips, C.; Lateltin, E. *J. Atmos. Chem.* **1998**, *30*, 173.
(137) Bösch, H.; Camy-Peyret, C.; Chipperfield, M. P.; Fitzenberger, R.; Harder, H.; Platt, U.; Pfeilsticker, K. *J. Geophys. Res.* **2003**, *108*, 4455.
(138) Berthet, G. l.; Renard, J.-B.; Chartier, M.; Pirre, M.; Robert, C. *J. Geophys. Res.* **2003**, *108*, 4161.

(139) Wittrock, F.; Müler, R.; Richter, A.; Bovensmann, H.; Burrows, J. P. *Geophys. Res. Lett.* **2000**, *27*, 1471.
(140) Bedjanian, Y.; Poulet, G. *Chem. Rev.* **2003**, *103*, 4639.
(141) Rossi, M. J. *Chem. Rev.* **2003**, *103*, 4823.
(142) Herrmann, H. *Chem. Rev.* **2003**, *103*, 4691.
(143) Atkinson, R.; Baulch, D. L.; Cox, R. A.; Crowley, J. N.; Hampson, R. F.; Hynes, R. G.; Jenkin, M. E.; Rossi, M. J.; Troe, J. *Atmos. Chem. Phys.* **2007**, *7*, 981.
(144) Sander, S. P.; Orkin, V. L.; Kurylo, M. J.; Golden, D. M.; Huie, R. E.; Kolb, C. E.; Finlayson-Pitts, B. J.; Molina, M. J.; Friedl, R. R.; Ravishankara, A. R.; Moortgat, G. K.; Keller-Rudek, H.; Wine, P. H. *Chemical kinetics and photochemical data for use in atmospheric studies*; Jet Propulsion Laboratory, California Institute of Technology: Pasadena, CA, 2006.
(145) Dillon, T. J.; Tucceri, M. E.; Hölscher, D.; Crowley, J. N. *J. Photochem. Photobiol., A* **2005**, *176* (1−3), 3.
(146) Gómez Martín, J. C.; Spietz, P.; Burrows, J. P. *J. Photochem. Photobiol., A* **2005**, *176*, 15.
(147) Harwood, M. H.; Burkholder, J. B.; Hunter, M.; Fox, R. W.; Ravishankara, A. R. *J. Phys. Chem. A* **1997**, *101*, 853.
(148) Gravestock, T. J. Ph.D. Thesis, University of Leeds: Leeds, U.K., 2006.
(149) Spietz, P.; Gómez Martín, J. C.; Burrows, J. P. *J. Photochem. Photobiol., A* **2005**, *176*, 50.
(150) Bloss, W. J.; Rowley, D. M.; Cox, R. A.; Jones, R. L. *J. Phys. Chem. A* **2001**, *105*, 7840.
(151) Gómez Martín, J. C. CIAC-CSIC, Unpublished work, 2011
(152) Laszlo, B.; Kurylo, M. J.; Huie, R. E. *J. Phys. Chem.* **1995**, *99*, 11701.
(153) Joseph, D. M.; Ashworth, S. H.; Plane, J. M. C. *J. Photochem. Photobiol., A* **2005**, *176*, 68.
(154) Tucceri, M. E.; Hölscher, D.; Rodriguez, A.; Dillon, T. J.; Crowley, J. N. *Phys. Chem. Chem. Phys.* **2006**, *8*, 834.
(155) Cox, R. A.; Bloss, W. J.; Jones, R. L.; Rowley, D. M. *Geophys. Res. Lett.* **1999**, *26*, 1857.
(156) Saiz-Lopez, A.; Saunders, R. W.; Joseph, D. M.; Ashworth, S. H.; Plane, J. M. C. *Atmos. Chem. Phys.* **2004**, *4*, 1443.
(157) Ingham, T.; Cameron, M.; Crowley, J. N. *J. Phys. Chem. A* **2000**, *104*, 8001.
(158) Ashworth, S. H.; Allan, B. J.; Plane, J. M. C. *Geophys. Res. Lett.* **2002**, *29*, 1456.
(159) Peterson, K. A. *Mol. Phys.* **2010**, *108*, 393.
(160) Gómez Martín, J. C.; Plane, J. M. C. *Chem. Phys. Lett.* **2009**, *474*, 79.
(161) Cox, R. A.; Coker, G. B. *J. Phys. Chem.* **1983**, *87*, 4478.
(162) Chambers, R. M.; Heard, A. C.; Wayne, R. P. *J. Phys. Chem.* **1992**, *96*, 3321.
(163) Vipond, A.; Canosa-Mas, C. E.; Flugge, M. L.; Gray, D. J.; Shallcross, D. E.; Shaha, D.; Wayne, R. P. *Phys. Chem. Chem. Phys.* **2002**, *4*, 3648.
(164) Atkinson, R.; Baulch, D. L.; Cox, R. A.; Crowley, J. N.; Hampson, R. F.; Hynes, R. G.; Jenkin, M. E.; Rossi, M. J.; Troe, J. *Evaluated kinetic and photochemical data for atmospheric chemistry*; http://www.iupac-kinetic.ch.cam.ac.uk/ (accessed Dec 2010).
(165) Marshall, P. In *Advances in Quantum Chemistry*; Goodsite, M. E. and Johnson, M. S., Eds.; Academic Press: London, 2008; Vol. 55.
(166) Mössinger, J. C.; Rowley, D. M.; Cox, R. A. *Atmos. Chem. Phys.* **2002**, *2*, 227.
(167) Burkholder, J. B.; Ravishankara, A. R.; Solomon, S. *J. Geophys. Res.* **1995**, *100*, 16793.
(168) Cotter, E. S. N.; Booth, N. J.; Canosa-Mas, C. E.; Gray, D. J.; Shallcross, D. E.; Wayne, R. P. *Phys. Chem. Chem. Phys.* **2001**, *3*, 402.
(169) Cotter, E. S. N.; Booth, N. J.; Canosa-Mas, C. E.; Wayne, R. P. *Atmos. Environ.* **2001**, *35*, 2169.
(170) Cotter, E. S. N.; Canosa-Mas, C. E.; Manners, C. R.; Wayne, R. P.; Shallcross, D. E. *Atmos. Environ.* **2003**, *37*, 1125.
(171) Carl, S. A.; Crowley, J. N. *Atmos. Chem. Phys.* **2001**, *1*, 1.
(172) Nakano, Y.; Ishiwata, T.; Kawasaki, M. *J. Phys. Chem. A* **2005**, *109*, 6527.
(173) Nakano, Y.; Ukeguchi, H.; Ishiwata, T. *Chem. Phys. Lett.* **2006**, *430*, 235.
(174) Ayhens, Y. V.; Nicovich, J. M.; McKee, M. L.; Wine, P. H. *J. Phys. Chem. A* **1997**, *101*, 9382.
(175) Enami, S.; Hashimoto, S.; Kawasaki, M.; Nakano, Y.; Ishiwata, T.; Tonokura, K.; Wallington, T. J. *J. Phys. Chem. A* **2005**, *109*, 1587.
(176) Enami, S.; Yamanaka, T.; Hashimoto, S.; Kawasaki, M.; Tonokura, K. *J. Phys. Chem. A* **2005**, *109*, 6066.
(177) Enami, S.; Sakamoto, Y.; Yamanaka, T.; Hashimoto, S.; Kawasaki, M.; Tonokura, K.; Tachikawa, H. *Bull. Chem. Soc. Jpn.* **2008**, *81*, 1250.
(178) Gravestock, T. J.; Blitz, M. A.; Heard, D. E. *J. Phys. Chem. A* **2008**, *112*, 9544.
(179) Dookwah-Roberts, V.; Nicovich, J. M.; Wine, P. H. *J. Phys. Chem. A* **2008**, *112*, 9535.
(180) Orlando, J. J.; Piety, C. A.; Nicovich, J. M.; McKee, M. L.; Wine, P. H. *J. Phys. Chem. A* **2005**, *109*, 6659.
(181) Enami, S.; Yamanaka, T.; Hashimoto, S.; Kawasaki, M.; Tonokura, K.; Tachikawa, H. *Chem. Phys. Lett.* **2007**, *445*, 152.
(182) Wayne, R. P.; Poulet, G.; Biggs, P.; Burrows, J. P.; Cox, R. A.; Crutzen, P. J.; Hayman, G. D.; Jenkin, M. E.; Bras, G. L.; Moortgat, G. K.; Platt, U.; Schindler, R. N. *Atmos. Environ.* **1995**, *29*, 2677.
(183) Nakano, Y.; Enami, S.; Nakamichi, S.; Aloisio, S.; Hashimoto, S.; Kawasaki, M. *J. Phys. Chem. A* **2003**, *107*, 6381.
(184) Enami, S.; Ueda, J.; Goto, M.; Nakano, Y.; Aloisio, S.; Hashimoto, S.; Kawasaki, M. *J. Phys. Chem. A* **2004**, *108*, 6347.
(185) Eskola, A. J.; Wojcik-Pastuszka, D.; Ratajczak, E.; Timonen, R. S. *Phys. Chem. Chem. Phys.* **2006**, *8*, 1416.
(186) Stefanopoulos, V. G.; Papadimitriou, V. C.; Lazarou, Y. G.; Papagiannakopoulos, P. *J. Phys. Chem. A* **2008**, *112*, 1526.
(187) Sehested, J.; Ellermann, T.; Nielsen, O. J. *Int. J. Chem. Kinet.* **1994**, *26*, 259.
(188) Masaki, A.; Tsunashima, S.; Washida, N. *J. Phys. Chem.* **1995**, *99*, 13126.
(189) Dillon, T. J.; Tucceri, M. E.; Crowley, J. N. *Phys. Chem. Chem. Phys.* **2006**, *8*, 5185.
(190) Larin, I. K.; Nevozhai, D. V.; Spasskii, A. I.; Trofimova, E. M.; Turkin, L. E. *Kinet. Catal.* **1999**, *40*, 487.
(191) Gómez Martín, J. C.; Spietz, P.; Burrows, J. P. *J. Phys. Chem. A* **2007**, *111*, 306.
(192) Sander, S. P. *J. Phys. Chem.* **1986**, *90* (10), 2194.
(193) Drougas, E.; Kosmas, A. M. *J. Phys. Chem. A* **2005**, *109*, 3887.
(194) Enami, S.; Hoshino, Y.; Kawasaki, M. *Int. J. Chem. Kinet.* **2007**, *39*, 688.
(195) Papayannis, D. K.; Kosmas, A. M. *Chem. Phys. Lett.* **2006**, *432*, 391–39.
(196) Tucceri, M. E.; Dillon, T. J.; Crowley, J. N. *Phys. Chem. Chem. Phys.* **2005**, *7*, 1657.
(197) Buben, S. N.; Larin, I. K.; Messineva, N. A.; Trofimova, E. M. *Sov. J. Chem. Phys.* **1991**, *8*, 200.
(198) Mellouki, A.; Laverdet, G.; Jourdain, J. L.; Poulet, G. *Int. J. Chem. Kinet.* **1989**, *21*, 1161.
(199) van den Bergh, H.; Troe, J. *J. Chem. Phys.* **1976**, *64*, 736.
(200) Dillon, T. J.; Blitz, M. A.; Heard, D. E. *J. Phys. Chem. A* **2006**, *110*, 6995.
(201) Allan, B. J.; Plane, J. M. C. *J. Phys. Chem. A* **2002**, *106*, 8634.
(202) Daykin, E. P.; Wine, P. H. *J. Phys. Chem.* **1990**, *94*, 4528.
(203) Hölscher, D.; Zellner, R. *Phys. Chem. Chem. Phys.* **2002**, *4*, 1839.
(204) Maguin, F.; Laverdet, G.; Le Bras, G.; Poulet, G. *J. Phys. Chem.* **1992**, *96*, 1775.
(205) Golden, D. M. *J. Phys. Chem. A* **2005**, *110*, 2940.
(206) Maguin, F.; Mellouki, A.; Laverdet, G.; Poulet, G.; LeBras, G. *Int. J. Chem. Kinet.* **1991**, *23*, 237.
(207) Barnes, I.; Bastian, V.; Becker, K. H.; Overath, R. D. *Int. J. Chem. Kinet.* **1991**, *23*, 579.
(208) Knight, G. P.; Crowley, J. N. *Phys. Chem. Chem. Phys.* **2001**, *3*, 393.

(209) Dillon, T. J.; Karunanandan, R.; Crowley, J. N. *Phys. Chem. Chem. Phys.* **2006**, *8*, 847.
(210) Drougas, E.; Kosmas, A. M. *J. Phys. Chem. A* **2007**, *111*, 3402.
(211) Bale, C. S. E.; Canosa-Mas, C. E.; Shallcross, D. E.; Wayne, R. P. *Phys. Chem. Chem. Phys.* **2005**, *7*, 2164.
(212) Enami, S.; Yamanaka, T.; Hashimoto, S.; Kawasaki, M.; Nakano, Y.; Ishiwata, T. *J. Phys. Chem. A* **2006**, *110*, 9861.
(213) Braban, C. F.; Adams, J. W.; Rodriguez, D.; Cox, R. A.; Crowley, J. N.; Schuster, G. *Phys. Chem. Chem. Phys.* **2007**, *9*, 3136.
(214) Holmes, N. S.; Adams, J. W.; Crowley, J. N. *Phys. Chem. Chem. Phys.* **2001**, *3*, 1679.
(215) Mössinger, J. C.; Cox, R. A. *J. Phys. Chem. A* **2001**, *105*, 5165.
(216) Enami, S.; Vecitis, C. D.; Cheng, J.; Hoffmann, M. R.; Colussi, A. J. *J. Phys. Chem. A* **2007**, *111*, 8749.
(217) Sakamoto, Y.; Yabushita, A.; Kawasaki, M.; Enami, S. *J. Phys. Chem. A* **2009**, *113*, 7707.
(218) Hayase, S.; Yabushita, A.; Kawasaki, M.; Enami, S.; Hoffmann, M. R.; Colussi, A. J. *J. Phys. Chem. A* **2010**, *114*, 6016.
(219) Wren, S. N.; Kahan, T. F.; Jumaa, K. B.; Donaldson, D. J. *J. Geophys. Res.* **2010**, *115*, D16309.
(220) Baker, A. R.; Thompson, D.; Campos, M. L. A. M.; Perry, S. J.; Jickells, T. D. *Atmos. Environ.* **2000**, *34*, 4331.
(221) O'Driscoll, P.; Lang, K.; Minogue, N.; Sodeau, J. *J. Phys. Chem. A* **2006**, *110*, 4615.
(222) O'Driscoll, P.; Minogue, N.; Takenaka, N.; Sodeau, J. *J. Phys. Chem. A* **2008**, *112*, 1677.
(223) Martino, M.; Liss, P. S.; Plane, J. M. C. *Geophys. Res. Lett.* **2006**, *33*, L06606.
(224) Jones, C. E.; Carpenter, L. J. *Geophys. Res. Lett.* **2007**, *34*, L13804.
(225) Pechtl, S.; Schmitz, G.; von Glasow, R. *Atmos. Chem. Phys.* **2007**, *7*, 1381.
(226) Dooley, K. S.; Geidosch, J. N.; North, S. W. *Chem. Phys. Lett.* **2008**, *457*, 303.
(227) Grant, D. J.; Garner, E. B.; Matus, M. H.; Nguyen, M. T.; Peterson, K. A.; Francisco, J. S.; Dixon, D. A. *J. Phys. Chem. A* **2010**, *114*, 4254.
(228) Aitken, J. *Trans. Roy. Soc. Edinburgh* **1895**, *37*, 17.
(229) Paugam, J. Y. *C. R. Acad. Sci., Ser. B* **1975**, *280*, 821.
(230) Bigg, E. K.; Turvey, D. E. *Atmos. Environ.* **1978**, *12*, 1643.
(231) ODowd, C. D.; Lowe, J. A.; Smith, M. H.; Davison, B.; Hewitt, N.; Harrison, R. M. *J. Geophys. Res., [Atmos.]* **1997**, *102*, 12839.
(232) Wiedensohler, A.; Covert, D. S.; Swietlicki, E.; Aalto, P.; Heintzenberg, J.; Leck, C. *Tellus B* **1996**, *48*, 213.
(233) Bonsang, B.; Cuong, N. B.; Paugam, J. Y. *C. R. Acad. Sci., Ser. B* **1976**, *283*, 1285.
(234) O'Dowd, C.; McFiggans, G.; Creasey, D. J.; Pirjola, L.; Hoell, C.; Smith, M. H.; Allan, B. J.; Plane, J. M. C.; Heard, D. E.; Lee, J. D.; Pilling, M. J.; Kulmala, M. *Geophys. Res. Lett.* **1999**, *26*, 1707.
(235) O'Dowd, C. D.; Hämeri, K.; Mäkelä, J. M.; Pirjola, L.; Kulmala, M.; Jennings, S. G.; Berresheim, H.; Hansson, H.-C.; de Leeuw, G.; Kunz, G. J.; Allen, A. G.; Hewitt, C. N.; Jackson, A.; Viisanen, Y.; Hoffmann, T. *J. Geophys. Res.* **2002**, *107*, 8108.
(236) Dal Maso, M.; Kulmala, M.; Lehtinen, K. E. J.; Makela, J. M.; Aalto, P.; O'Dowd, C. D. *J. Geophys. Res., [Atmos.]* **2002**, *107*, 8097.
(237) Flanagan, R. J.; Geever, M.; O'Dowd, C. D. *Environ. Chem.* **2005**, *2*, 256.
(238) Mäkelä, J. M.; Hoffmann, T.; Holzke, C.; Väkevä, M.; Suni, T.; Mattila, T.; Aalto, P. P.; Tapper, U.; Kauppinen, E. I.; O'Dowd, C. D. *J. Geophys. Res.* **2002**, *107*, 8110.
(239) Heard, D. E.; Read, K. A.; Methven, J.; Al-Haider, S.; Bloss, W. J.; Johnson, G. P.; Pilling, M. J.; Seakins, P. W.; Smith, S. C.; Sommariva, R.; Stanton, J. C.; Still, T. J.; Brooks, B.; Leeuw, G. D.; Jackson, A. V.; McQuaid, J. B.; Morgan, R.; Smith, M. H.; Carpenter, L. J.; Carslaw, N.; Hamilton, J.; Hopkins, J. R.; Lee, J. D.; Lewis, A. C.; Purvis, R. M.; Wevill, D. J.; Brough, N.; Green, T.; Mills, G.; Penkett, S. A.; Plane, J. M. C.; Saiz-Lopez, A.; Worton, D.; Monks, P. S.; Fleming, Z.; Rickard, A. R.; Alfarra, M.; Allan, J. D.; Bower, K.; Coe, H.; Cubison, M.; Flynn, M.; McFiggans, G.; Gallagher, M.; Norton, E. G.; O'Dowd, C. D.; Shillito, J.; Topping, D.; Vaughan, G.; Williams, P.; Bitter, M.; Ball, S. M.; Jones, R. L.; Povey, I. M.; O'Doherty, S.; Simmonds, P. G.; Allen, A.; Kinnersley, R. P.; Beddows, D. C. S.; Dall'Osto, M.; Harrison, R. M.; Donovan, R. J.; Heal, M. R.; Jennings, S. G.; Noone, C.; Spain, G. *Atmos. Chem. Phys.* **2006**, *6*, 2241.
(240) Huang, R. J.; Seitz, K.; Neary, T.; O'Dowd, C. D.; Platt, U.; Hoffmann, T. *Geophys. Res. Lett.* **2010**, *37*, L03803.
(241) O'Dowd, C. D. O. *J. Geophys. Res., [Atmos.]* **2001**, *106*, 1545.
(242) McFiggans, G.; Bale, C. S. E.; Ball, S. M.; Beames, J. M.; Bloss, W. J.; Carpenter, L. J.; Dorsey, J.; Dunk, R.; Flynn, M. J.; Furneaux, K. L.; Gallagher, M. W.; Heard, D. E.; Hollingsworth, A. M.; Hornsby, K.; Ingham, T.; Jones, C. E.; Jones, R. L.; Kramer, L. J.; Langridge, J. M.; Leblanc, C.; LeCrane, J. P.; Lee, J. D.; Leigh, R. J.; Longley, I.; Mahajan, A. S.; Monks, P. S.; Oetjen, H.; Orr-Ewing, A. J.; Plane, J. M. C.; Potin, P.; Shillings, A. J. L.; Thomas, F.; von Glasow, R.; Wada, R.; Whalley, L. K.; Whitehead, J. D. *Atmos. Chem. Phys.* **2010**, *10*, 2975.
(243) Whitehead, J. D.; McFiggans, G. B.; Gallagher, M. W.; Flynn, M. J. *Geophys. Res. Lett.* **2009**, *36*, L04806.
(244) Väkevä, M.; Hameri, K.; Aalto, P. P. *J. Geophys. Res., [Atmos.]* **2002**, *107*, 8104.
(245) Fjellvag, H.; Kjekshus, A. *Acta Chem. Scand.* **1994**, *48*, 815.
(246) Selte, K.; Kjekshus, A. *Acta Chem. Scand.* **1970**, *24*, 1912.
(247) Daehlie, G.; Kjekshus, A. *Acta Chem. Scand.* **1964**, *18*, 144.
(248) Kumar, R.; Saunders, R. W.; Mahajan, A. S.; Plane, J. M. C.; Murray, B. J. *Atmos. Chem. Phys.* **2010**, *10*, 12251.
(249) Selte, K.; Kjekshus, A. *Acta Chem. Scand.* **1968**, *22*, 3309.
(250) Katzin, L. I. *J. Chem. Phys.* **1953**, *21*, 490.
(251) Pirjola, L.; O'Dowd, C.; Yoon, Y. J.; Sellegri, K. *Environ. Chem.* **2005**, *2*, 271.
(252) McFiggans, G.; Artaxo, P.; Baltensperger, U.; Coe, H.; Facchini, M. C.; Feingold, G.; Fuzzi, S.; Gysel, M.; Laaksonen, A.; Lohmann, U.; Mentel, T. F.; Murphy, D. M.; O'Dowd, C. D.; Snider, J. R.; Weingartner, E. *Atmos. Chem. Phys.* **2006**, *6*, 2593.
(253) Kulmala, M.; Korhonen, P.; Napari, I.; Karlsson, A.; Berresheim, H.; O'Dowd, C. D. *J. Geophys. Res., [Atmos.]* **2002**, *107*, 8111.
(254) O'Dowd, C. D.; De Leeuw, G. *Philos. Trans. R. Soc. a: Math. Phys. Eng. Sci.* **2007**, *365*, 1753.
(255) Kulmala, M.; Kerminen, V.-M. *Atmos. Res.* **2008**, *90*, 132.
(256) Chebbi, A.; Carlier, P. *Atmos. Environ.* **1996**, *30*, 4233.
(257) Saxena, P.; Hildemann, L. M. *J. Atmos. Chem.* **1996**, *24*, 57.
(258) Lemoine, G. *C. R. Hebd. Seances Acad. Sci.* **1921**, *173*, 192.
(259) Abel, E.; Hilferding, K.; Smetana, O. *Z. Phys. Chem. Abt. B* **1936**, *32*, 85.
(260) Cobb, R. L. *J. Org. Chem.* **1958**, *23*, 1368.
(261) Vuollekoski, H.; Kerminen, V. M.; Anttila, T.; Sihto, S. L.; Vana, M.; Ehn, M.; Korhonen, H.; McFiggans, G.; O'Dowd, C. D.; Kulmala, M. *J. Geophys. Res.* **2009**, *114*, D02206, DOI: 10.1029/2008JD010713.
(262) Duce, R. A.; Woodcock, A. H.; Moyers, J. L. *Tellus* **1967**, *19* (3), 367.
(263) Seto, F. Y. B.; Duce, R. A. *J. Geophys. Res.* **1972**, *77*, 5339.
(264) Laniewski, K.; Dahlen, J.; Boren, H.; Grimvall, A. *Chemosphere* **1999**, *38*, 771.
(265) Gilfedder, B. S.; Petri, M.; Biester, H. *Atmos. Chem. Phys.* **2007**, *7*, 2661.
(266) Gilfedder, B. S.; Petri, M.; Biester, H. *J. Geophys. Res.* **2007**, *112*, D07301.
(267) Lai, S. C.; Hoffmann, T.; Xie, Z. Q. *Geophys. Res. Lett.* **2008**, *35*, L21803.
(268) Xu, S.-Q.; Xie, Z.-Q.; Liu, W.; Yang, H.-X.; Li, B. *Chin. J. Anal. Chem.* **2010**, *38*, 219.
(269) Kanthale, P.; Ashokkumar, M.; Grieser, F. *Ultrason. Sonochem.* **2008**, *15*, 143.
(270) Liu, S.-C.; Wu, H. *J. Am. Chem. Soc.* **1934**, *56*, 1005.
(271) Tsukada, H.; Hara, H.; Iwashima, K.; Yamagata, N. *Bull. Chem. Soc. Jpn.* **1987**, *60*, 3195.
(272) Xu, S.; Xie, Z.-Q.; Li, B.; L., S.; Kang, H.; Yang, H.; Zhang, P. *Environ. Chem.* **2010**, *7*, 406.

(273) Gilfedder, B. S.; Chance, R.; Dettmann, U.; Lai, S. C.; Baker, A. R. *Anal. Bioanal. Chem* **2010**, *398* (1), 519.
(274) Hou, X. L.; Aldahan, A.; Nielsen, S. P.; Possnert, G. *Environ. Sci. Technol.* **2009**, *43*, 6522.
(275) Truesdale, V. W.; Jones, S. D. *J. Hydrol.* **1996**, *179*, 67.
(276) Campos, M. L. A. M.; Nightingale, P. D.; Jickells, T. D. *Tellus B* **1996**, *48*, 106.
(277) O'Dowd, C. D.; Facchini, M. C.; Cavalli, F.; Ceburnis, D.; Mircea, M.; Decesari, S.; Fuzzi, S.; Yoon, Y. J.; Putaud, J. P. *Nature* **2004**, *431*, 676.
(278) Truesdale, V. W.; Luther, G. W. *Aq. Geochem.* **1995**, *1*, 89.
(279) Murphy, D. M.; Thomson, D. S.; Middlebrook, A. M. *Geophys. Res. Lett.* **1997**, *24*, 3197.
(280) Middlebrook, A. M.; Murphy, D. M.; Thomson, D. S. *J. Geophys. Res.* **1998**, *103*, 16475.
(281) Murphy, D. M.; Thomson, D. S. *Geophys. Res. Lett.* **2000**, *27*, 3217.
(282) Jenkin, M. E.; Cox, R. A.; Candeland, D. E. *J. Atmos. Chem.* **1985**, *2*, 359.
(283) Chatfield, R. B.; Crutzen, P. J. *J. Geophys. Res.* **1990**, *95D*, 22319.
(284) Davis, D. J.; Crawford, J.; Liu, S.; McKeen, S.; Bandy, A.; Thornton, D.; Rowland, F.; Blake, D. *J. Geophys. Res.* **1996**, *101*, 2135.
(285) McFiggans, G.; Cox, R. A.; Mössinger, J. C.; Allan, B. J.; Plane, J. M. C. *J. Geophys. Res., [Atmos.]* **2002**, *107*, 4271.
(286) Lindberg, S. E.; Brooks, S.; Lin, C. J. *Environ. Sci. Technol.* **2002**, *36* (6), 1245.
(287) Sander, R.; Vogt, R.; Harris, G. W.; Crutzen, P. J. *Tellus:B* **1997**, *49*, 522.
(288) von Glasow, R.; Sander, R.; Bott, A.; Crutzen, P. J. *J. Geophys. Res.* **2002**, *107*, 4341.
(289) Stutz, J.; Hebestreit, K.; Alicke, B.; Platt, U. *J. Atmos. Chem.* **1999**, *34*, 65.
(290) Sommariva, R.; Bloss, W. J.; Brough, N.; Carslaw, N.; Flynn, M.; Haggerstone, A.-L.; Heard, D. E.; Hopkins, J. R.; Lee, J. D.; Lewis, A. C.; McFiggans, G.; Monks, P. S.; Penkett, S. A.; Pilling, M. J.; Plane, J. M. C.; Read, K. A.; Saiz-Lopez, A.; Rickard, A. R.; Williams, P. I. *Atmos. Chem. Phys.* **2006**, *6*, 1135.
(291) O'Dowd, C. D.; Hameri, K.; Makela, J.; Vakeva, M.; Aalto, P.; de Leeuw, G.; Kunz, G. J.; Becker, E.; Hansson, H. C.; Allen, A. G.; Harrison, R. M.; Berresheim, H.; Geever, M.; Jennings, S. G.; Kulmala, M. *J. Geophys. Res., [Atmos.]* **2002**, *107*, 8107.
(292) Shall, C.; Heumann, K. G. *Fresenius J. Anal. Chem.* **1993**, *346*, 717.
(293) Bassford, M. R.; Nickless, G.; Simmonds, P. G.; Lewis, A. C.; Pilling, M. J.; Evans, M. J. *Atmos. Environ.* **1999**, *33*, 2373.
(294) Krummel, P.; Krummel, P.; Krummel, P. In *Baseline Atmospheric Program Australia 2005−2006*; Cainey, J., Derek, N., Krummel., P., Eds.; Australian Bureau of Meteorology: Melbourne, Victoria, Australia, 2007.
(295) Li, H. J.; Y., Y.; Akimoto, H. *Atmos. Environ.* **1999**, *33*, 1881.
(296) Reifenhäuser, W.; Heumann, K. G. *Atmos. Environ.* **1992**, *26A*, 2905.
(297) Atlas, E.; Pollock, W.; Greenberg, J.; Heidt, L.; Thompson, A. M. *J. Geophys. Res.* **1993**, *98*, 16993.
(298) Yokouchi, Y.; Mukai, H.; Yamamoto, H.; Otsuki, A.; Saitoh, C.; Nojiri, Y. *J. Geophys. Res.* **1997**, *102*, 8805.
(299) Li, H. J.; Yokouchi, Y.; Akimoto, H.; Narita, Y. *Geochem. J.* **2001**, *35*, 137.
(300) Zhou, Y.; Varner, R. K.; Russo, R. S.; Wingenter, O. W.; Haase, K. B.; Talbot, R.; Sive, B. C. *J. Geophys. Res.* **2005**, *110*, D21302.
(301) Varner, R. K.; Zhou, Y.; Russo, R. S.; Wingenter, O. W.; Atlas, E.; Stroud, C.; Mao, H.; Talbot, R.; Sive, B. C. *J. Geophys. Res.* **2008**, *113*, D10303.
(302) Rattingan, O. V.; Shallcross, D. E.; Cox, R. A. *J. Chem. Soc., Faraday Trans* **1997**, *93*, 2839.
(303) Mössinger, J.; Shallcross, D. E.; Cox, R. A. *J. Chem. Soc., Faraday Trans* **1998**, *94*, 1391.
(304) Rancher, J.; Kritz, M. A. *J. Geophys. Res.* **1980**, *85*, 5581.
(305) Duce, R. A.; Winchester, J. W.; van Nahl, T. W. *J. Geophys. Res.* **1965**, *70* (8), 1775.
(306) Moyers, J. L.; Duce, R. A. *J. Geophys. Res.* **1972**, *77*, 5229.
(307) Duce, R. A.; Arimoto, R.; Ray, B. J.; Unni, C. K.; Harder, P. J. *J. Geophys. Res.* **1983**, *88*, 5321.
(308) Sturges, W. T.; Barrie, L. A. *Atmos. Environ.* **1988**, *22*, 1179.
(309) Barrie, L. A.; Barrie, M. J. *J. Atmos. Chem.* **1990**, *11*, 211.
(310) Barrie, L. A.; Staebler, R.; Toom, D.; Georgi, B.; Denhartog, G.; Landsberger, S.; Wu, D. *J. Geophys. Res., [Atmos.]* **1994**, *99*, 25439.
(311) Arimoto, R.; Duce, R. A.; Ray, B. J.; Ellis, W. G., Jr.; Cullen, J. D.; Merrill, J. T. *J. Geophys. Res.* **1995**, *100*, 1199.
(312) Zieman, J. J.; Holmes, J. L.; Connor, D.; Jensen, C. R.; Zoller, W. H.; Hermann, D. M.; Parrington, J. R.; Gordon, G. E. *J. Geophys. Res.* **1995**, *100*, 25979.
(313) Jalkanen, L.; Manninen, P. *Environmetrics* **1996**, *7*, 27.
(314) Cheng, Z. L.; Lam, K. S.; Chan, L. Y.; Wang, T.; Cheng, K. K. *Atmos. Environ.* **2000**, *34*, 2771.
(315) Duce, R. A.; Winchester, J. W.; van Nahl, T. W. *Tellus* **1966**, *18* (2−3), 238.
(316) Lininger, R. L.; Duce, R. A.; Winchester, J. W.; Matson, W. R. *J. Geophys. Res.* **1966**, *71* (10), 2457.
(317) Duce, R. A.; Zoller, W. H.; Moyers, J. L. *J. Geophys. Res.* **1973**, *78*, 7802.
(318) Yoshida, S.; Muramatsu, Y. *J. Radioanal. Nucl. Chem.* **1995**, *196*, 295.
(319) Maenhaut, W. R.; Zoller, W. H.; Duce, R. A.; Hoffman, G. L. *J. Geophys. Res.* **1979**, *84C*, 2421.
(320) Cunningham, W. C.; Zoller, W. H. *J. Aerosol Sci.* **1981**, *12*, 367.
(321) Tuncel, G.; Aras, N. K.; Zoller, W. H. *J. Geophys. Res.* **1989**, *94*, 13025.
(322) Maenhaut, W.; Salma, I.; Cafmeyer, J.; Annegarn, H. J.; Andreae, M. O. *J. Geophys. Res., [Atmos.]* **1996**, *101*, 23631.
(323) Gäbler, H. E.; Heumann, K. G. *Int. J Anal. Chem.* **1993**, *50*, 129.
(324) Wimschneider, A.; Heumann, K. G. *Fresenius. J. Anal. Chem.* **1995**, *353*, 191.
(325) Baker, A. R. *Geophys. Res. Lett.* **2004**, *31*, L23S02.
(326) Allan, J. D.; Topping, D. O.; Good, N.; Irwin, M.; Flynn, M. J.; Williams, P. I.; Coe, H.; Baker, A. R.; Martino, M.; Niedermeier, N.; Wiedensohler, A.; Lehmann, S.; Muller, K.; Herrmann, H.; McFiggans, G. *Atmos. Chem. Phys.* **2009**, *9*, 9299.
(327) Richter, U.; Wallace, D. W. R. *Geophys. Res. Lett.* **2004**, *31*, L23S03.
(328) Bröske, R. Ph.D. Thesis, University of Wuppertal, Wuppertal, Germany, 1999.